LINEAR VISCOELASTIC CHARACTERIZATION

OF SAND-ASPHALT MIXTURES

BY

JOSEPH ELIAS SOUSSOU
Ingenieur de l'Ecole Centrale
des Arts et Manufactures - Paris
(1966)

Submitted in partial fulfillment

of the requirements for the degree of

Master of Science

at the

Massachusetts Institute of Technology

1968

Signature of Author ....
                Department of Civil Engineering, May 17, 1968

Certified by ....
                                        Thesis Supervisor

Accepted by ....
        Chairman, Departmental Committee on Graduate Students

ABSTRACT

LINEAR VISCOELASTIC CHARACTERIZATION

OF SAND-ASPHALT MIXTURES

by

JOSEPH ELIAS SOUSSOU

Submitted to the Department of Civil Engineering on
May 17, 1968 in partial fulfillment of the requirements
for the degree of Master of Science.

        One of the important requirements for the development
of a rational method for pavement design is the determina-
tion of the constitutive equations of the materials used.
Asphaltic materials and bituminous mixtures exhibit visco-
elastic behavior. This study reviews the theory of linear
viscoelastic characterization and the mathematical methods
available to analyze the applicability of the theory to
real materials. A sand-asphalt mixture is taken as an
example and creep and relaxation tests are performed at
different temperatures. The material is found to be linear
and the time-temperature superposition principle is also
found to be valid. The theoretical relationships are
applied by making use of appropriate computer programs
developed for this study. This includes correction of the
relaxation curves for the finite rise time of strain,
approximation of the master curves by means of Dirichlet
series, and comparison of the creep and relaxation results
in Laplace domain. The two series of test results are
also interconverted directly in the real time domain
through numerical integration, and the complex functions
are derived from the analytical expressions.

Thesis Supervisor: Fred Moavenzadeh

Title: Associate Professor of Civil Engineering

ACKNOWLEDGEMENT

CONTENTS

I. INTRODUCTION

The development of a rational method of design for
flexible pavements requires the description of some
failure criteria and their application to the results of
an analysis of stresses and displacements. Such an
analysis requires the determination of the interrelations
between forces acting on a material body and the resulting
deformations. These interrelations are called constitutive
equations and are generally assumed to be linear in form,
thus avoiding the mathematical complications which may
arise otherwise. The rheological behavior of asphaltic
mixtures is found to be time and temperature dependent,
thus these variables should be included in the constitutive
equations of such materials.

The present rational methods of pavement design
generally do not take into account the time and temperature
dependency of the materials. This has resulted in large
discrepancies between experimentally measured stresses and
displacements and those calculated theoretically. Moreover,
variables such as the duration of load and the rate of
loading cannot be accounted for with the present design
methods using elastic assumptions. Similarly the theories
of elasticity cannot be used to explain the accumulation

of deflection which is observed experimentally in a pavement. Some methods of analysis developed recently [7] take into consideration the time-dependent behavior of materials. A wide variety of time-dependent materials may be characterized as linear viscoelastic materials as a first approximation. Such characterization requires the availability of easy and accurate methods in either analytical or numerical form for the application of the theory to the actual data.

Objective and Scope:

The objective of this study was to characterize the time-dependent behavior of a sand-asphalt mixture so as to determine the applicability of the theory of linear visco-elasticity to the mechanical response of such a mixture at different temperatures. The applicability of the time-temperature superposition principle to the viscoelastic response of this mixture was also investigated. Furthermore, a review of the relations which exist among various visco-elastic methods of representation and the available mathe-matical methods of application of these methods to visco-elastic characterizations of sand-asphalt mixtures was made.

For this purpose, static creep tests and stress relaxation tests were conducted at six different temperatures

for a sand-asphalt mixture. Different levels of stress and strain were used to demonstrate the linear behavior of the mixture. The use of the time-temperature superposition principle yielded creep compliance and relaxation modulus master curves. The two curves were fitted to a Dirichlet series of exponentials and their Laplace transforms were compared. A numerical inversion procedure was also used to compare them in the real time domain. The complex functions were derived from the transient functions, and the results obtained from the creep tests were also compared with those obtained from the stress relaxation tests.

II. CHARACTERIZATION OF
LINEAR VISCOELASTIC MATERIALS

The mechanical behavior of materials can be studied at three different levels [19]; the atomic and molecular level, the structural level and the phenomenological level. Engineering design is mainly concerned with the phenomenological or macroanalytical level of representation. At this level, by appropriate dimensional considerations, the material is generally considered as continuous, even though certain materials such as sand-asphalt mixtures are clearly made of various distinct phases. The assumption of continuity will allow the notions of stress and strain to be defined for such material bodies.

Phenomenological Characterization of Materials:

Internal force equilibrium of a body yields the notion of stress [4]. The change in shape and volume yields the notion of strain. The consideration of forces on an infinitesimal cubical element shows, at the limits when the cube is shrunk to a point, the stress at that point can be represented by a second order tensor, having nine elements σ_{ij}. Similarly, calling the displacements of a point along

the axes of a reference system U_i and considering its variation with space change, results in the definition of a strain tensor (ε_{ij}) which will also contain nine elements ε_{ij} and will represent the infinitesimal shape changes at a point.

Geometrical considerations and the definition of strains yield nine kinematic relations between strains and displacements:

$$\varepsilon_{ij} = \frac{1}{2} (U_{i,j} + U_{j,i} + U_{k,i}U_{k,j}) \qquad (2.1)$$

where the comma indicates partial differentiation with respect to the coordinate associated with the index following the comma. The symmetry of this expression results in the strain tensor being symmetric and the number of the kinematic relations being reduced to six. For small displacements the second order terms are usually neglected which will further simplify the kinematic equations.

By satisfying equilibrium requirements, for stresses due to applied loads and inertial forces due to acceleration, six equations of equilibrium can be defined. Three of them are derived from the equilibrium of the coupled stresses, which result in a stress tensor being symmetric ($\sigma_{ij} = \sigma_{ji}$) for non-polar cases. The other three equations are:

$$\sigma_{ij,j} + F_i = \rho \frac{\partial^2 U_i}{\partial t^2} \qquad (2.2)$$

where σ_{ij} is the stress acting along x_j on a plane
perpendicular to direction x_i; F_i is the body force
acting along x_i and ρ is the density of the material,
assumed to be a continuous function of the volume.

A point in a body is, thus, mechanically defined by
six components of stresses, six components of strains and
three components of displacements. Thus, in addition to
equations of equilibrium and strain-displacement, six
additional equations are required to define a point in a
body. These additional equations are obtained by establish-
ing relationships which exist between kinematical and
dynamical variables in a material. Such relationships,
which depend entirely upon the mechanical properties of
a material, are referred to as constitutive equations.

Constitutive Equations:

The constitutive equations can be generally written
in the form of implicit functions:

f(stresses, deformations, time, temperature, geometry) = 0

In their general form these equations are complicated and

are often in non-linear form. In an explicit form the
stress tensor is given as a function of the past history
of the displacements or motion. The simple materials,
moreover, are defined as materials for which the stress
tensor depends on the history of the first spatial gradient
of the displacements [15, 52]. For such materials the
constitutive equations are expressed in operational forms
such as, differential, integral, or integro-differential
relations. For example in an integral operator form the
constitutive equations are written as:

$$[\sigma_{ij}] = \int_{-\infty}^{t} f([\sigma_{ij}], x, t, t', T)[\epsilon_{ij}] \, dt' \qquad (2.3)$$

where $[\sigma_{ij}]$ is the stress tensor, x is the space variable,
t and t' are the present time and the time as a parameter
of history respectively, and T is the temperature. $[\epsilon_{ij}]$
is the strain tensor which may be a function of time. The
simplest form of such equations is that of linear elastic
materials where the stress is a linear function of strain
only.

The constitutive equations may be dependent on time
as a result of the variation in properties, structure, or
composition of the material. This could correspond to a
chemical degradation or a building up of a structure or
other similar mechanisms. Such time effects are included

in the variable t' of the above equation. Disregarding the influence of such parameters, the forms of the constitutive equations of materials can be divided into time dependent and time independent systems.

Time Independent Systems: For time independent systems the time effect is neglected in the mechanical response. The linear elastic materials are a special case of such systems with the constitutive equations of the following form:

$$[\sigma_{ij}] = [E_{ijhk}][\epsilon_{hk}] \qquad (2.4)$$

where E_{ijhk} are the constants defining the properties of the material. These constants are related to the second derivatives of the free energy F, and thus for the most general case of anisotropic material, there are only twenty-one independent elastic constants [27]. For an isotropic material, these constants reduce to only two independent parameters such that:

$$\sigma_{ij} = \lambda\theta\delta_{ij} + 2\mu \epsilon_{ij} \qquad (2.5)$$

where $\theta = \sum_i \epsilon_{ii}$, δ_{ij} is the Kronecker delta, defined such that $\delta_{ij} = 1$ for $i = j$, and $\delta_{ij} = 0$ for $i \neq j$. λ and μ are Lame's constants. Mathematically, the stress

and strain tensors can be resolved into the sum of a mean normal tensor and deviatoric tensor which represent the pressure-volume and pure shear effects, respectively [36].

$$[\sigma_{ij}] = [S_{ij}] + [\sigma]$$

$$[\varepsilon_{ij}] = [e_{ij}] + [\varepsilon] \tag{2.6}$$

where $\sigma = (\sigma_{ii})/3$ and $\varepsilon = (\varepsilon_{ii})/3$, and $S_{ij} = \sigma_{ij} - \delta_{ij}\sigma$ and $e_{ij} = \varepsilon_{ij} - \delta_{ij}\varepsilon$.

The two constants characterizing a linear isotropic elastic material can be written as:

$$\sigma = 3K\varepsilon \quad\text{and}\quad S_{ij} = 2Ge_{ij} \tag{2.7}$$

where K is the bulk modulus and G is the shear modulus. Of course, K, G, λ and μ are interrelated. Although K and G represent more fundamental mechanical behaviors of a material, Young's modulus E and Poisson's ratio ν are more commonly used.

Time Dependent Systems: For most of the materials the mechanical response is not truly time independent, and in certain cases the time variable cannot be neglected in the constitutive equation. A particular case of the time dependent systems is a Newtonian viscous fluid. The one dimensional Constitutive equation of such material is a linear

relation between stress and the first derivative of the strain with respect to time: $\sigma = \eta\frac{d\varepsilon}{dt}$. The three-dimensional characterization is analogous to that of elasticity if the strain rate is substituted for strain. The response of this material can also be resolved into volumetric and deviatoric tensors.

Viscoelastic materials represent a general class of the time dependent materials. The assumption of linearity requires that the effect be proportional to the cause for a given point at a given time.

One Dimensional Linear Viscoelastic Theory:

Assumption of the linearity of the material transforms equation 2.3 into a simple form:

$$\sigma_{ij} = \int_{o}^{t} f(x, t-t', T) \, \varepsilon_{ij} \, dt' \qquad (2.8)$$

which is based on the principle of the fading memory. This principle states that the deformations which occurred in the distant past have less influence in determining the present stress than those that occurred in the recent past. Consequently identical materials having similar recent past histories of deformation, will have the same mechanical response, even though their distant past histories could be different. Thus if the material was essentially unstressed

during the recent past, the integral summation could be made on the interval (0,t) instead of (-∞,t).

The assumptions of homogeneity and isothermal condition reduce equation 2.8 to:

$$\sigma_{ij} = \int_0^t f(t-t') \, \varepsilon_{ij} \, dt' \qquad (2.9)$$

These functions of time will replace the constants characterizing a linear elastic material. They are separated into two groups; the creep functions and the relaxation functions. The creep functions are derived from stress-controlled tests and the relaxation functions are derived when deformations are controlled. The creep compliance function is defined as:

$$D_c(t) = \frac{\varepsilon(t)}{\sigma_o h(t)} \qquad (2.10)$$

where $\varepsilon(t)$ is the axial strain,

σ_o is the applied constant axial stress, and

h(t) is the Heaviside step function $\begin{cases} = 0 & t < 0 \\ = 1 & t \geq 0 \end{cases}$

Similarly the stress relaxation modulus is defined as:

$$E_r(t) = \frac{\sigma(t)}{\varepsilon_o h(t)} \qquad (2.11)$$

In this case the strain ε_o is applied instantaneously and maintained constant.

The assumption of the linearity of the material allows the application of discrete or continuous summations to obtain the stresses or strains caused by any pattern of deformation or loading [28]. Letting $\Delta\varepsilon(\tau_k)$ and $\Delta\sigma(\tau_k)$ be instantaneous increases of strains or stresses at times τ_k, yields the summations:

$$\varepsilon(t) = \sum_{k=1}^{n} D_c(t-\tau_k)\, \Delta\sigma(\tau_k)$$

and (2.12)

$$\sigma(t) = \sum_{k=1}^{n} E_r(t-\tau_k)\, \Delta\varepsilon(\tau_k)$$

These summations can be extended to integral forms [22], [28] which are the general expressions of Boltzman's superposition principle.

$$\sigma(t) = \int_o^t E_r(t-\tau)\, \frac{d\varepsilon(\tau)}{d\tau}\, d\tau$$

(2.13)

$$\varepsilon(t) = \int_o^t D_c(t-\tau)\, \frac{d\sigma(\tau)}{d\tau}\, d\tau$$

The superposition principle can also be expressed as:

$$\sigma(t) = \int_o^t \varepsilon(t-\tau)\, \frac{dE_r(\tau)}{d\tau}\, d\tau$$

(2.14)

or:

$$\varepsilon(t) = \int_0^t \sigma(t-\tau) \frac{dD_c(\tau)}{d\tau} d\tau \qquad (2.14)$$

Substitution of one of the above equations into the other will result in an explicit relationship between $E_r(t)$ and $D_c(t)$ in the form of a Volterra integral equation [53]:

$$\int_0^t E_r(t-\tau) D_c(\tau) d\tau = \int_0^t D_c(t-\tau) E_r(\tau) d\tau = t \qquad (2.15)$$

or

$$\int_0^t E_r(t-\tau) \frac{dD_c(\tau)}{d\tau} d\tau = \int_0^t D_c(t-\tau) \frac{dE_r(\tau)}{d\tau} d\tau = h(t) \qquad (2.16)$$

Many engineering materials manifest an instantaneous mechanical response which corresponds to a discontinuity at the origin in their relaxation and creep functions. Such discontinuity in these functions generally results in certain mathematical complications. Gurtin and Sternberg [23] have shown that the definition of one of the two transient functions yields, if it is a continuous function, a unique value for the other. They have extended this proof to the case where discontinuities are included as a limiting case of continuous functions.

Differential Operators: The constitutive equation of a

viscoelastic material may also be written in an operational

form:

$$P[\epsilon(t)] = Q[\sigma(t)] \qquad (2.17)$$

where   P   and   Q   instead of being integral operators as

in equations 2.14 are differential operators.   For linear

viscoelastic materials   P   and   Q   are linear differential

operators, such that:

$$P = \sum_{k=0}^{p} P_k \frac{\partial^k}{\partial t^k}$$

and   (2.18)

$$Q = \sum_{k=0}^{q} Q_k \frac{\partial^k}{\partial t^k}$$

Gurtin and Sternberg [23] have shown such a differential

representation can be derived from the integral representa-

tion if   P   can be found such that $P[E_r(t)] = Q_o$ for

$0 \leqslant t < \infty$.   They have further shown that when $p \neq q$

only one of the two integral representations can be found

from a differential representation unless generalized

discontinuity functions are used such as the Heaviside step

function and the Dirac delta function or its successive

derivatives.

Mechanical Models: To visualize the behavior of visco-
elastic materials, and more precisely the differential
operator representation, an interpretation in terms of a
finite network of springs and dashpots is often used.
Springs represent an elastic law: $\sigma = K\epsilon$ and dashpots
represent purely viscous fluid where $\sigma = \eta\frac{d\epsilon}{dt}$. The mecha-
nical response of a combination of these elements can be
represented in differential operator form. These models
have been used to represent actual materials. To represent
the behavior of real materials over an extended time period,
elaborate mechanical models are used. The interest in the
mechanical models seems to be more of historic and academic
value than ease of representation.

Following consideration of some mechanical models,
terms corresponding to pure linear elastic response and
the pure viscous flow are sometime separated from the
remaining terms in the integral representation [22,32]:

$$\sigma(t) = E_r(0)\epsilon(t) + \eta_0\delta(t) + \int_0^t E_\psi(t-\tau)\frac{d\epsilon(\tau)}{d\tau}\, d\tau$$

$$(2.19)$$

$$\epsilon(t) = D_c(0)\sigma(t) + \frac{t}{\eta_\infty} + \int_0^t D_\phi(t-\tau)\frac{d\sigma(\tau)}{d\tau}\, d\tau$$

These expressions are derived directly from the consideration

of mechanical models of springs and dashpots. The terms
which were taken out from the integrals represent the
degenerated elements in a generalized model. $D_c(0)$ and
$E_r(0)$ are terms corresponding to the isolated springs and
η_∞ and η_0 are the terms related to the isolated dashpots
in a generalized Voigt and Maxwell model respectively [5]
(Figure 1). These terms can be kept in the integral
definitions, but their separation may allow a better
understanding of the mechanical behavior. For cross-linked
polymers $\frac{1}{\eta_\infty} = 0$, thus the creep compliance reaches a
finite value for an infinite time; while for uncross-linked
polymers there is a constant flow for extended time. In
what follows, since only linear viscoelastic solids are
studied, the term corresponding to long term flow is
separated from the creep compliance. This separation
prevents any confusion which may otherwise arise in some
of the approximate formulas, and it also assures the
convergence of integrals.

The instantaneous viscosity term is also neglected
since its physical existence is doubtful, and it has not
yet been actually measured. Its existence would mean that
the stress would go to infinity when the straining time
approaches zero. Actually, when the rate of straining

Generalized Voigt Model
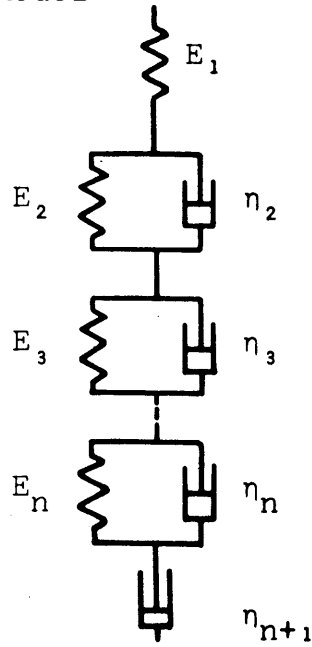
$$D_c(t) = \frac{\varepsilon(t)}{\sigma_o h(t)} = [\frac{1}{E_1} + \sum_{i=2}^{n} \frac{1}{E_i} (1 - e^{-\frac{E_i}{\eta_i}t}) + \frac{t}{\eta_{n+1}}]$$

Generalized Maxwell Model
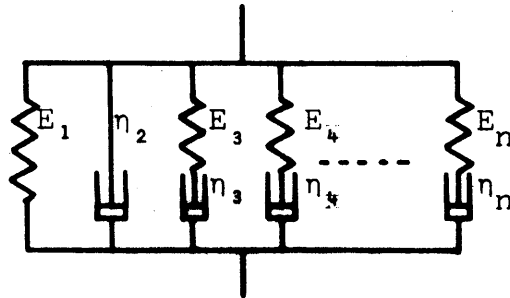
$$E_r(t) = \frac{\sigma(t)}{\varepsilon_o h(t)} = [E_1 + \eta_2 \delta(t) + \sum_{i=3}^{n} E_i e^{-\frac{E_i}{\eta_i}t}]$$

Figure 1.   Mechanical Models

increases, the instantaneous stress seems to level off at a finite value.

The instantaneous responses $D_c(0)$ and $E_r(0)$ will, however, be left in the integral expressions for this study.

Complex Functions: These functions aan be derived directly from the hereditary representation and can be measured by subjecting the material to a cyclic loading. Letting

$$\sigma(t) = \sigma_o e^{i\omega t}$$

$$\varepsilon(t) = \varepsilon_o e^{i\omega t}$$

or

(2.20)

in equations 2.13, the following expressions can be derived [22]:

$$\sigma^*(i\omega) = i\omega\varepsilon_o e^{i\omega t} \int_o^\infty e^{-i\omega\tau} E_r(\tau)d\tau$$

(2.21)

and

$$\varepsilon^*(i\omega) = i\omega\sigma_o e^{i\omega t} \int_o^\infty e^{-i\omega\tau} D_c(\tau)d\tau$$

Thus, the steady state response to a sinusoidal excitation with a circular frequency ω will also be sinusoidal with the same frequency.

Defining

$$\sigma^*(i\omega) = E^*(i\omega)\varepsilon^*(i\omega)$$

(2.22)

and

$$\varepsilon^*(i\omega) = D^*(i\omega)\sigma^*(i\omega)$$

-24-

leads to

$$E^*(i\omega) = i\omega \int_0^\infty E_r(\tau)e^{-i\omega t} \, d\tau$$

(2.23)

$$D^*(i\omega) = i\omega \int_0^\infty D_c(\tau)e^{-i\omega t} \, d\tau$$

These complex functions are the Fourier transforms
of the transients functions defined in equations 2.13.
Combining equations 2.22 yields:

$$E^*(i\omega) \, D^*(i\omega) = 1$$

(2.24)

The complex modulus E^* and complex compliance D^*
can be separated into a real and an imaginary component:

$$E^*(i\omega) = E_1(\omega) + iE_2(\omega)$$

(2.25)

and $\qquad D^*(i\omega) = D_1(\omega) + iD_2(\omega)$

The real component is associated with the recoverable
energy and the imaginary part is a measure of the loss energy
[17]. A loss tangent is defined to relate these two
components:

$$\tan \delta(\omega) = \frac{-D_2(\omega)}{D_1(\omega)} = \frac{E_2(\omega)}{E_1(\omega)}$$

(2.26)

$\delta(\omega)$ is also the phase angle between the vectors repre-
senting $\epsilon^*(i\omega)$ and $\sigma^*(i\omega)$.

The relationships derived from equations 2.23 give these two components in terms of transient functions [17, 33]:

$$E_1(\omega) = \omega \int_0^\infty [E_r(\tau) - E_\infty] \sin \omega\tau \, d\tau + E_\infty$$

$$E_2(\omega) = \omega \int_0^\infty [E_r(\tau) - E_\infty] \cos \omega\tau \, d\tau$$

$$(2.27)$$

$$D_1(\omega) = \omega \int_0^\infty [D_c(\tau) - D_\infty - \frac{t}{\eta}] \sin \omega\tau \, d\tau + D_\infty$$

$$D_2(\omega) = -\omega \int_0^\infty [D_c(\tau) - D_\infty - \frac{t}{\eta}] \cos \omega\tau \, d\tau + \frac{1}{\omega\eta}$$

D_∞ and E_∞ are the equilibrium values for an infinite time after the flow term is subtracted. These terms are separated from the expressions of $D_c(t)$ and $E_r(t)$ to avoid the difficulties of the integrations.

The real and imaginary components of complex modulus and complex compliance are related to each other by the following equations, derived from equation 2.4:

$$E_1(\omega) = \frac{D_1(\omega)}{[D_1(\omega)]^2 + [D_2(\omega)]^2} \qquad E_2(\omega) = \frac{-D_2(\omega)}{[D_1(\omega)]^2 + [D_2(\omega)]^2}$$

or

$$(2.28)$$

$$D_1(\omega) = \frac{E_1(\omega)}{[E_1(\omega)]^2 + [E_2(\omega)]^2} \qquad D_2(\omega) = \frac{-E_2(\omega)}{[E_1(\omega)]^2 + [E_2(\omega)]^2}$$

The inverse Fourier transformation gives transient functions from the complex function components [17]:

$$E_r(t) = E_\infty + \frac{2}{\pi} \int_0^\infty \left\{ [E_1(\omega) - E_\infty]/\omega \right\} \sin \omega t \ d\omega$$

$$(2.29)$$

$$E_r(t) = E_\infty + \frac{2}{\pi} \int_0^\infty [E_2(\omega)/\omega] \ \cos \omega t \ d\omega$$

$$D_c(t) = D_0 + \frac{2}{\pi} \int_0^\infty \left\{ [D_1(\omega) - D_0]/\omega \right\} \sin \omega t \ d\omega + \frac{t}{\eta}$$

$$(2.30)$$

$$D_c(t) = D_0 + \frac{2}{\pi} \int_0^\infty [D_2(\omega)/\omega - 1/\omega^2\eta][1 - \cos \omega t] \ d\omega + \frac{t}{\eta}$$

Similar algebraic relationships can be obtained between the various viscoelastic functions using Laplace transformation. Applying this transformation to a stress relaxation test [54]:

$$E_r(t) = \frac{\sigma(t)}{\varepsilon_0 h(t)}$$

$$(2.31)$$

we obtain
$$\overline{E}(p) = \frac{\overline{\sigma}(p)}{\overline{\varepsilon}(p)} = p \ \overline{E}_r(p)$$

$$(2.32)$$

The relationship between the creep function and the relaxation function in the real time domain becomes algebraic between their images in the Laplace domain: $\overline{E}(p) \times \overline{D}(p) = p^2 \overline{E}_r(p) \times \overline{D}_c(p) = 1$. This transformation may be interesting for the characterization of a viscoelastic material because

the relations of linear elasticity can be applied to the

associated functions in the Laplace domain. However, since

the inverse transform is not easy to obtain, the approximate

techniques applied to the direct conversion are often

preferable.

Spectral Representation: The spectral distribution functions

of a viscoelastic material cannot be measured experimentally,

and should be derived mathematically from the experimental

functions. They are of interest for two principal reasons:

They make certain relationships between characteristic

functions easier to handle. They also will eventually

permit the description of the molecular phenomena. A

spectral distribution function can be expressed as:

$$F(t) = \int_{0}^{\infty} H(\tau)f(t,\tau)d\tau \qquad (2.33)$$

where H would be the spectrum related to the function F.

The kernel $f(t,\tau)$ could be any function. Often by

analogy with the mechanical models it is either $f(t,\tau) =$

$e^{-t/\tau}$ or $f(t,\tau) = \dfrac{e^{-t/\tau}}{\tau}$. Different authors use different

definitions. The spectrum $H(t)$ can be continuous or

discontinuous.

On a natural scale, the spectrum is defined as [22]:

$$E_r(t) = E_{\infty} + \int_{0}^{\infty} H_n(\tau) e^{-t/\tau} d\tau \qquad (2.34)$$

where $H_n(t)$ is the relaxation spectrum corresponding
to the relaxation function $E_r(t)$. This expression can be
written as:

$$E_r(t) = E_\infty + L[H_n(\tau)] \qquad (2.35)$$

which leads to Stieltjes integral equations as:

$$\overline{E}_r(p) = E_\infty + \int_0^\infty \frac{H_n(\tau)}{\tau+p} \, d\tau \qquad (2.36)$$

The spectra, however, are generally defined on a logarithmic
scale such that:

$$D_c(t) = D_0 + \int_0^\infty L(\tau)(1-e^{-t/\tau})d(\ln\tau) + \frac{t}{\eta}$$

$$\qquad (2.37)$$

$$E_r(t) = E_\infty + \int_0^\infty H(\tau) \, e^{-t/\tau} \, d(\ln\tau)$$

where $L(\tau)$ and $H(\tau)$ are also respectively the retar-
dation and relaxation distribution functions. This defini-
tion will be retained for the remainder of this presentation.
It is useful to note that these two definitions of distri-
bution functions are related:

$$H(\tau) = \tau H_n(\tau)$$

$$\qquad (2.38)$$

$$L(\tau) = \tau L_n(\tau)$$

Similarly, if one wants to use logarithmic time to the base 10 [6]:

$$H(\log_{10}\tau) = 2.303\ H(\ell n\tau) = 2.303\ \tau\ H_n(\tau)$$

$$ (2.39) $$

$$L(\log_{10}\tau) = 2.303\ L(\ell n\tau) = 2.303\ \tau\ L_n(\tau)$$

where the definitions of H and L are in terms of logarithms to the base 10, in terms of natural logarithms and in terms of linear time, respectively.

The dynamic functions are also related to the spectral representation as defined in equations 2.37, by Stieltjes integral equations [45]. Thus the components of the relaxation complex modulus are:

$$E_1(\omega) = E_\infty + \int_o^\infty \frac{H(\tau)\omega^2\tau^2}{1 + \omega^2\tau^2}\ d(\ell n\tau)$$

$$ (2.40) $$

$$E_2(\omega) = \int_o^\infty \frac{\omega\tau}{1+\omega^2\tau^2}\ H(\tau)\ d(\ell n\tau)$$

Through change of variables these expressions can be transformed into convolution integrals, which are sometimes easier to solve.

Letting

$$\alpha = \ell n(\tau/\tau_o)$$

$$\beta = \ell n(\omega\tau_o)$$

$$\phi(\alpha) = H(\tau)/\tau$$

and $\qquad \tau = \tau_o e^{\alpha}$ where τ_o is arbitrary, yields

$$E_1(\beta) = \frac{1}{2} \int_{-\infty}^{+\infty} \phi(\alpha)[1 + \tanh (\alpha-\beta)] \, d\alpha$$

$$(2.41)$$

$$E_2(\beta) = \frac{1}{2} \int_{-\infty}^{+\infty} \phi(\alpha) \operatorname{sech} (\beta-\alpha) \, d\alpha$$

Similar expressions can be derived for the creep functions. Fuoss and Kirkwood [21] derived exact inverse relationships to obtain the spectral distributions from the components of the complex functions.

$$H(\tau = \frac{1}{\omega}) = \pm\frac{1}{\pi} \lim_{\epsilon \to 0} \operatorname{Im}(-\omega \pm i\epsilon) = \pm\frac{1}{\pi} \operatorname{Im} E^*(\omega e^{\pm i\pi}) \qquad (2.42)$$

These equations are also discussed in Reference [17] and [22]. The relations relating directly the two spectral distributions and all the remaining interrelationships are summarized in Tables 1 and 2.

Effect of Temperature: The constitutive equations of materials are in general functions of temperature. In general the effect of temperature on the properties of materials is quite involved. In special cases, however, the well-known time-temperature superposition principle may be

TABLE 1

DIAGRAM OF MATHEMATICAL RELATIONSHIP
OF THE CHARACTERISTIC FUNCTIONS
(After B. Gross)
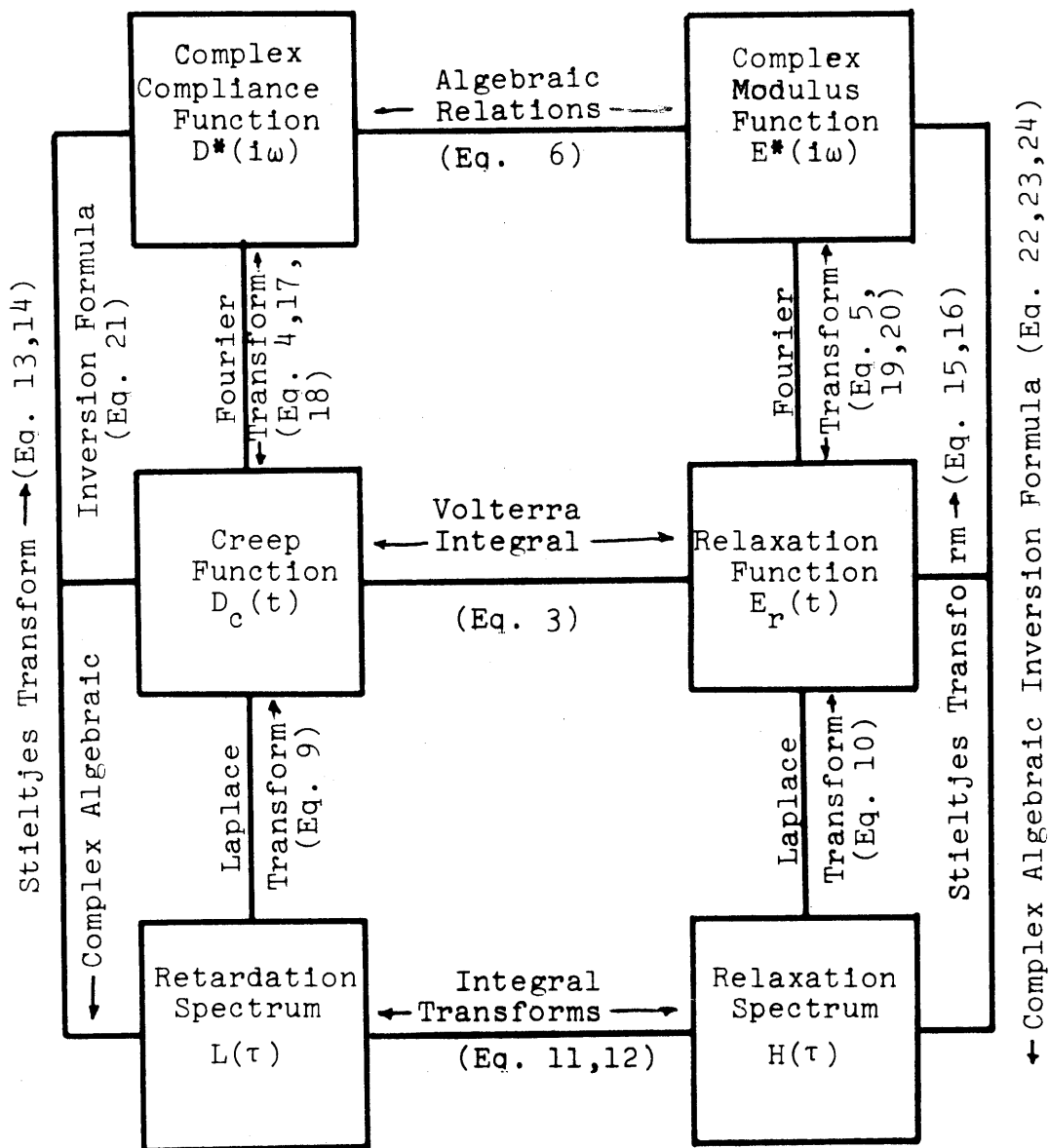
Note: The equations are summarized in Table 2.

TABLE 2

A Summary of the Transformations

Applied in Linear Viscoelasticity

$$D_c(t) = \frac{\varepsilon(t)}{\sigma_o h(t)} \qquad (1)$$

$$E_r(t) = \frac{\sigma(t)}{\varepsilon_o h(t)} \qquad (2)$$

$$\text{where} \quad h(t) = \begin{cases} 0 & t < 0 \\ 1 & t \geq 0 \end{cases}$$

$$\int_o^t E_r(\tau) D_c(t-\tau) d\tau = t \qquad (3)$$

$$D^*(i\omega) = i\omega \int_o^\infty D_c(t) e^{-i\omega t} dt \qquad (4)$$

$$E^*(i\omega) = i\omega \int_o^\infty E_r(t) e^{-i\omega t} dt \qquad (5)$$

$$E^*(i\omega) D^*(i\omega) = 1 \qquad (6)$$

TABLE 2 (Continued)

$$D^*(i\omega) = D_1(\omega) + iD_2(\omega) \tag{7}$$

$$E^*(i\omega) = E_1(\omega) + iE_2(\omega) \tag{8}$$

$$D_c(t) = \int_0^\infty L(\tau)(1 - e^{-t/\tau})\frac{d\tau}{\tau} + D_0 + \frac{t}{\eta} \tag{9}$$

$$E_r(t) = \int_0^\infty H(\tau)e^{-t/\tau} \frac{d\tau}{\tau} + E_\infty \tag{10}$$

$$L(\tau) = \frac{H(\tau)}{[E_\infty - \int_0^\infty \frac{H(u)}{(\frac{u}{\tau}-1)} d(\ln u)]^2 + \pi^2 H^2(\tau)]} \tag{11}$$

$$H(\tau) = \frac{L(\tau)}{[D_0 + \int_0^\infty \frac{L(u)}{(1-\frac{u}{\tau})} d(\ln u)-\frac{\tau}{\eta}]^2 + \pi^2 L^2(\tau)} \tag{12}$$

$$D_1(\omega) = D_0 + \int_0^\infty \frac{L(\tau)}{1+\omega^2\tau^2} d(\ln\tau) \tag{13}$$

$$D_2(\omega) = \int_0^\infty \frac{\omega\tau}{1+\omega^2\tau^2} L(\tau) d(\ln(\tau)) + \frac{1}{\omega\eta} \tag{14}$$

TABLE 2 (Continued)

$$E_1(\omega) = E_\infty + \int_0^\infty \frac{H(\tau)\omega^2\tau^2}{1+\omega^2\tau^2} \, d(\ln\tau) \qquad (15)$$

$$E_2(\omega) = \int_0^\infty \frac{\omega\tau}{1+\omega^2\tau^2} H(\tau) \, d(\ln\tau) \qquad (16)$$

$$D_c(t) = D_0 + \frac{2}{\pi} \int_0^\infty [(D_1(\omega) - D_0)/\omega] \sin \omega t \, d\omega + \frac{t}{\eta} \qquad (17)$$

$$D_c(t) = D_0 + \frac{2}{\pi} \int_0^\infty [D_2(\omega)/\omega - 1/\omega^2\eta](1 - \cos \omega t) \, d\omega + \frac{t}{\eta} \qquad (18)$$

$$E_r(t) = E_\infty + \frac{2}{\pi} \int_0^\infty [(E_1(\omega) - E_\infty)/\omega] \sin \omega t \, d\omega \qquad (19)$$

$$E_r(t) = E_\infty + \frac{2}{\pi} \int_0^\infty [E_2(\omega)/\omega] \cos \omega t \, d\omega \qquad (20)$$

$$L_{(\tau=\frac{1}{\omega})} = \pm \frac{1}{\pi} \lim_{\varepsilon \to 0} \text{Im } D^* (-\omega \mp i\varepsilon) = \pm \frac{1}{\pi} \text{Im } D^* (\omega e^{\mp i\pi}) \qquad (21)$$

$$H_{(\tau=\frac{1}{\omega})} = \pm \frac{1}{\pi} \lim_{\varepsilon \to 0} \text{Im } E^* (-\omega \pm i\varepsilon) = \pm \frac{1}{\pi} \text{Im } E^* (\omega e^{\pm i\pi}) \qquad (22)$$

TABLE 2 (Continued)

$$H_{(\tau = \frac{1}{\omega})} = \pm \frac{2}{\pi} \lim_{\epsilon \to 0} \mathrm{Im}\ E_1\ (\epsilon \pm i\omega) = \pm \frac{2}{\pi} \mathrm{Im}\ E_1\ (\omega e^{\pm i\pi/2}) \qquad (23)$$

$$H_{(\tau = \frac{1}{\omega})} = \frac{2}{\pi} \lim_{\epsilon \to 0} \mathrm{Re}\ E_2\ (\epsilon \pm i\omega) = \frac{2}{\pi} \mathrm{Re}\ E_2\ (\omega e^{\pm i\pi/2}) \qquad (24)$$

used to account for the effect of temperature. This principle was found experimentally and proposed by Leaderman [28] and Tobolsky and Andrews [50]. It simply states that the viscoelastic functions obtained at different temperatures can be derived one from the other by two consecutive shifts on a log-log plot. If one has $E(T)$ and wants to get $E(T_o)$, one has to use a vertical shift first by plotting $\frac{\rho_o T_o}{\rho T} E(T)$. This corresponds to the fact that an increase in temperature brings about corresponding increases in entropy and modulus. A horizontal shift log a_T is then made. This shift corresponds to an acceleration of the relaxation or retardation process due to an increase of temperature. The shift factor has been related to the activation energy ΔE_A of polymeric materials;

$$a_T = e^{\frac{\Delta Ea}{R} \left(\frac{1}{T} - \frac{1}{T_o}\right)} \qquad (2.43)$$

which in the case of a multiphase system is difficult to evaluate. For unfilled elastomeric systems an empirical equation due to Williams, Landel, and Ferry known as the WLF equation gives the value of a_T [54]. The application of the time-temperature superposition principle yields plots which, in terms of the reduced variables, are independent of the temperature. The reduced variables are;

$$\frac{\rho_o T_o}{\rho T} E_r(t), \quad \frac{\rho T}{\rho_o T_o} D_c(t), \quad \text{and} \quad t^* = \frac{t}{a_T}.$$

The shift factor a_T may be determined experimentally by measuring the amount of shift necessary to superpose experimental curves on a log-log plot. This principle of time-temperature superposition can be applied when the curves superpose exactly, and the plot of a_T vs. temperature is a smooth curve. The material obeying such principle is called thermorheologically simple. Schwarzl and Staverman [44] show that materials are thermorheologically simple if either they do not exhibit Newtonian flow, or their long term viscosity has the same temperature dependency as the remaining part of the creep function. The shift procedure is also shown to apply to the spectral distribution functions when they are defined on a logarithmic scale.

The complete characterization of linear viscoelastic materials, becomes rather straightforward once the time-temperature superposition principle is applicable. To determine the viscoelastic functions for very short times, many difficulties arise. One is the limitation of the recording apparatus; another is the introduction of inertia effects, which will produce vibrations whenever the loading or the straining is very fast. Hence the loading time is finite while the transient functions were defined mathematically with a Heaviside step function. Consequently the mechanical response observed will be mathematically inaccurate for about 10 times the loading time.

At long times, due to experimental inconvenience, the experimental data are limited. Since the viscoelastic behavior is essentially exponential and may cover more than 10 decades of time, the time limitation can be quite serious.

Similarly, dynamic tests are limited to narrow ranges of frequencies because of apparatus limitations. The time-temperature superposition can be used to assist in establishing the behavior of the material at above instances.

Extension to Three-Dimensional Cases:

For the three-dimensional case the relations discussed above are still valid in form, but the scalar functions are replaced by tensors.

$$[\sigma(t)] = \int_o^t F(t-t')[\epsilon(t')]\, dt' \qquad (2.44)$$

In this expression $F(t-t')$ is a linear transformation of the space of symmetric tensors into itself [15]. This representation and similar expressions can be extended immediately from the one-dimensional theory. The mathematical foundation of the theory was laid recently through axiomatization of the principles [15,23,52]. Coleman and Noll [15] based their derivation on macroscopic assumptions about

the mechanical behavior of materials with memory. They

treated the general case of finite linear viscoelasticity

for anisotropic materials. Biot [9] applied the methods

of Lagrangian mechanics for a network of interconnected

springs and dashpots and obtained the constitutive equations

in the form of differential operators. Khazanovitch [26]

derived the general constitutive equation of linear visco-

elastic materials under the form of hereditary functions

from the general principle of statistical physics, similar

to the derivation of the laws of viscous flow from statis-

tical considerations. In all these derivations the consti-

tutive equations separate explicitly a time independent

transformation (elastic) from a time dependent one. This

separation corresponds to a general case where the time-

dependent and time-independent behavior of the material

has two different microstructural explanations. Thus two

different anisotropies can coexist. The time-independent

transformation is either the reaction at the origin of

time [9, 26], or the equilibrium condition for large

times [15]. For the case of isotropic materials all these

derivations show that only two functions are needed over

the whole viscoelastic range if the time-independent

transformation can be included as discontinuity functions

with the time dependent transformation.

Hilton [24] used mechanical models to define a three-

dimensional characterization of materials in differential operator form.

Gurtin and Sternberg [23] have given a mathematical development of the viscoelastic theory based upon the hypothesis of hereditary expressions. They gave the mathematical proofs to relations accepted intuitively. They also showed that the functions required for the case of isotropy reduce to two; the functions in shear and in isotropic deformation. The implication of two different functions means that the molecular explanation in the two modes of deformation is different. Often the materials are assumed to be incompressible and there is only one function left to be determined.

Thus, by analogy with the elastic theory, stresses and strains can be separated into deviatoric and volumetric components or simple shear and bulk compression [48,49]. All the expressions developed for the case of uniaxial loading can be repeated for three dimensional case. The main relationships would be:

$$\epsilon_{ij} = \frac{\delta_{ij}}{3} \int_o^t B(t-\tau) \frac{d\sigma_{ij}(\tau)}{d\tau} d\tau + \frac{1}{2} \int_o^t J(t-\tau) \frac{dS_{ij}}{d\tau} d\tau$$

$$(2.45)$$

$$\sigma_{ij} = 3\delta_{ij} \int_o^t K(t-\tau) \frac{d\epsilon_{ij}(\tau)}{d\tau} + 2 \int_o^t G(t-\tau) \frac{de_{ij}}{d\tau} d\tau$$

or, for the normal components of a one-dimensional case:

$$\sigma_{ii}(t) = \int_0^t E(t-\tau)\frac{d\varepsilon_{ii}(\tau)}{d\tau}\,d\tau$$

$$\varepsilon_{ii}(t) = \int_0^t D(t-\tau)\frac{d\sigma_{ii}(\tau)}{d\tau}\,d\tau$$

(2.46)

The deviatoric components would be:

$$S_{ij}(t) = 2\int_0^t G(t-\tau)\frac{de_{ij}(\tau)}{d\tau}\,d\tau$$

$$e_{ij}(t) = \int_0^t J(t-\tau)\frac{dS_{ij}(\tau)}{d\tau}\,d\tau$$

(2.47)

and the mean hydrostatic pressure and volumetric deformation would be:

$$\sigma_{ii}(t) = 3\int_0^t K(t-\tau)\frac{d\varepsilon_{ii}(\tau)}{d\tau}\,d\tau$$

$$\varepsilon_{ii}(t) = \frac{1}{3}\int_0^t B(t-\tau)\frac{d\sigma_{ii}(\tau)}{d\tau}\,d\tau$$

(2.48)

where

$$\sigma_{ii}(t) = \sum_i \sigma_{ii}(t) \qquad\qquad \varepsilon_{ii}(t) = \sum_i \varepsilon_{ii}(t)$$

$$S_{ij}(t) = \sigma_{ij}(t) - \frac{1}{3}\sigma_{ii}(t) \qquad e_{ij}(t) = \varepsilon_{ij}(t) - \frac{1}{3}\varepsilon_{ii}(t)$$

$E(t)$, $G(t)$, $K(t)$ are the uniaxial, shear and bulk moduli,

while $D(t)$, $J(t)$ and $B(t)$ are the corresponding compliances. These two groups are related through convolution integrals:

$$\int_0^t E(t-\tau)\, D(\tau)\, d\tau = t$$

$$\int_0^t G(t-\tau)\, J(\tau)\, d\tau = t \qquad (2.49)$$

$$\int_0^t K(t-\tau)\, B(\tau)\, d\tau = t$$

which can be obtained by combining the preceding equations, and lead to the following inequalities [55]:

$$E(t)\, D(t) \leqslant 1$$

$$G(t)\, J(t) \leqslant 1 \qquad (2.50)$$

$$K(t)\, B(t) \leqslant 1$$

The similitude with elasticity brings also the definition of viscoelastic Poisson's ratio [48] for

$$\varepsilon_x(t) = \varepsilon_0 h(t) \qquad \nu_r(t) = \frac{-\varepsilon_y(t)}{\varepsilon_x(t)}$$

and for $\hspace{8cm} (2.51)$

$$\sigma_x(t) = \sigma_0 h(t) \qquad \nu_c(t) = \frac{-\varepsilon_y(t)}{D_0(t)\sigma_x(t)}$$

These equations can be written as an integral form:

$$-\varepsilon_y(t) = \int_0^t \nu_r(t-\tau)\frac{d\varepsilon_x(\tau)}{d\tau}\ d\tau = \int_0^t \nu_c(t-\tau)D_0(t-\tau)\frac{d\sigma_x(\tau)}{d\tau}\ d\tau$$

$$(2.52)$$

thus yielding:

$$\int_0^t \nu_r(t-\tau)\nu_c^{-1}(\tau)\ d\tau = 1 \qquad (2.53)$$

Through combinations of the preceding equations, Volterra equations of the second kind can be obtained [49]. These equations establish relations similar to those obtained in elasticity. They can be obtained more easily through the Laplace images of the different functions, since the different well-known elastic relationships yield algebraic relations in Laplace domain. Table 3 lists some of the relations derived by Theocaris [49]. When temperature variation occurs, the constitutive equations are affected as for the one-dimensional case. However, for the volumetric deformation tensors, strains due to thermal expansion are to be added to the relation [24].

TABLE 3

THREE-DIMENSIONAL RELATIONSHIPS

$$D(t) = \frac{J(t)}{3} + \frac{B(t)}{9} \qquad (2.54)$$

$$D(t) = \frac{J_o}{2[1+\nu_c(t)]} + \frac{1}{2} \int_o^t \frac{1}{[1+\nu_c(\tau)]} \frac{dJ(t-\tau)}{d\tau} d\tau \qquad (2.55)$$

$$D(t) = \frac{B_o}{6[\frac{1}{2} - \nu_c(\tau)]} + \frac{1}{6} \int_o^t \frac{1}{[\frac{1}{2} - \nu_c(\tau)]} \frac{dB(t-\tau)}{d\tau} d\tau \qquad (2.56)$$

$$B(t) = 3D(t)[1-2\nu_o] - 6 \int_o^t \frac{d\nu_c(t-\tau)}{d\tau} D(\tau)d\tau \qquad (2.57)$$

$$J(t) = 2D(t)[1+\nu_o] + 2 \int_o^t \frac{d\nu_c(t-\tau)}{d\tau} D(\tau)d\tau \qquad (2.58)$$

$$E(t) = 3K(t)[1-2\nu_o] - 6 \int_o^t \frac{d\nu_r(t-\tau)}{d\tau} K(\tau)d\tau \qquad (2.59)$$

$$E(t) = 2G(t)[1+\nu_o] + 2 \int_o^t \frac{d\nu_r(t-\tau)}{d\tau} G(\tau)d\tau \qquad (2.60)$$

TABLE 3 (Continued)

$$\nu_c(t) = [\frac{J_o}{2D(t)} - 1] + \frac{1}{2} \int_o^t \frac{dJ(t-\tau)}{d\tau} \frac{d\tau}{D(\tau)} \qquad (2.61)$$

$$\nu_c(t) = \frac{1}{2} [1 - \frac{B_o}{3D(t)}] + \frac{1}{6} \int_o^t \frac{dB(t-\tau)}{d\tau} \frac{d\tau}{D(\tau)} \qquad (2.62)$$

$$\nu_r(t) = [\frac{E_o}{2G(t)} - 1] + \frac{1}{2} \int_o^t \frac{dE(t-\tau)}{d\tau} \frac{d\tau}{G(\tau)} \qquad (2.63)$$

$$\nu_r(t) = \frac{1}{2} [1 - \frac{E_o}{3K(t)}] - \frac{1}{6} \int_o^t \frac{dE(t-\tau)}{d\tau} \frac{d\tau}{K(\tau)} \qquad (2.64)$$

III. METHODS OF APPLICATION

OF THE THEORY

The mechanical response of a material to different
programs of loading or deformation can be analyzed in
terms of either the transient or the complex functions as
defined in the preceding section. The simplest programs
of deformation (or load) are the static tests, the constant
rate of strain (or stress) tests, and the sinusoidal
strain (or stress). In the case of static tests, strains
(or stresses) are applied instantaneously and maintained
throughout the test and stresses (or strains) are
measured. These tests give directly the transient charac-
teristic functions. The results of these tests are limited
to a certain range of time. Short time results are
inaccurate and long time results are limited by experimental
practicality. These tests can simultaneously give the
relaxation moduli (or creep compliances) in two mutually
perpendicular directions by making two measurements in those
directions. Shear or bulk modulus (or compliance) can also
be measured directly.

Transient functions can be determined easily from
constant rate of strain (or stress) tests. Assuming

$\varepsilon(t) = Rt$; where R is the constant rate of strain and using a Laplace transform, it can be shown that [54]:

$$[\frac{d\sigma(t)}{d\varepsilon}]_{\varepsilon=Rt} = E_r(t) \qquad (3.1)$$

This means that the slope of a stress-strain curve is equal to the relaxation modulus. The limitations of this test are; a) the determination of slopes from experimental curves is highly inaccurate and, b) the range of time for which the modulus is determined is generally limited. To extend the time range one should use a large number of tests with different strain rates. This test can be used in conjuntion with a relaxation test and can allow the determination of the relaxation modulus during the short times. Similarly, for the case of a constant rate of loading tests it can be shown that [45]:

$$[\frac{d\varepsilon}{d\sigma}]_{\sigma=Rt} = [D(t) + \frac{t}{\eta}] \qquad (3.2)$$

The third common type of test uses a cyclic deformation or loading, usually a sinusoidal function. The complex functions are then determined directly by measuring the phase lag between the excitation and the mechanical response, and the ratio between their peak values. To

obtain the response of material at short and long testing times, the dynamic tests are generally performed over a wide range of frequency. The limitations arise from the experimental difficulty to produce a wide range of frequencies with the same apparatus.

In the case of a thermorheologically simple material, different temperatures can be used to extend the experimental functions by the application of the time-temperature shift procedure.

The characteristic functions determined experimentally can then be transformed to derive the other functions by using the equations of linear viscoelasticity. Detailed reviews of the characterization procedures can be found in References [12] and [39]. The latter also lists the available computer programs for characterization of viscoelastic materials. The following is a brief description of the different methods of characterization. First, methods of solution for the exact interrelationships between viscoelastic functions are presented. Then the approximate relationships are summarized.

Analytical Fittings:

Different analytical expressions can be used to represent the experimental data and make the viscoelastic interrelationships readily usable. The polynomial repre-

sentations used for such expressions include Legendre,
Chebycheff and Laguerre polynomials [16, 38]. These
polynomial representations have been used to obtain the
inversion of Laplace transforms of viscoelastic functions.

Fourier series have also been applied to solve
convolution type integrals [40]:

$$f(s) = \int_{-\infty}^{+\infty} K(s-t) \, g(t) \, dt \qquad (3.3)$$

where the unknown is $g(t)$. The eigenvalues of $K(s-t)$
are first computed:

$$\frac{1}{\lambda(\nu)} = \int_{-\infty}^{+\infty} K(\zeta) \, \exp(i\nu\zeta) \, d\zeta \qquad (3.4)$$

and equation (3.3) is then solved.

The most widely used methods of representation are
those based on Dirichlet or Prony series. These series of
exponential expansions are directly based upon the mechani-
cal model representations and they often provide a satis-
factory approximation of the mechanical behavior.

Alfrey [4] and Bland [10] have suggested various
techniques for representing the experimental curves by such
series. When the spectra of real materials are broad and
cover many decades of time the exponential series representa-

tion of viscoelastic functions may result in unrealistic description of the materials. There are two methods commonly used to determine the appropriate Dirichlet series representation of a viscoelastic function. One is suggested by Tobolsky [51] and the other is proposed by Schapery [42].

Tobolsky's Graphical Procedure: This method is basically a graphical technique whereby the creep or the relaxation functions are expressed as:

$$E(t) = E_\infty + E_1 e^{-t/\tau_1} + \ldots + E_n e^{-t/\tau_n} \qquad (3.5)$$

The graphical procedure will determine E_1 and τ_1 from a semi-logarithmic plot. If the plot of log $(E(t) - E_\infty)$ vs. t is extended to large enough times t, the curve can be approximated by a straight line. τ_n is the negative slope of this line divided by 2.303 and E_n is obtained from the intercept of this line with $t = 0$.

The next step is to plot the difference between this line and the original curve in the same manner on a semi-logarithmic plot. This plot will give E_{n-1} and τ_{n-1}. The procedure is repeated until the remaining difference can be completely represented by a straight line. This procedure gives a good approximation to the experimental

curve and has the "advantage" of giving a mechanical model that permits the visualization of the mechanical behavior of the material.

Schapery's Procedure: This procedure obtains a set of linear equations by arbitrarily choosing the exponents τ_i.

$$E(t) = E_\infty + \sum_{i=1}^{n} E_i e^{-t/\tau_i}$$

or   (3.6)

$$D(t) = D_\infty + \sum_{i=1}^{n} D_i e^{-t/\tau_i}$$

Taking n experimental points:

$$[E(t_j) = E_\infty + \sum_{i=1}^{n} E_i e^{-t_j/\tau_i}]_{\text{for } 1 \leqslant j \leqslant n}$$ (3.7)

τ_i is assumed to be equal to $2t_i$. This technique not only allows one to express the viscoelastic characteristic functions of a material in an analytical form, but it also provides an excellent means to establish the relationships which exist among the various viscoelastic functions of a material. The number of terms in Schapery's method is chosen approximately equal to the number of decades of time where the curves have a significant slope. Increasing the

-52-

number of terms will result in an oscillation of the
fitted curve around the experimental data. This is because
some of the terms of the series become of opposite sign.
These terms of opposite signs are not basically wrong, but
they have a difficult mechanical and physical interpretation.
They could be represented by elements in Voigt or Maxwell
generalized models, which are in tension when all the other
elements are in compression, or vice versa.

Least Squares Fitting Procedure: Schapery's procedure
can be changed into a least squares fitting technique if
the data is not very smooth or if more experimental data
are to be included while keeping the number of terms in the
series constant, so as to avoid excessive oscillations.
This can be done by determining the coefficients of the series

$$E(t) = E_{\infty} + \sum_{i=1}^{n} E_i \, e^{-t/\tau i} \qquad (3.8)$$

while τ_i are chosen arbitrarily. If there are m experi-
mental data points; (E_j, t_j) for $1 \leqslant j \leqslant m$ and $m \geqslant n$
the total square error will be:

$$(\Delta E)^2 = \sum_{j=1}^{m} [E(t_j) - \sum_{i=1}^{n} E_i e^{-t_j/\tau i}]$$

Minimizing the square error with respect to the coefficients E_i.

$$\frac{d(\Delta E)^2}{dE_i} = 2 \sum_{j=1}^{m} [E(t_j) - \sum_{i=1}^{n} E_i e^{-t_j/\tau_i}][-e^{-t_j/\tau_i}] = 0$$

This is a set of n linear equations with n unknowns:

$$\sum_{j=1}^{m} E(t_j) = \sum_{i=1}^{n} X_i \left(\sum_{j=1}^{m} e^{-t_j/\tau_i} \right) \tag{3.9}$$

For the creep curves the procedure is identical, but the coefficients D_i will be negative. One way to obtain a more accurate representation of the creep, for t approaching zero, is to modify slightly the equation by writing:

$$D(t) = D_o + \sum_{i=1}^{n} D_i(1-e^{-t/\tau_i}) \tag{3.10}$$

In this form the value of D(t) does not appear as a difference of two large numbers for $t \to 0$.

Application of the Dirichlet Series: The series of expo-
nential expansions are very convenient to apply to some interconversion equations. Laplace transforms and the complex functions are readily available for these expressions.

Gross [22] also shows that the coefficients of the series have the meaning of a discrete spectral representation.

Brisbane [11] suggested the use of these series representations for the correction of experimental data obtained for short times. In an actual experiment the application of load or deformation cannot be instantaneous. To account for this delay in loading or deformation of the specimens, a correction should be made in the measured data. This correction, in case of the relaxation modulus, is based on the assumption that the relaxation modulus of the material can be expressed in a Dirichlet series:

$$E(t) = E_\infty + \sum_{i=1}^{n} E_i \, e^{-\alpha_i t}$$

When such a material is subjected to a stress relaxation test, the deformation being applied at a constant rate of strain R, the stress S(t) will also be given as a Dirichlet series:

$$S(t) = S_\infty + \sum_{i=1}^{n} S_i \, e^{-\alpha_i t}$$

The coefficients of the two series are related. When the origin of time is taken at the end of the loading, an accurate fitting series can be obtained for S(t), and the

relationships between the coefficients of the series are:

$$E_i = \frac{-S_i \alpha_i e^{\alpha_i t_o}}{R[1-e^{\alpha_i t_o}]} \qquad (3.11)$$

and $\qquad E_\infty = S_\infty / Rt_o$

where $\qquad t_o$ = loading time.

Use of this technique will provide a more accurate representation of relaxation data, especially for times or temperatures where the material is sensitive to loading.

Numerical Integration of Convolution Integrals:

The creep and relaxation functions of a linear visco-elastic material are related to each other by a Riemann Convolution integral which in general form can be written as:

$$g(t) = \int_o^t \phi(t-\tau)\psi(\tau)\,d\tau \qquad (3.12)$$

Hopkins and Hamming [25] suggested in 1957 a numerical method to integrate this integral equation. The solution assumes that $g(t)$ and $\psi(t)$ are known functions and $\phi(t)$ is unknown. $\psi(t)$ and $g(t)$ are furthermore assumed to be known only at discrete points. The procedure to obtain $\psi(t)$ is as follows:

-56-

Introducing the integral $\psi(t)$

$$f(t) = \int_0^t \psi(t) \, d\tau$$

gives $f(0) = 0$ and $\frac{df(t)}{dt} = \psi(t)$.

The time interval is then divided into n intervals t_i ($i=0\ldots n$) which can be arbitrarily small. Equation (3.12) can be written then as:

$$g(t_{n+1}) = \int_0^{t_{n+1}} \phi(\tau)\psi(t_{n+1}-\tau) \, d\tau$$

$$g(t_{n+1}) = \sum_{i=0}^{n} \int_{t_i}^{t_{i+1}} \phi(\tau) \, \psi(t_{n+1}-\tau) \, d\tau$$

To calculate the integrals, the trapezoidal rule of integration is then applied:

$$\int_{t_i}^{t_{i+1}} \phi(\tau)\psi(t_{n+1}-\tau)d\tau = \phi(t_{n+1/2})\int_{t_i}^{t_{i+1}} \psi(t_{n+1}-\tau) \, d\tau$$

$$= -\phi(t_{i+1/2}) \, [f(t_{n+1}-t_{i+1}) - f(t_{n+1}-t_i)]$$

Then the sum becomes:

$$g(t_{n+1}) = -\sum_{i=0}^{n-1} \phi(t_{i+1/2})[f(t_{n+1}-t_{i+1}) - f(t_{n+1}-t_i)]$$

$$+ \phi(t_{n+1/2}) \, f(t_{n+1}-t_n)$$

This can be written as:

$$\phi(t_{n+1/2}) = \frac{g(t_{n+1}) - \sum_{i=0}^{n-1} \phi(t_{i+1/2})[f(t_{n+1}-t_i) - f(t_{n+1}-t_{i+1})]}{f(t_{n+1}-t_n)}$$

(3.13)

Thus the function $\phi(t)$ can be computed point by point by recurrence, the first value being:

$$\phi(t_{1/2}) = \frac{g(t_1)}{f(t_1)} \quad .$$

Hopkins and Hamming demonstrated that this finite difference integration is stable and that the effect of errors introduced at different times dies out rapidly in subsequent stages of the computation.

This finite difference procedure was used by Hopkins and Hamming [25] to solve the Volterra integral equation of the first kind relating creep and relaxation. It was also used by Lee and Rogers [30] to solve a particular problem in viscoelastic stress analysis, leading to a convolution type integral.

Theocaris [48, 49] in the so-called indirect method uses a similar procedure to solve Volterra's integral equation of the second kind. He shows that for a cross-linked polymer, all transient functions can be determined

-58-

to a good approximation, if only one of them is known along the whole viscoelastic range and another function is known for initial condition.

For example assuming that $D(t)$, the creep function, and initial value of $\nu_c(0)$, Poisson's ratio, or $B(0)$, bulk modulus, are known, Theocaris [48] by applying the finite difference procedure to equations (2.57) and (2.62) finds:

$$B(t_{n+1}) = 3[D(t_n) - 2D_0\nu_c(t_n)] - 6\nu_c(t_n) \sum_{i=1}^{n} [D(t_{n+1}-t_{i+1}) -$$

$$D(t_{n+1}-t_i)] \qquad (3.14)$$

and

$$\nu_c(t_{n+1}) = \frac{1}{2}[1 - \frac{B(t_n)}{3D_0}] - \frac{B(t_n)}{6} \sum_{i=1}^{n} [D(t_{n+1}-t_{i+1}) -$$

$$D(t_{n+1}-t_i)]^{-1} \qquad (3.15)$$

where $D_0 = D(t_1)$, $\nu_{co} = \nu_c(t_1)$ and $B_0 = B(t_1)$ are the initial values of these three functions. The integration may start either from the rubbery region and proceed back to the glassy region or the reverse. The iteration process is to use alternatively equation (3.14) and (3.15) starting at

one end of the time scale, after dividing the time scale
into arbitrarily small intervals, such that the different
functions can be approximated by a constant. Starting
from one equation or the other would yield an upper or
lower bound for the computed functions. When the number of
subintervals increases indefinitely these two values tend
to approximate the exact value of the functions. Considering
the viscoelastic range divided into n double subintervals,
Theocaris [49] derives the following expressions to yield
an upper and lower bound for B(t) and $v_c(t)$ satisfying
his assumptions:

$$[\frac{1}{2} - v_c(2n)] = \frac{D(2n-2)}{D(2n-1)} \cdot \frac{D(2n-4)}{D(2n-3)} \cdot \ldots \cdot \frac{D(2)}{D(3)} [\frac{1}{2} - v_c(2)]$$

$$B(2n) = \frac{D(2n)}{D(2n-1)} \cdot \frac{D(2n-2)}{D(2n-3)} \cdot \ldots \cdot \frac{D(2)}{D(1)} \cdot B(0)$$

(3.16)

$$[\frac{1}{2} - v_c(2n)] = \frac{D(2n-1)}{D(2n)} \cdot \frac{D(2n-3)}{D(2n-2)} \cdot \ldots \cdot \frac{D(1)}{D(2)} [\frac{1}{2} - v_c(0)]$$

$$B(2n) = \frac{D(2n-1)}{D(2n-2)} \cdot \frac{D(2n-3)}{D(2n-4)} \cdot \ldots \cdot \frac{D(3)}{D(2)} \cdot B(2)$$

And similar expressions for the relaxation functions.

The so-called indirect method is obviously an approxi-
mation which may happen to be correct just in special cases.

By introducing an arbitrary assumption concerning the derivatives of these functions, this method reduces an undetermined system of two equations with three unknown functions to a determined system. This is in fact what the finite difference method represents. A more fundamental approach could be achieved by making clearer assumptions with respect to the basic shear and volumetric functions. For example assuming the material is incompressible $(K(t) = \infty)$ or has a constant bulk modulus $(K = constant)$, or its viscoelastic bulk modulus is similar to its shear modulus $(\frac{G(t)}{G_O} = \frac{K(t)}{K_O})$. In any case the assumption made cannot be generalized but has to be tested for each particular material.

Iteration Procedures:

Roesler and Twyman [41] proposed an iteration procedure which, when it converges, can be applied to solve the Volterra integral equations:

Let
$$f(s) = \int K(s-t)\ g(t)\ dt \qquad\qquad (3.17)$$

where $f(s)$ and $K(s-t)$ are known functions. An approximation (n) of $g(t)$ will be:

$$f_{(n)}(s) = \int K(s-t)\, g_{(n)}(t)\, dt \qquad (3.18)$$

Next approximation is defined by:

$$g_{(n+1)}(t) - g_{(n)}(t) = p[f(s) - f_{(n)}(s)] \qquad (3.19)$$

where p is arbitrary. They show that the convergence
is assured if the kernel [K(s-t)] has all its eigenvalues
obtained from a Fourier expansion, of the same sign and
when p satisfies the relation $0 < p/\lambda_{min} < 2$.
Generally iteration procedures can be applied to any of the
equations when convergence can be shown.

Approximate Relationships:

Numerous approximate methods are suggested in the
literature for determining complete viscoelastic functions
of a material from the results of a limited laboratory
test. In following sections several of these methods are
briefly reviewed.

Inversion of any Transient Function to any Other: A
crude approximation based on the inequalities of equations
(2.50) are suggested for solution of Volterra integral

equations of the first kind.

$$\int_0^t D(t-\tau)\ E(\tau)\ d\tau = t$$

At very short times $t \to 0$ or at very large times $t \to \infty$ the Volterra equation may be approximated by

$$D(t)\ E(t) = 1$$

In the transition region, however, the above equality is a crude approximation to the integral equation and results in unrealistic values for the unknown function. To provide a better approximation Leaderman [28] and Aklonis and Tobolsky [1] suggested that line tangents over small portions of a master curve ($\log D_c$ or $\log E_r$ vs. $\log t$) can be approximated by straight line tangents. This approximation results in:

$$E_r(t) = \frac{\frac{\sin m\pi}{m\pi}}{D_c(t)}$$

where m is the slope of the straight line tangent to the master curve at the point $\log t$. The validity of the expression requires that $m < 1$.

Taylor [46] suggests that, instead of solving

$\int_o^t E(t-\tau)\ D(\tau)\ d\tau = t$, the Volterra equations can be
solved in an easier manner if it is written as:

$$D(t)E(0) - \int_o^t D(\tau)\ \frac{dE(t-\tau)}{d\tau}\ d\tau = 1 \qquad (3.20)$$

He also suggested that the solution would be more stable if
the flow term is removed from the creep expression. Thus
decomposing the creep function into:

$$D(t) = S(t) + Rt$$

which after substitution in equation (3.20) results in:

$$S(t)E(0) - \int_o^t S(\tau)\ \frac{dE(t-\tau)}{d\tau}\ d\tau = 1 - R \int_o^t E(\tau)\ d\tau \qquad (3.21)$$

and $\quad R = 1/ \int_o^\infty E(t)dt$

Determination of the Spectra from Transient Functions: The
exact relationship between a transient function and the
spectrum distribution function is:

$$E(t) = E_\infty + \int_o^\infty H(\tau)\ e^{-t/\tau}\ d(\ell n\tau)$$

Alfrey [4] proposed a very simple approximation for solution
of this equation. The method assumes that the intensity
function $(e^{-t/\tau})$ behaves as a step function and has a

-64-

value of 0 or 1 at $\tau = t$. By differentiation, the first order approximation is then obtained:

$$- \left. \frac{dE(t)}{d(\ln t)} \right|_{t=\tau} \cong H(\tau)$$

Thus the relaxation or retardation spectra are approximated by the slope of the transient functions. The above equation can also be solved using Laplace transformations.

Cost [16] presents a critical discussion of the different methods of approximating the inverse of a Laplace transform, which is the case for the determination of the spectra. The inversion can be done rigorously if the transient functions are analytical. For experimental functions, however, approximate procedures have to be used. A general inversion formula is that of Widder's which approximates an intensity function:

$$[t^n e^{-pt}]$$

by a Dirac function. The inverse of $\overline{f}(p) = \int_0^t f(t)e^{-pt}dt$ is then:

$$f(t) = \lim_{n \to \infty} \left[\frac{(-1)^n}{n!} p^{n+1} \frac{d^n}{dp^n} \overline{f}(p) \right]_{p=n/t} \qquad (3.22)$$

This formula is exact when n goes to infinity. So for finite values of n one can get different approximations. However, the formula involves the use of successive derivatives of an experimental function and it is difficult to obtain such derivatives accurately. This has resulted in the use of only first and second derivatives. He shows that Alfrey's rule described above is a first approximation of his expression for $n = 1$.

Ter Haar [41] in a similar manner, assumed that $(te^{-pt}]$ can be approximated by a Delta function, and proposed the following inversion equation:

$$f(t) = [pf(p)]_{p=\frac{1}{t}} \tag{3.23}$$

or

$$H(\ell n\tau) = E(\ell n\tau)$$

Schwarzl and Staverman [43] have shown that in general ter Haar's approximation can be considered as a zero order approximation:

$$L(\ell n\tau) \approx \psi_{\infty} - \psi(t) \tag{3.24}$$

and that of Alfrey is of the first order approximation:

$$L(\ell nt) \approx \frac{d\psi(t)}{d\ell nt} \qquad\qquad (3.25)$$

They then suggest an expression, of a second order approximation for the determination of spectra functions:

$$L(\ell nt) \approx \frac{d\psi(2t)}{d\ell nt} - \frac{d^2\psi(2t)}{d(\ell nt)^2}$$

or $\qquad\qquad (3.26)$

$$H(\ell nt) \approx - \frac{dE(2t)}{d\ell nt} - \frac{d^2E(2t)}{d(\ell nt)^2}$$

Ferry and Williams [18] also provide a second order approximation method which is derived from the consideration that a double logarithmic plot of the spectral functions can be approximated locally by straight lines of (-m) for relaxation and (+m) for creep such that:

$$H(\tau) = - M(m) \ E(t) \left. \frac{dlogE(t)}{dlogt} \right|_{t=\tau}$$

$$(3.27)$$

and

$$L(\tau) = M(-m) \ [D(t) - \frac{t}{\eta}] \left. \frac{dlog[D(t) - \frac{t}{\eta}]}{dlogt} \right|_{t=\tau}$$

where $M(m) = 1/\Gamma(m+1)$. The method is limited to positive values of m. The calculation is done by successive approxi-

mations. Comparing the preceding two second order approximation methods it appears that they are equivalent for their use because even though the procedure indicated by Ferry and Williams does not require the second derivative of E(t) or D(t), it requires the determination of the slope of their spectra. Moreover η has to be known for Williams-Ferry method. A completely different method is proposed by Roesler [40] where the transient functions are expanded in Fourier series and the spectra are also given in terms of Fourier series, coefficients of which are related to the first series.

Schapery [42] has proposed two methods for the inversion of a Laplace transform associated with the determination of spectra functions. His first method is similar to the methods suggested by Alfrey and by ter Haar with a slight change, which resulted from a different location used by Schapery for the approximate delta functions.

$$F(t) = [p\bar{f}(p)]_{p = \frac{0.5}{t}}$$

(3.28)

or

$$H(\tau) = - \left. \frac{dE(t)}{d\ell nt} \right|_{t = 0.5\tau}$$

The second method is based on the principle of least

squares, which gives a discrete spectral representation derived from the Dirichlet series.

Cost [16] also presents a method of inversion of Laplace transforms using Legendre polynomial expansions. Solutions obtained from this method may be unstable and may oscillate. Clauser and Knauss [14] describe the direct numerical inversion and state that Cost's solution is unstable and yields increasing oscillation if one wants to evaluate the spectra with more accuracy. They present an improved method which imposes minimization of the curvature with arbitrary constraint. The method, however, is not general and may provide severe oscillations in certain cases.

Determination of Spectra from Complex Functions: Fuoss and Kirkwood [21] and Gross [22] derived exact and simple relationships to obtain the distribution functions, given in equation (2.42) in terms of complex functions. These formulas are exact and do not require any approximation methods. The Williams-Ferry Method provides two formulas to obtain the spectral distributions from the real parts of the complex functions depending on whether m the negative slope of a doubly logarithmic plot is greater than or less than 1.

For m < 1:

$$H(\tau) = AE'(\omega) \left.\frac{d\log E'(\omega)}{d\log\omega}\right|_{\frac{1}{\omega} = \tau} \qquad (3.29)$$

where: $A = (2-m)/2\Gamma(2-\frac{m}{2})(1+\frac{m}{2})$

and for 1 < m < 2:

$$H(\tau) = A'E'(\omega) \left.\frac{2 - d\log E'(\omega)}{d\log\omega}\right|_{\frac{1}{\omega} = \tau} \qquad (3.30)$$

where: $A' = m/2\Gamma(1+\frac{m}{2})(2-\frac{m}{2})$

IV. MATERIALS AND PROCEDURE

In this section the materials used in this study are presented, and the test procedures used to determine the viscoelastic functions of sand-asphalt mixtures are discussed.

Aggregate:

The introduction of large volumes (80%) of aggregates into sand-asphalt mixtures makes the selection of the right quality of aggregate very important. It is necessary that aggregates be inert, sound, durable and well graded. Ottawa sand, used in this study, satisfies the above requirements. The gradation of sand was within the specification limits of ASTM D1663-59T for sheet asphalts as shown in Table 4. Flint powder was used as mineral fillers (passing 200 sieve).

Asphalt:

The asphalt used in this study was AC-20 grade asphalt cement coded B-3056 from the "Asphalt Institute - Bureau of Public Roads Cooperative Study of Viscosity - Graded Asphalts".

Table 4

GRADATION OF AGGREGATES

Sieve Size	ASTM Specification D1663-59T	Selected Gradation % Passing*
No. 16	85 - 100	100
30	70 - 95	75
50	45 - 75	45
100	20 - 40	26
200	9 - 20	15

* Percent of the total weight of material passing a given sieve size.

Table 5

THE RESULTS OF CONVENTIONAL TESTS ON ASPHALT

USED IN THIS STUDY

Test	
Specific Gravity 77/77°F	1.020
Ductility 77°F	250 + CM
Penetration 200gm., 60 sec., 39.9°F	30
Flash Point, Cleveland Open Cup	545°F

The results of conventional tests on this asphalt are shown in Table 5. An asphalt content of 9% by weight of aggregate was used for this study, which was within the range recommended by ASTM D1663-59T for sheet asphalt.

Preparation of Mix:

The asphalt and a pre-weighed amount of aggregate were heated separately to a uniform temperature of 325°F, along with the mixing bowl and plates from the mechanical mixer. The exact amount of heated asphalt was added to the pre-heated sand, and mixed for one minute in a mechanical mixer. The bowl was scraped and mixed for another minute. The mix was then removed from the bowl and spaded for another minute with a heated spatula to obtain uniformity. Mixtures were then wrapped and stored in a refrigerator for less than one day.

Preparation of Specimens:

A miniature Marshal Compaction Apparatus was used to fabricate the specimens from the mix. The specimens were 1.4 inches in diameter and 3 inches in length. About 170 grams of sand-asphalt mixtures were heated along with molds and collars in an oven for 15 minutes at 275°F. The mix was

then compacted under the medium compactive effort corresponding to medium traffic design category. The method of compaction used was as follows:

A predetermined weight of asphalt mixture was placed in the mold. The mixture was given one-half the number of hammer blows calculated for the amount of compaction desired, that is 25 out of 50 blows. Each blow delivered 15 foot pounds of energy. The specimen was then turned over and 25 compaction blows were given on the second end. The specimen was cooled for a short time and removed from the mold by means of a special hydraulic jack extrusion apparatus and brought to room temperature and stored in a refrigerator until ready for testing.

It was found that the above compaction procedure yields specimens that are uniform and of almost identical bulk densities.

The density of the samples used in this study was determined by weighing the specimens in air and then in water. The expression used for the bulk density of the specimens was:

$$\rho = \frac{\text{weight in air}}{\text{weight in air} - \text{weight in water}}$$

The table of densities for some of the specimens tested is given in Table 6. The average density and void content is also given in the same table.

Test Procedure:

Creep Tests: In order to conduct a static creep test, a constant axial stress was applied to the specimen and maintained for a certain period of time under a constant temperature and the deformation was continuously recorded. The creep apparatus used is shown in Figure 2.

Each specimen was brought to equilibrium at the testing temperature by placing it at least one hour prior to testing in the appropriate water bath. During the test, the temperature was maintained at desired temperature by circulating water around the specimen in a triaxial test chamber. A thermostat and a heater in the cell maintained the temperature to within .1°C of that desired. Loading was done by means of consolidation weights applied to the loading frame with a hydraulic jack. Deformation was recorded by means of an LVDT transducer (Daytronic Model 102B-600) connected to a Varian Recorder (Model G-14A-1). The amount of strain was limited to 1%. At low testing temperatures, below 0°C, ethylene-glycol was added to the circulating water to prevent freezing.

Table 6

SAMPLE DENSITIES

Sample Number	Densities	Sample Number	Densities
1	2.20	21	2.26
2	2.22	22	2.27
3	2.26	23	2.27
4	2.27	24	2.25
5	2.30	25	2.28
6	2.28	26	2.25
7	2.28	27	2.26
8	2.25	28	2.27
9	2.28	29	2.26
10	2.29	30	2.27
11	2.28	31	2.27
12	2.25	32	2.27
13	2.24	33	2.27
14	2.25	34	2.26
15	2.27	35	2.26
16	2.27	36	2.25
17	2.23	37	2.25
18	2.24	38	2.23
19	2.25	39	2.26
20	2.27	40	2.26

Average Density for the 9% Mix

ρ = 2.26

Void Content = 7%
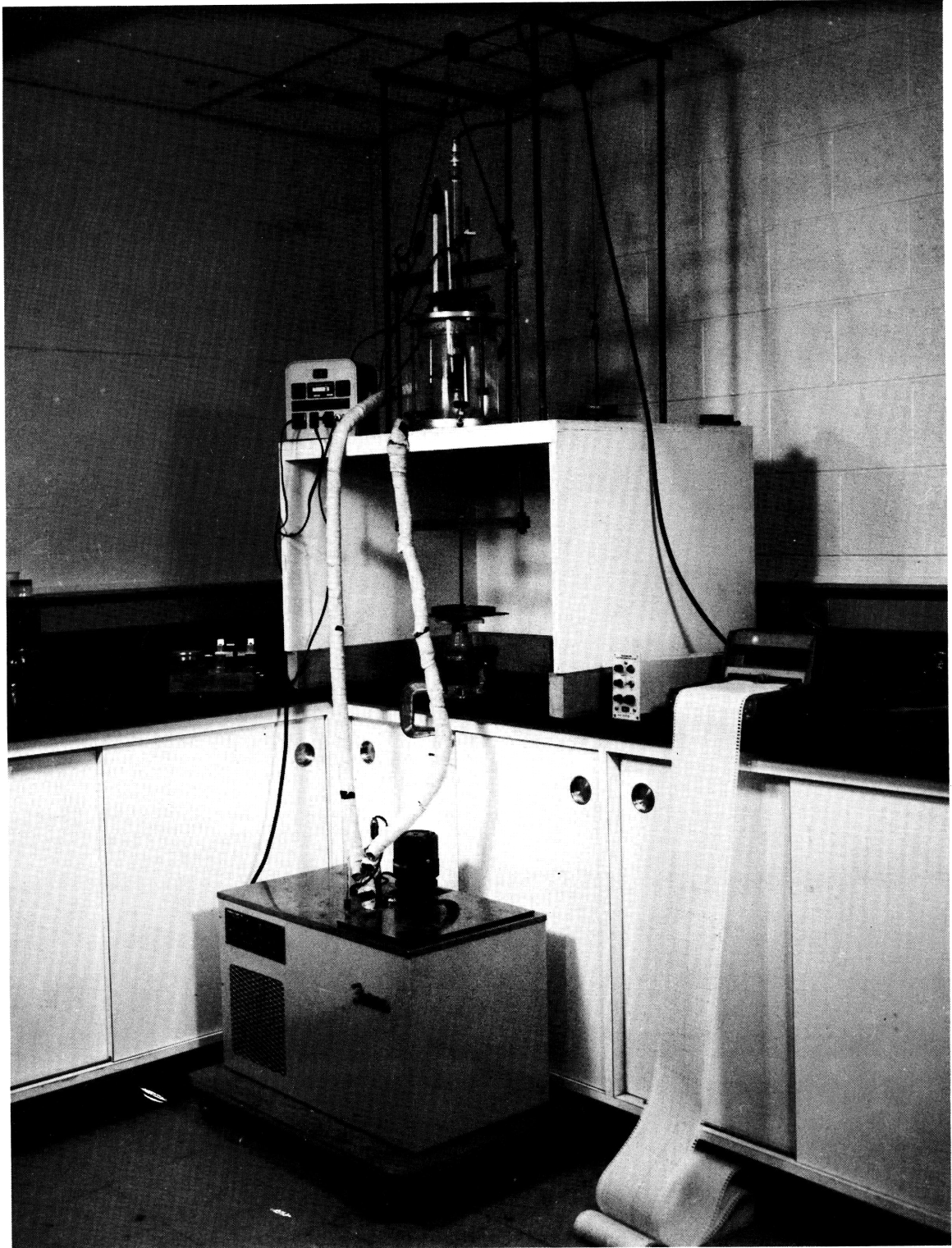
FIGURE 2. CREEP APPARATUS

The specimens were also mechanically preconditioned prior to testing. The recorder was allowed to run and the load was applied carefully and kept for ten minutes, after which the load was removed for a period of ten minutes. Each specimen was loaded and unloaded three times using the same load in order to minimize end effects and to control the uniformity of specimens. For each temperature and each stress level three identical specimens were tested.

Relaxation: Stress relaxation tests were performed by applying a predetermined strain on the compacted specimen and measuring the stress necessary to maintain this strain as a function of time. Temperature equilibrium was attained by keeping the specimens at the test temperature for at least an hour prior to testing. The actual tests were done utilizing an Instron testing machine. The fastest rise rate of the crosshead that could be applied was .2 inches/minute. This rate of deformation was used to approximate as closely as practically possible the step strain input used in an ideal relaxation test. The test cell (in which temperature was maintained) was placed directly on the crosshead of the Instron. The specimens were preconditioned by straining each sample to about .3% and letting the stress relaxation of the specimen occur for five minutes. Then the deformation was removed, allowing the specimen to reach an

equilibrium position under zero stress. This cycle was
repeated twice more before testing. Various strain levels
were used for the actual tests.

V. EXPERIMENTAL RESULTS AND DISCUSSION

Asphalts have been shown to be a linear viscoelastic liquid above the glass transition temperature [8]. The time-temperature superposition principle was found valid for asphalts and the WLF equation is obeyed over a wide range of temperature.

Bituminous concrete mixtures have also been analyzed using rheological principles. Papazian [37] tested asphalt mixtures dynamically to arrive at general stress-strain relations of a linear viscoelastic material in the frequency domain. Alexander [3] performed creep, constant rate-of-strain and relaxation-type tests on bituminous concrete and determined the limits of linear viscoelastic behavior. He also compared the behavior in tension and in compression and concluded that the properties were different in the two cases.

The effect of temperature on the response of asphalt-aggregate composite has also been investigated. Pagen [36] and Lottman [31] found that time-temperature superposition was applicable to such mixtures.

The experimental phase of this investigation consisted of the determination of the rheological response of a sand-

asphalt mixture by using transient creep tests and stress relaxation tests. The viscoelastic functions were extended over a wide range of temperature by using the time-temperature superposition principles. The two series of experiments were then compared and the complex functions were predicted from the results of the transient functions.

Creep:

Effect of Repetition of Loading: Characterization of a material requires that experimental tests be repeatable and reproducible.

The first quality is directly related to the principle of Fading Memory. If this principle can be applied, the repetition of the load will not have a significant effect on the response of the material providing enough time is left between the different loadings. However, Figure 3 which is a typical example at 45°C shows that the rheological response of the material is influenced by the loading history, and the same specimen undergoing the same creep test gives a different creep function after each loading. This behavior is not surprising since the mixture is expected to behave primarily as a granular soil because of the large percentage of the aggregates. Al-Ani [2] performing creep tests on a similar type of material,
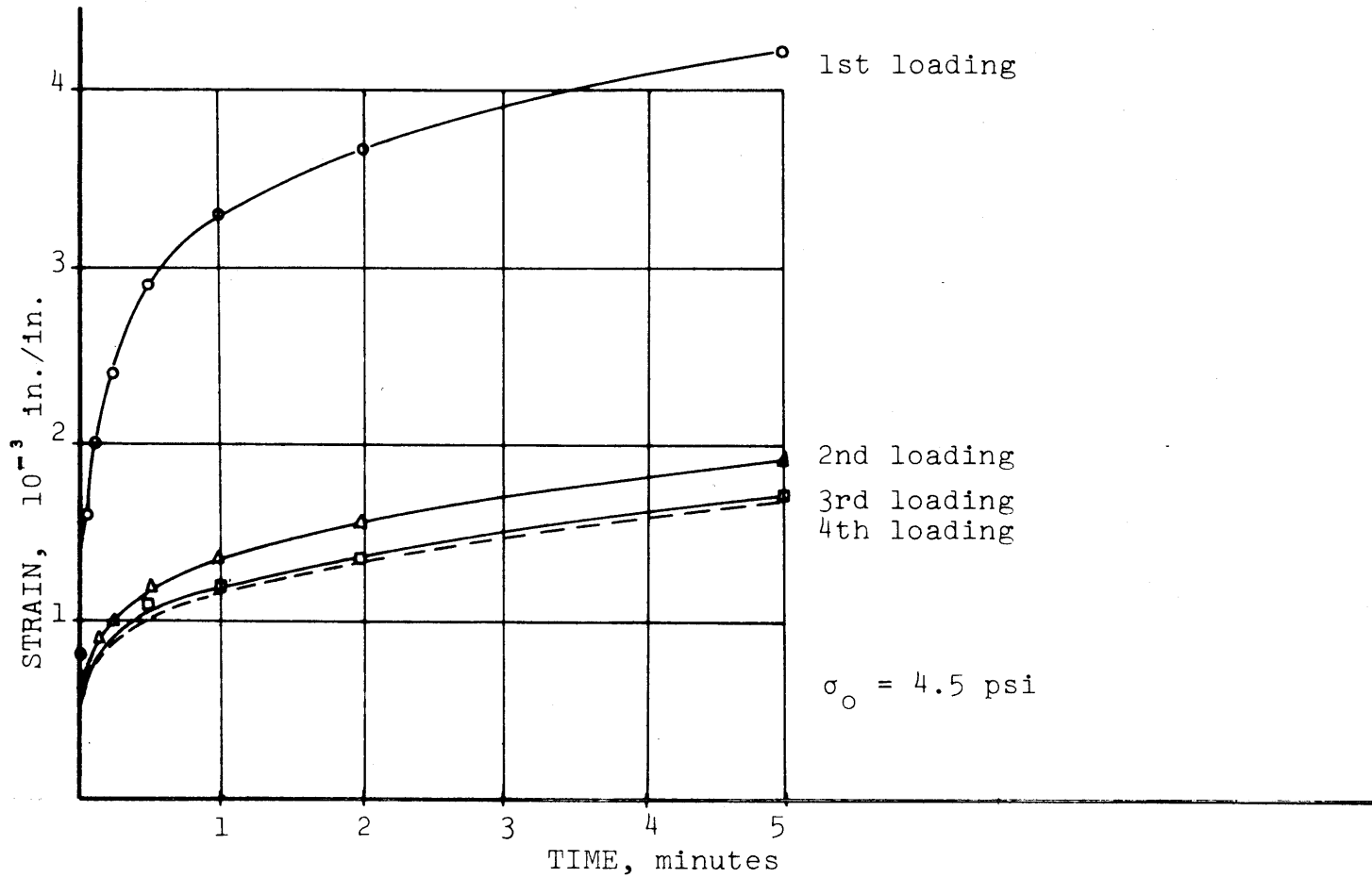
Figure 3.   Effect of Repetition of Loading on Creep Curves at 45°C

found the same behavior. The curves show that after
three cycles the effect of the repetition of the load
becomes small.

The second required test quality is reproducibility.
This refers to the possibility of obtaining identical
results from similar tests performed on identical specimens.
It was found that the scatter observed for the first cycle
due to slight variations in the densities or due to any end
defect is larger than that obtained from the subsequent
loadings. During the first cycle the specimen work
hardens, and the increase in stiffness is mainly due to the
interlocking of the sand particles and due to a slight
increase in density. The creep compliance is thus expected
to tend asymptotically towards a minimum value, and possibly
increase again later on under fatigue processes. This work
hardening is a transient state in which the properties of
the material are changing and it significantly interferes
with linear viscoelastic characterization.

For this study, all the specimens were preconditioned
by three cycles of loading as described above to insure a
better repeatability and reproducibility of the tests. It
is believed that the choice of the fourth cycle rather
than the first cycle to describe the material is also
preferrable when the results are used for prediction of the
dynamic functions of the material. The material after three

cycles of loading is closer to a steady state rheological configuration. Ideally a larger number of preconditioning cycles are required to obtain a better uniformity in the specimens tested at different temperatures and at different stress levels.

Effect of Finite Loading Time: The definition of creep functions assumes an instantaneous application of the load which would correspond to a Heaviside step function. This cannot be achieved in reality. Application of a load requires a finite time. The shorter this loading time is, the better would be the approximation of a Heaviside step function. Unfortunately for very fast loading, the inertia forces could not be neglected and damped oscillations could occur. The loading procedure, however, affects only the results at short times. This is also a consequence of the principle of fading memory. Generally results are unaffected by duration loading time after ten times the loading time has elapsed.

In this study the specimens were loaded mutually and the time required to place the load was of the order of a tenth of a second. Results reported are for times larger than two seconds.

Creep Curves: Figure 4 shows typical creep curves at 25°C where strains are shown as functions of time on an
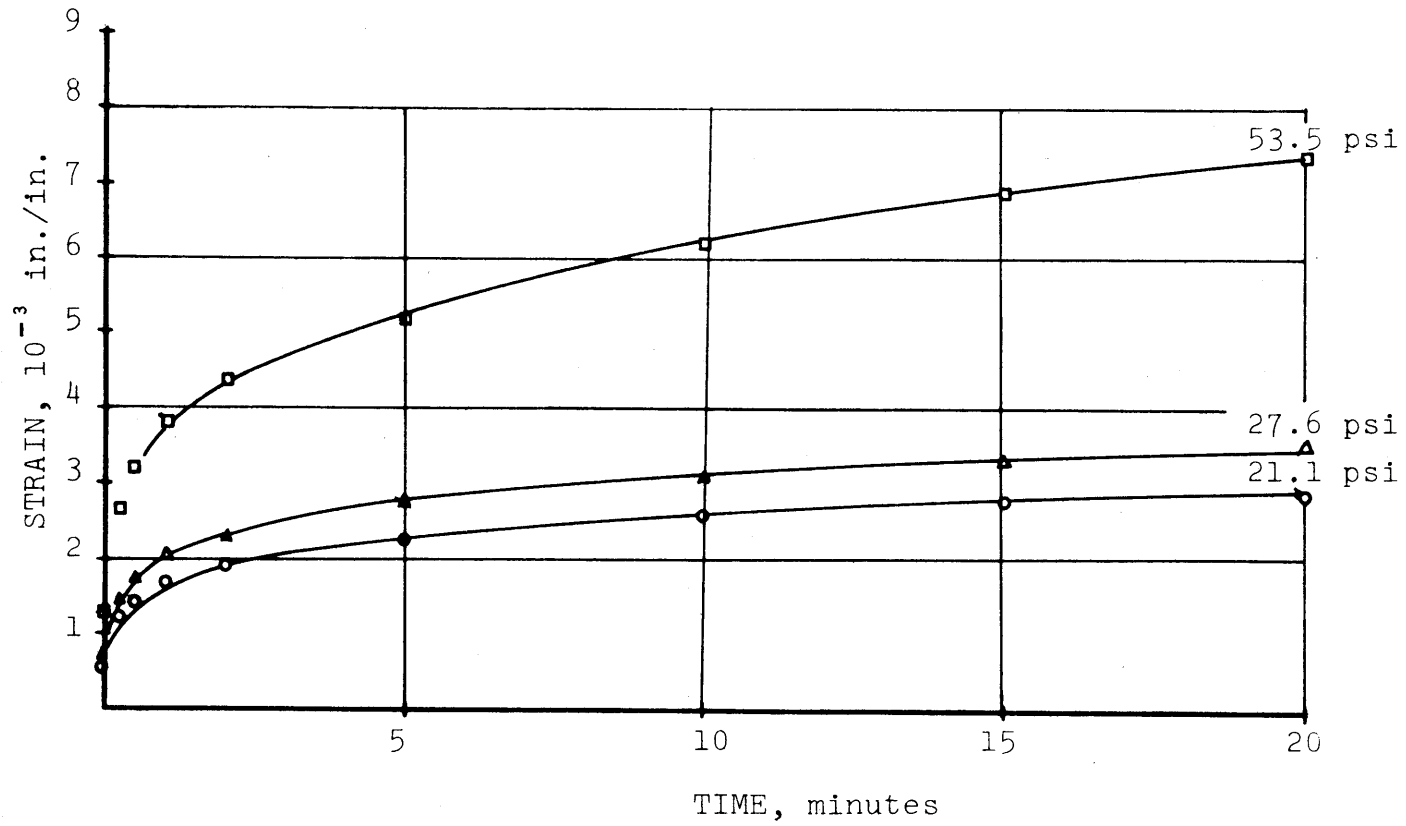
Figure 4.   Typical Creep Curves at 25°C

algebraic scale for different stress levels. Semi-
logarithmic plots of creep tests, as shown in Figure 5,
are more useful for the analysis of the data in the short
time region. Figure 5 also shows the amount of variations
generally obtained among identical specimens tested under
the same load.

Tests of Linearity: To test the linearity assumption, two
series of plots are used; the isochrones and the compliances.
Figure 6 represents a typical isochrone plot for the results
of creep tests at 25°C. The stress-strain relationships, at
any given time, are well approximated by straight lines
which indicate that the material tested is linear when
tested in creep. Similarly, Figure 7 which shows the com-
pliances obtained from the results of tests performed at
different stress levels can also be used as a check of the
linearity. The creep compliance is defined as the strain
response to a unit stress applied instantaneously. When such
compliance curves can be superimposed, the material is
considered to be linear.

Temperature Effects: Since the asphaltic mixtures are
shown to be temperature sensitive the results of the creep
tests are also very sensitive to temperature changes. The
limits of linearity thus vary at different temperatures. To
assure that material is linear, the linearity was checked
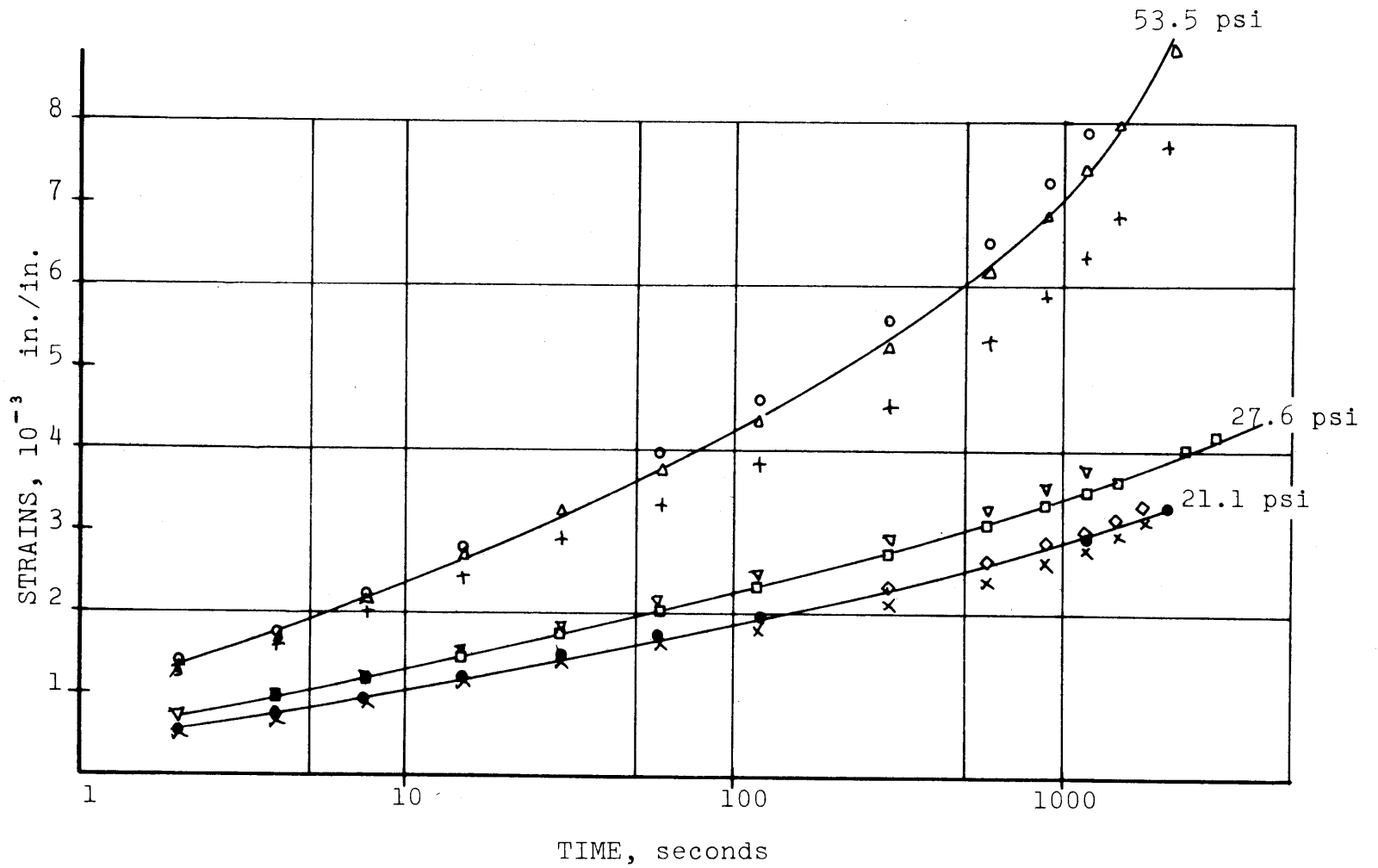
Figure 5.   Typical Creep Curves at 25°C: semi-logarithmic plot
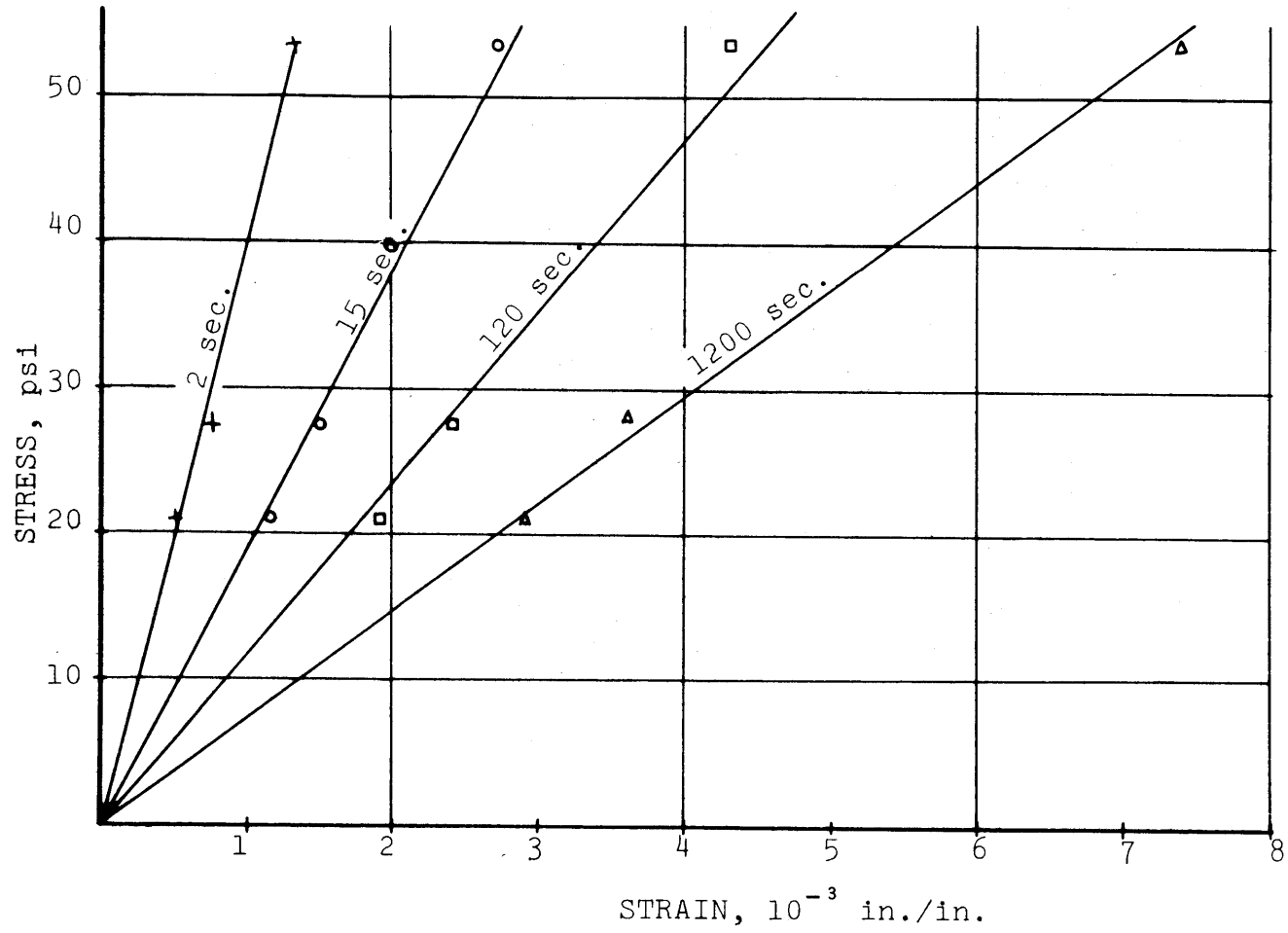
Figure 6.   Isochrones from Creep at 25°C
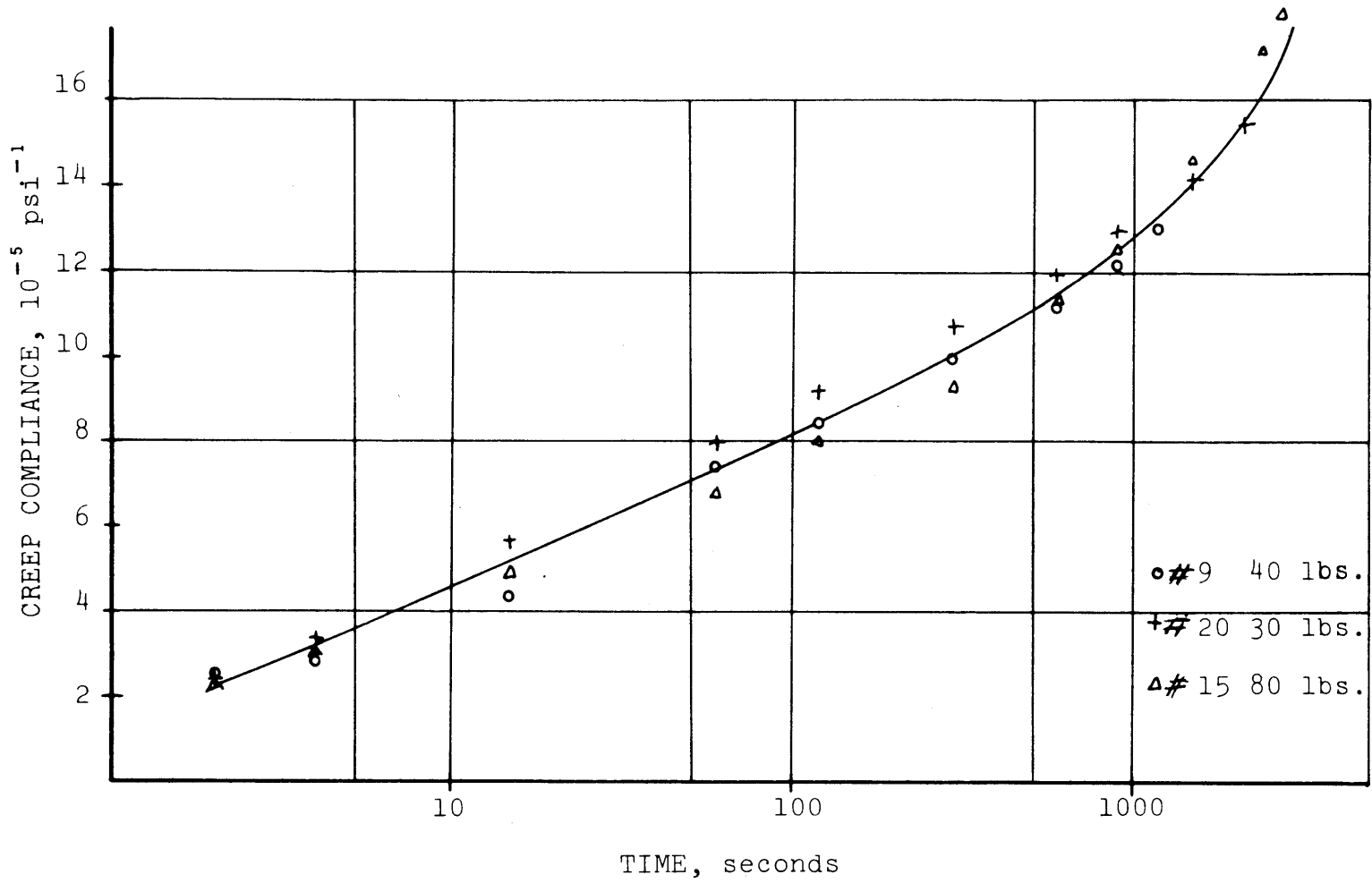
Figure 7. Creep Compliance at 25°C

at all the six temperatures used in this study. The
figures showing the creep compliance curves and the iso-
chrones obtained at these temperatures are presented in
the Appendix.

Time-Temperature Superposition Principle: Figure 8
presents the creep compliances obtained at six different
temperatures. The compliances are plotted as reduced
variables $D_c \dfrac{T}{T_o}$ corrected for the entropy temperature
change. The reference temperature was chosen as 25°C. The
correction for density change was neglected since the
levels of deformations were very small, and the density
changes were less than .5%. The application of the time-
temperature superposition principle was tested on the
curves of Figure 8 and the creep compliance master curve
was obtained for the reference temperature. The shift
factors were measured graphically by evaluating the hori-
zontal translation necessary to superpose the different
curves. They were then plotted on Figure 10 vs. the recipro-
cal of the absolute temperature. This plot was found to
be close to a straight line and this corroborates with
the theoretical expression relating it to the activation
energy. The master creep curve in Figure 9 shows three
different regions of viscoelastic behavior:

    1. A glassy region, where the effect of time is

       not very important, corresponding to low tempera-
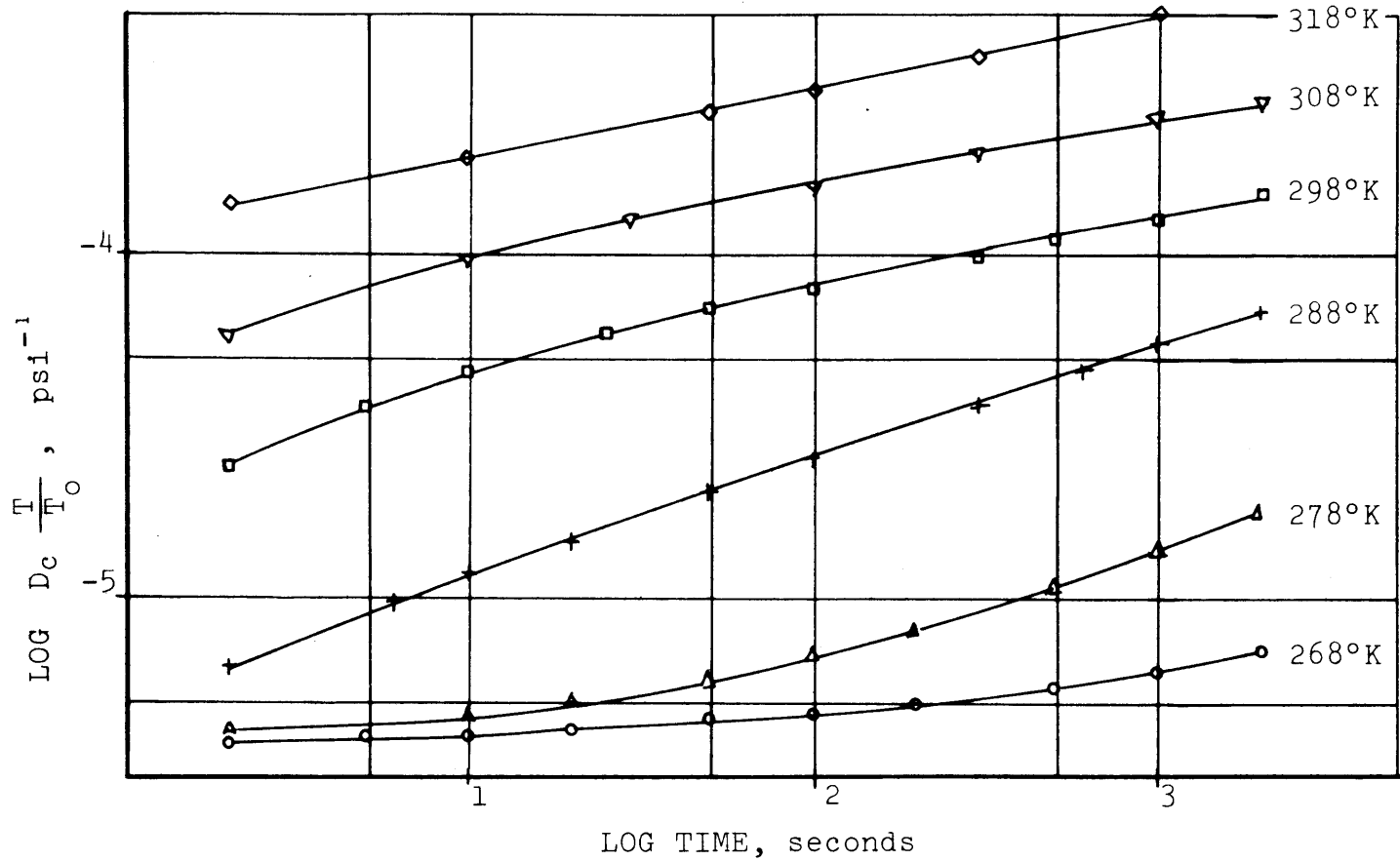
Figure 8.　Reduced Creep Compliances at Different
　　　　　　Temperatures
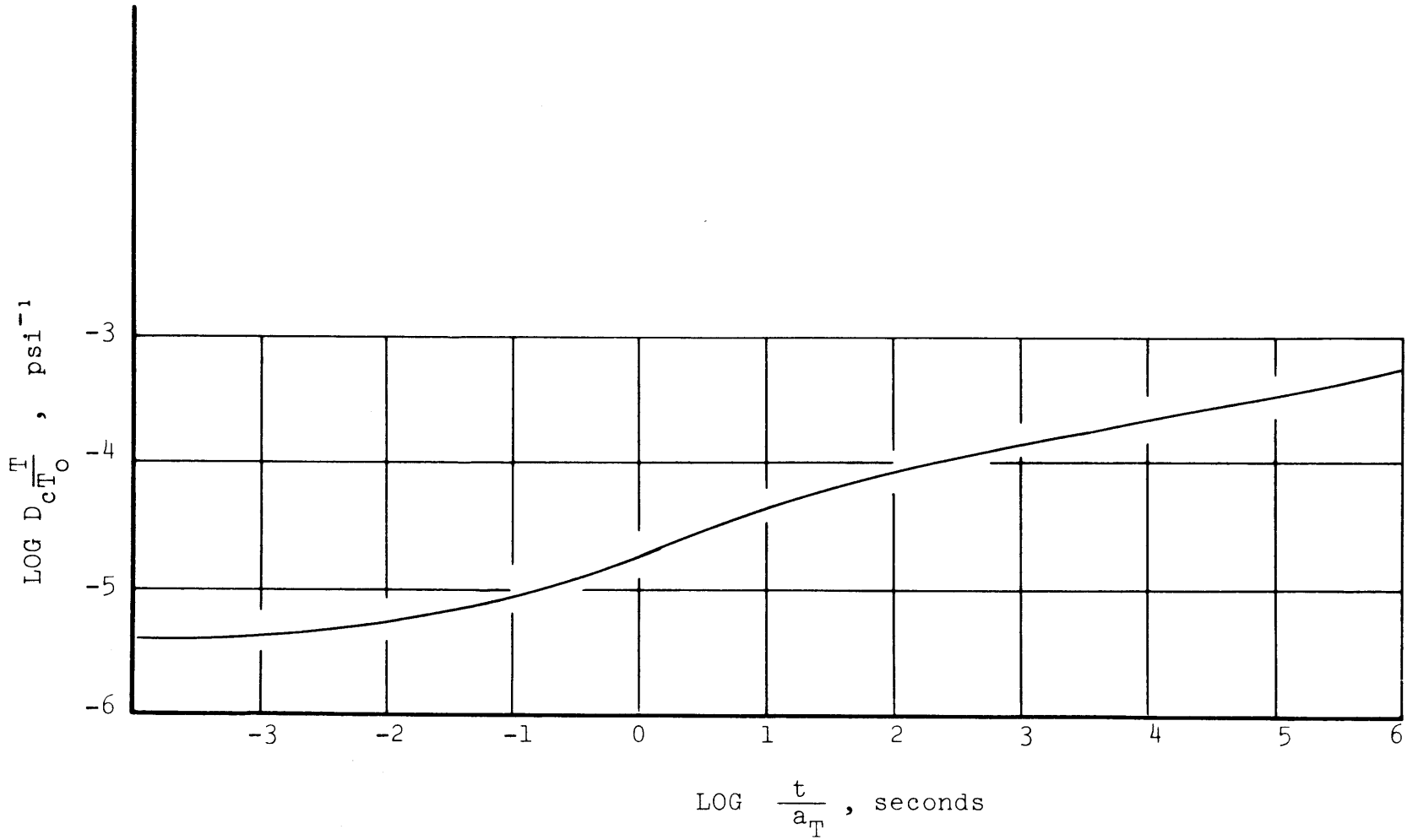
Figure 9.   Creep Compliance Master Curve Reduced at T_o = 298°K
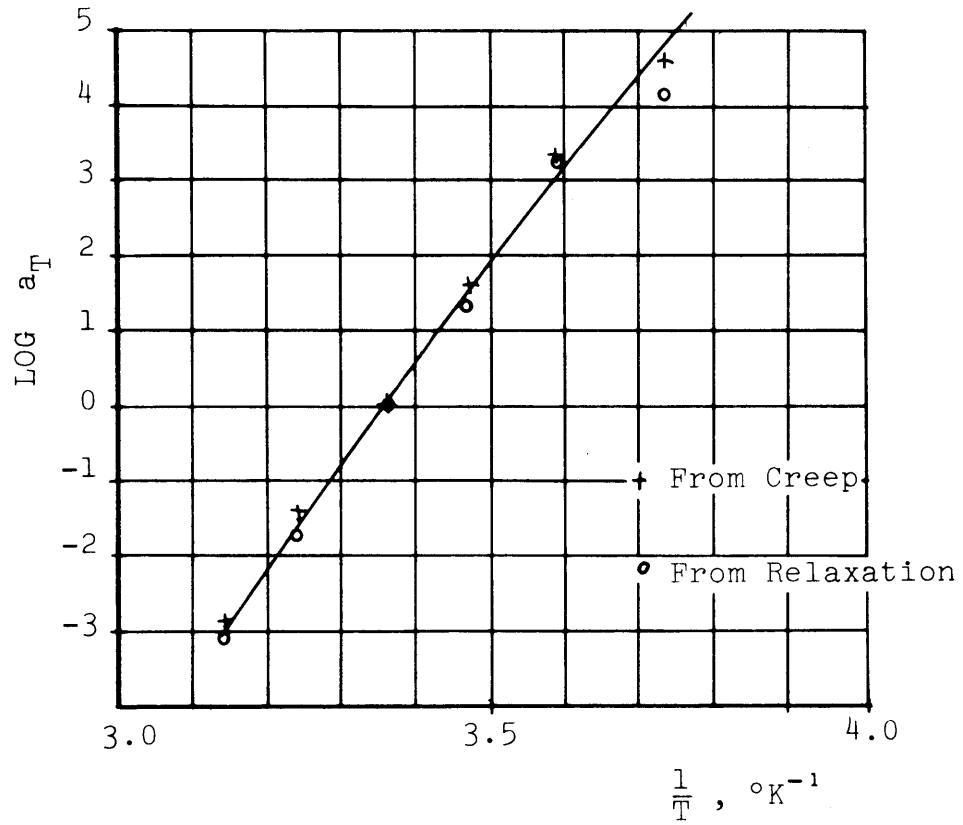
Figure 10. Shift Factors vs. $\frac{1}{T}$

ture or short time response of the material.

2.   A transition region in which the reduced
compliance changes very rapidly with time and
temperature.

3.   The onset of a rubbery region where the
time effect diminishes.

Relaxation:

Effect of Repetition of Straining: A parallel study was
made on the relaxation tests. The effect of the repeti-
tion of the straining was checked and it was found to be
very important. Figure 11 is a typical example of the
effect of repetition of the deformation at a relatively
high test temperature. In relaxation, a higher number of
cycles is required to reach the steady state response
particularly at high temperatures. This is easy to under-
stand since in a creep preconditioning the sample attains
large strains at the first loading, while if preconditioned
in relaxation, the amount of deformation introduced in the
material is very small. Thus for elevated temperatures,
the samples were either preconditioned with six cycles or
preconditioned with a constant load similar to the pre-
conditioning realized for the creep tests. The straining
was performed on the Instron Testing Machine.
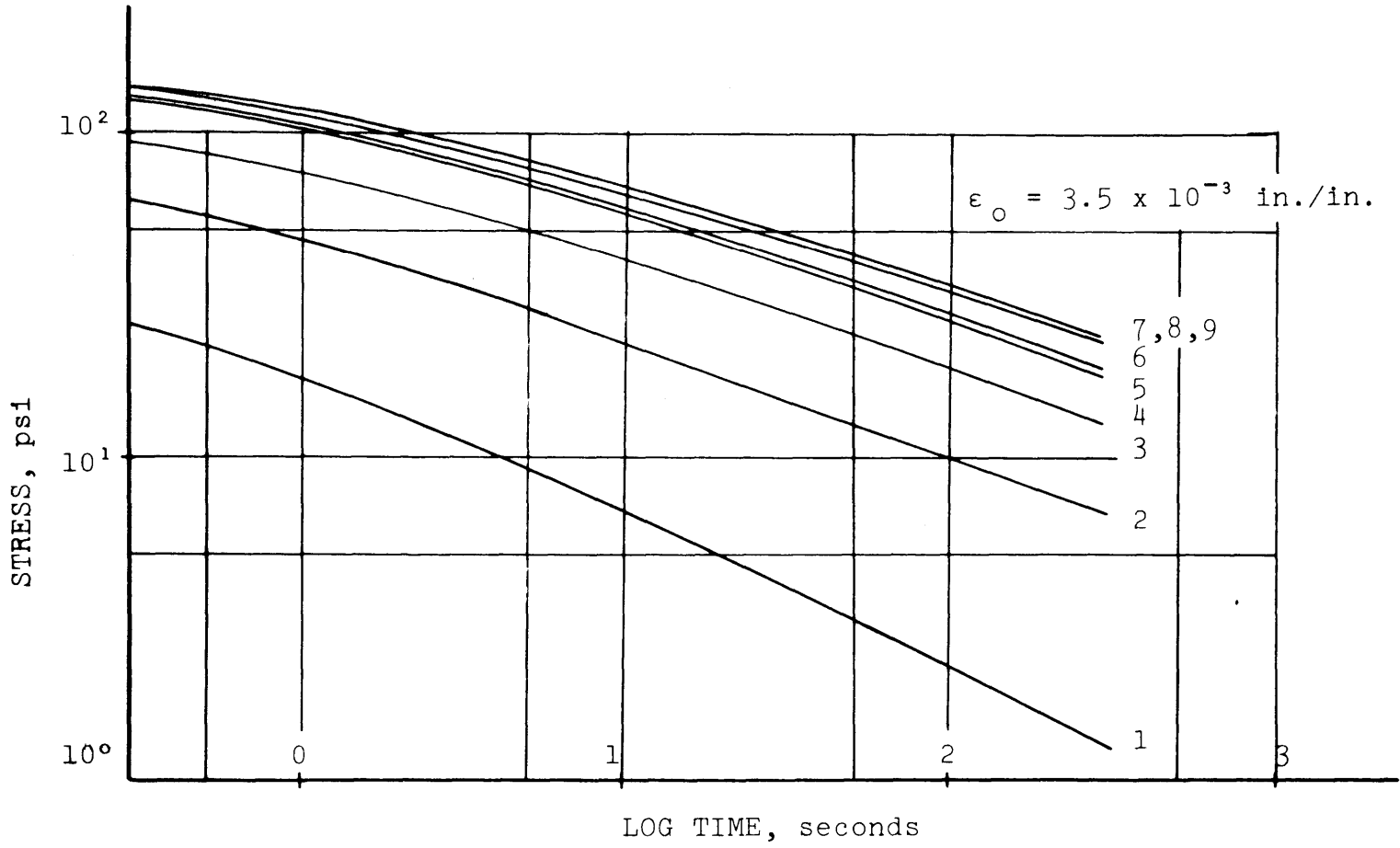
Figure 11.   Effect of Repetition of Straining on Relaxation
Curves at 35°C

Effect of Finite Loading Time: As discussed above for
the creep tests, the application of the strain cannot be
instantaneous. A high rate of loading can be used, but
it may produce wave propagation and the inertia forces
would become significant. Also the inertia of the
recording apparatus would not permit significant observa-
tions of fast varying results. To avoid these difficulties
the specimen was deformed at a rate of 0.2 inches/minute
which corresponded to a strain rate of 1.12×10^{-3} inches/
inches/second. A numerical method using a collocation
technique, which was described in section III was used to
correct for the error introduced by the stress relaxation
occurring during the loading period. The results of such
a correction are shown in Figures 12 and 13 for two
different test temperatures. To emphasize the variations
of the results at short times, the time axis is plotted in
logarithmic scale. The origin of time is taken at the
end of the loading time. Relaxation modulus is defined as
$E_r(t) = E(t)/\varepsilon_o$, ε_o being the strain applied at zero time
as a step function. Figure 12 contains the results of
stress relaxation tests at -5°C. At this temperature the
response of the material does not vary significantly with
time and it is referred to as the glassy region, hence
the correction for finite straining time is not very sig-
nificant. Figure 13, however, represents the relaxation
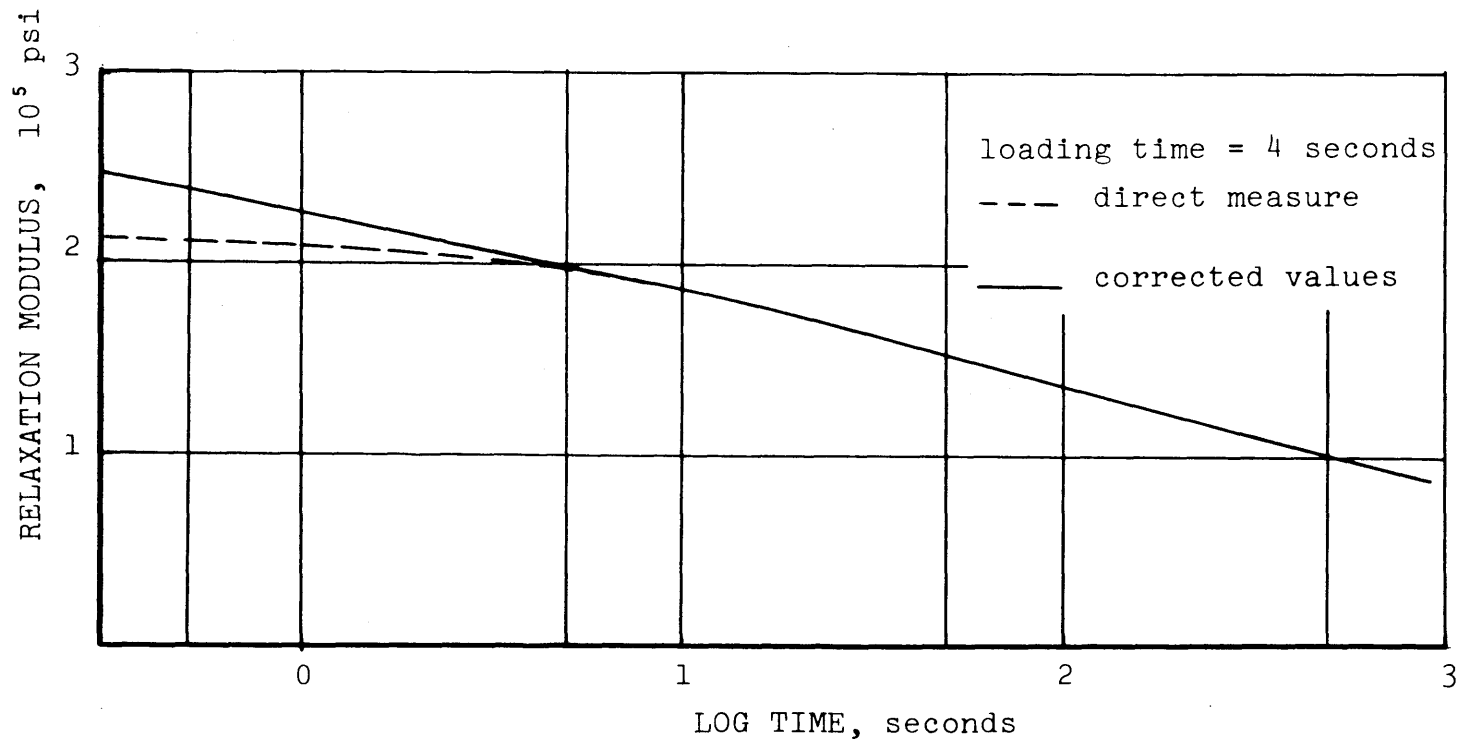
Figure 12. Correction for Finite Rise Time at -5°C
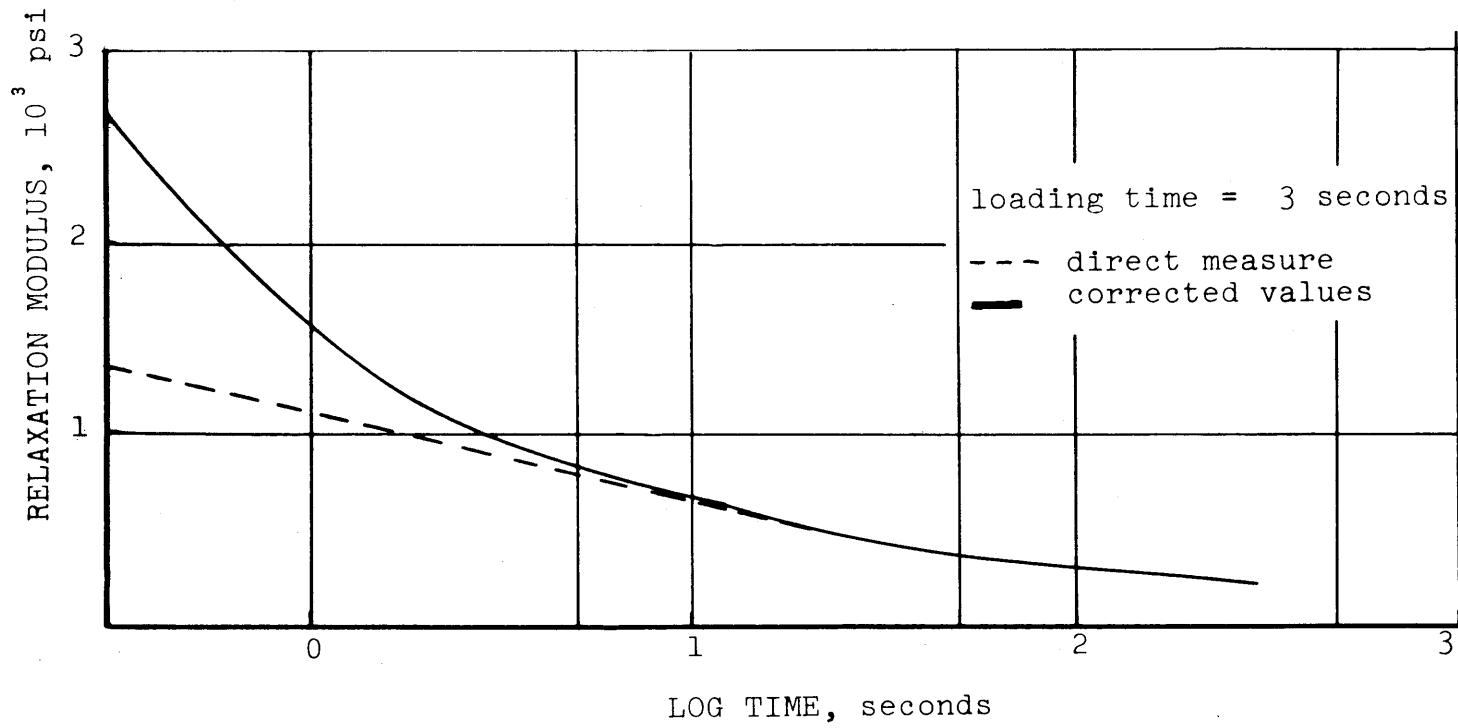
Figure 13. Correction for Finite Rise Time at 35°C

modulus at 35°C, the transition region. The correction
in this region is significant and the results should thus
be accounted for. The feasibility of the correction
method was tested on a three-element mechanical model,
and it was found to improve the validity of the experi-
mental curve for short times. However, the accuracy of
the correction depends highly on an accurate experimental
curve and a good fitting for the short times. Moreover,
it was found that when time-temperature superposition
principle is applied to the corrected relaxation results,
the superposition would be better than that for uncorrected
results. Thus all the relaxation results in this study
were corrected for finite straining time prior to their
use. Figure 14 shows typical stress relaxation curves at
25°C.

Tests of Linearity: Linearity of the relaxation results
are also shown in two series of plots, the isochrones and
the moduli. Figure 15 shows the isochrones of relaxation
curves. The results are similar to Figure 6 which shows
the isochrones for creep data. The relaxation modulus at
25°C is plotted in Figure 16. The fact that the relaxa-
tion moduli determined from the results of tests under
different levels of applied strain are superposed indicate
that the material is linear viscoelastic.
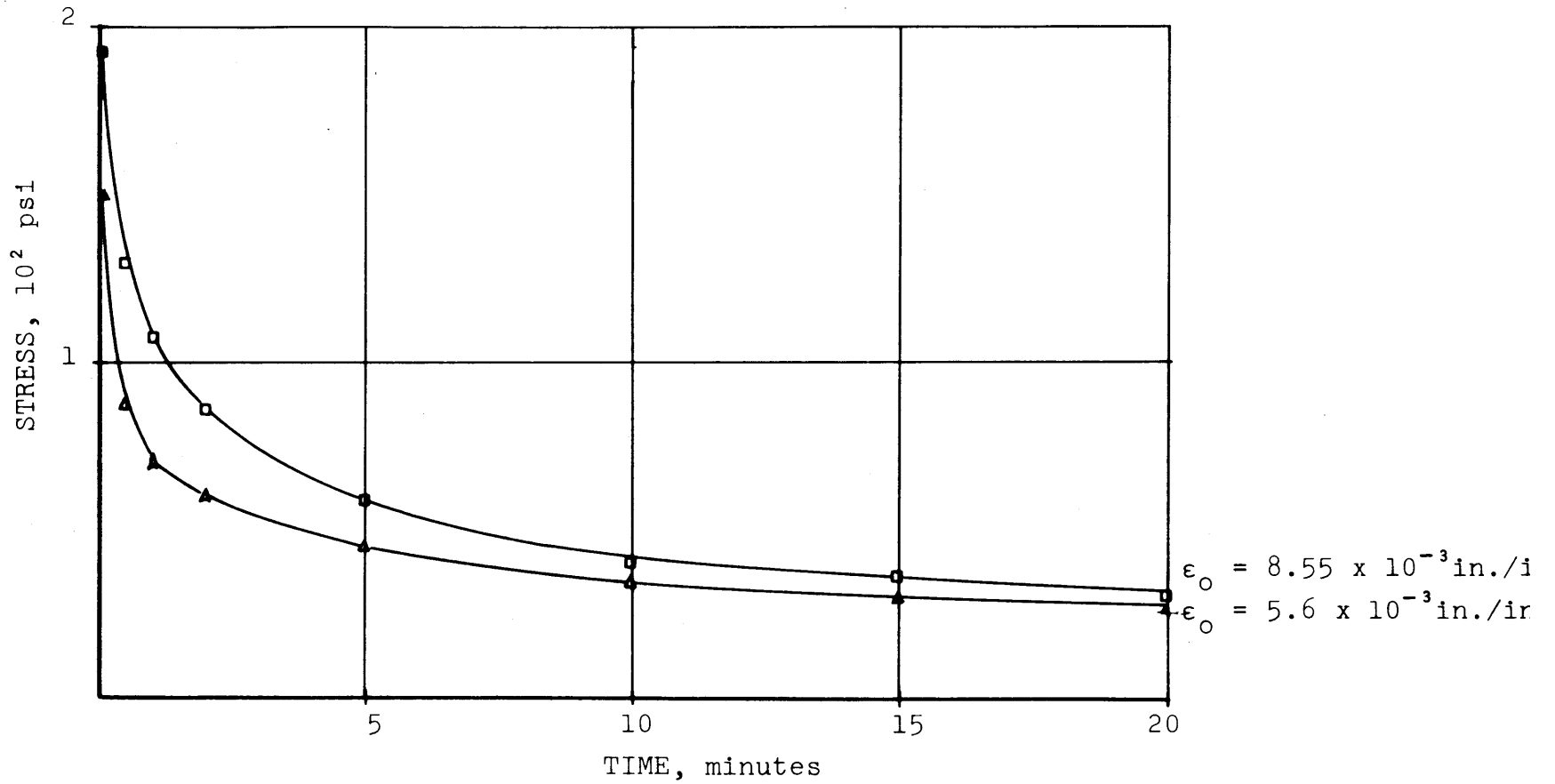
Figure 14. Typical Stress Relaxation Curves at 25°C
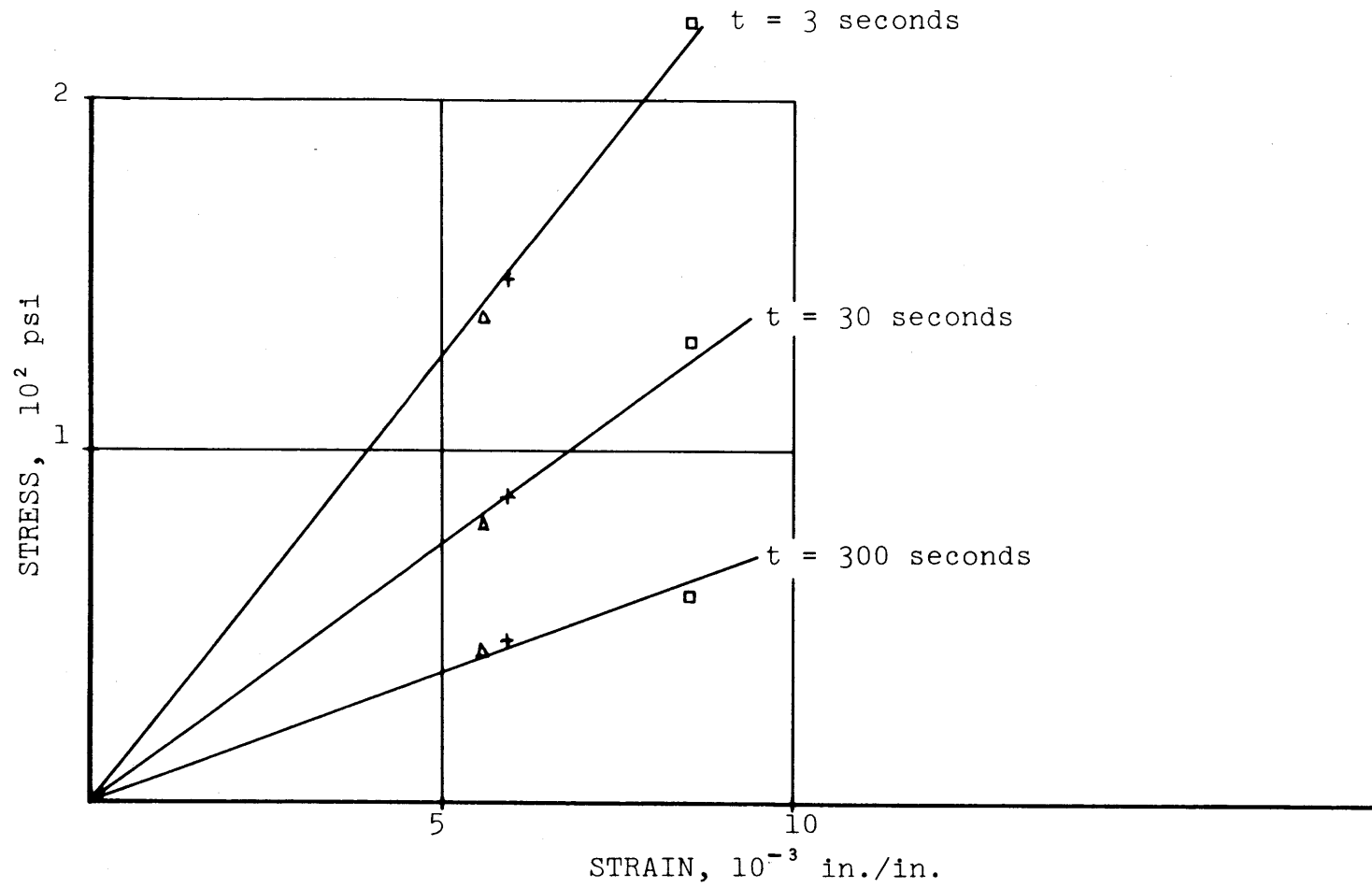
Figure 15.   Isochrones from Stress Relaxation at 25°C
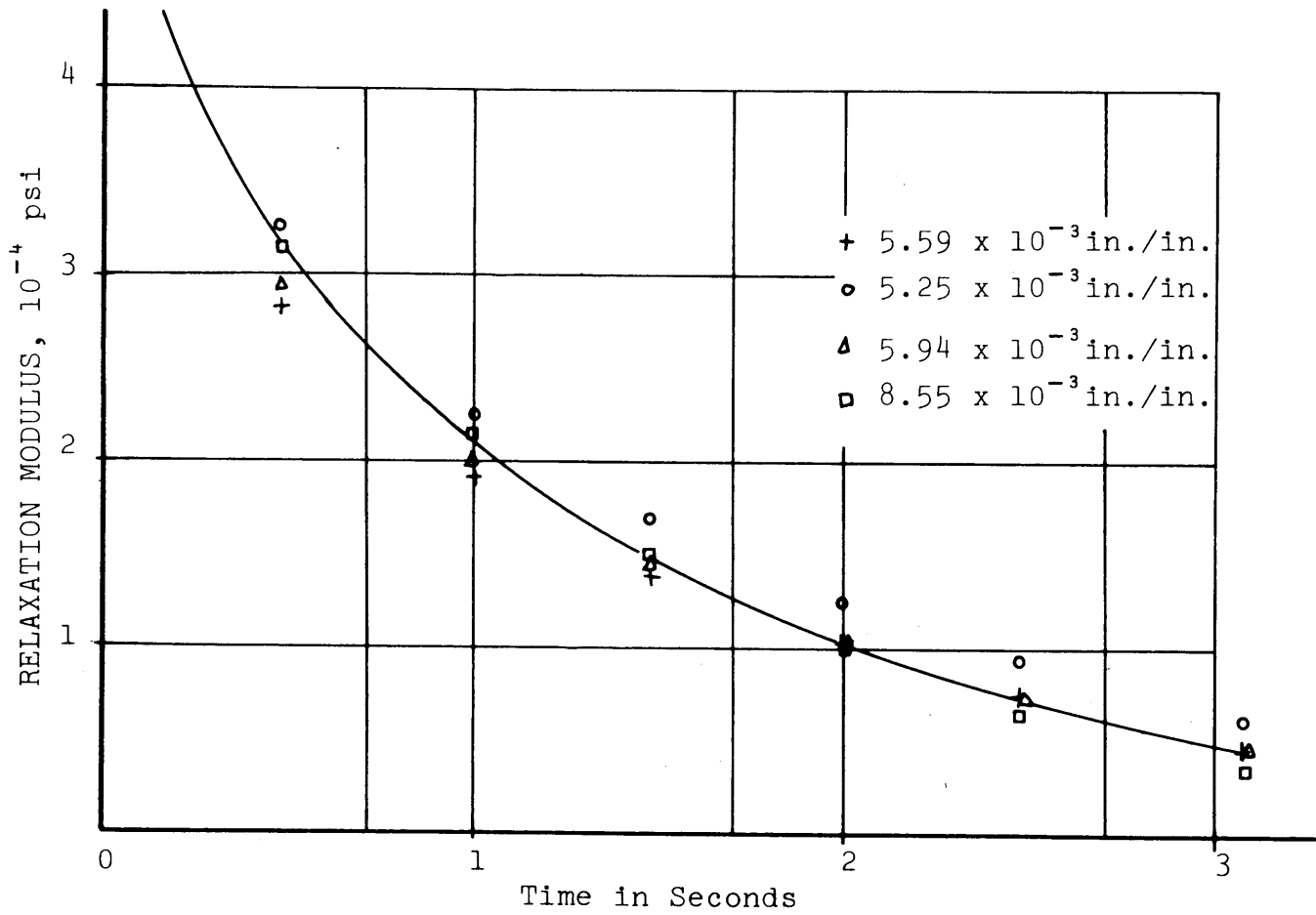
Figure 16.   Relaxation Modulus at 25°C

Temperature Effects: A complete characterization of a

material requires the determination of the viscoelastic

functions at different temperatures.   For relaxation

tests, six different temperatures were used and the

relaxation curves and the isochrones are shown in the

Appendix.

Time-Temperature Superposition Principle: In Figure 17,

all the relaxation moduli of the sand-asphalt mixture

obtained in this study are plotted as reduced variables

$E_r \frac{T_o}{T}$ vs. time to an arbitrary base temperature of 25°C.

By appropriate horizontal shifts of these reduced curves,

the relaxation master curve at the reference temperature

of 25°C is constructed in Figure 18.   The procedure used

here is similar to that used for the creep compliance

master curve.   The master curve of relaxation modulus

shows also three different regions; glassy region, transi-

tion region, and rubbery region.

Comparison of Creep and Relaxation:

Shift Factors: The values of the shift factors obtained

from both the creep and relaxation results are compared in

Figure 10.   Within the limits of experimental accuracy,

the shift factors obtained from the relaxation and the
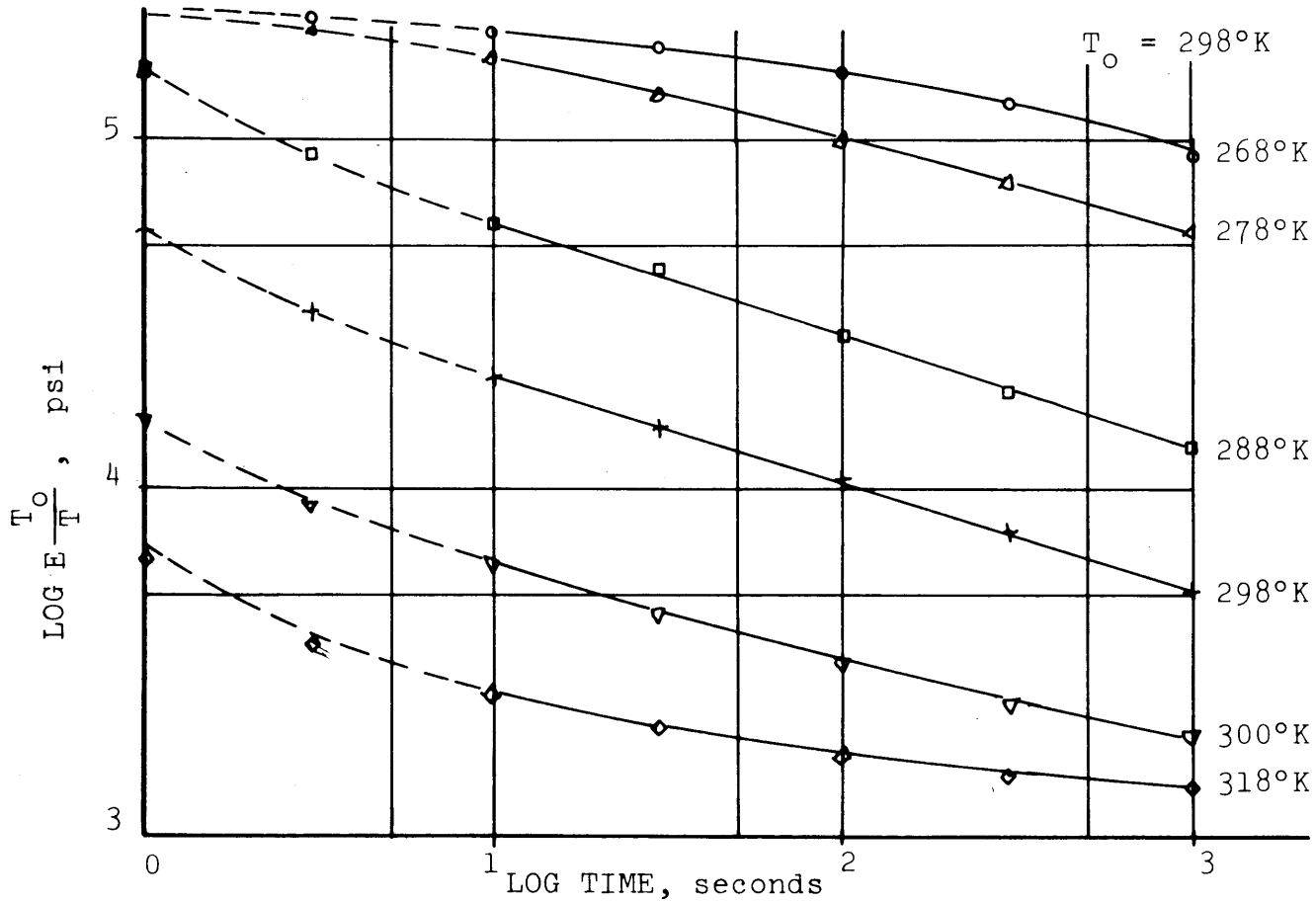
Figure 17.   Reduced Relaxation Moduli at Different Temperatures
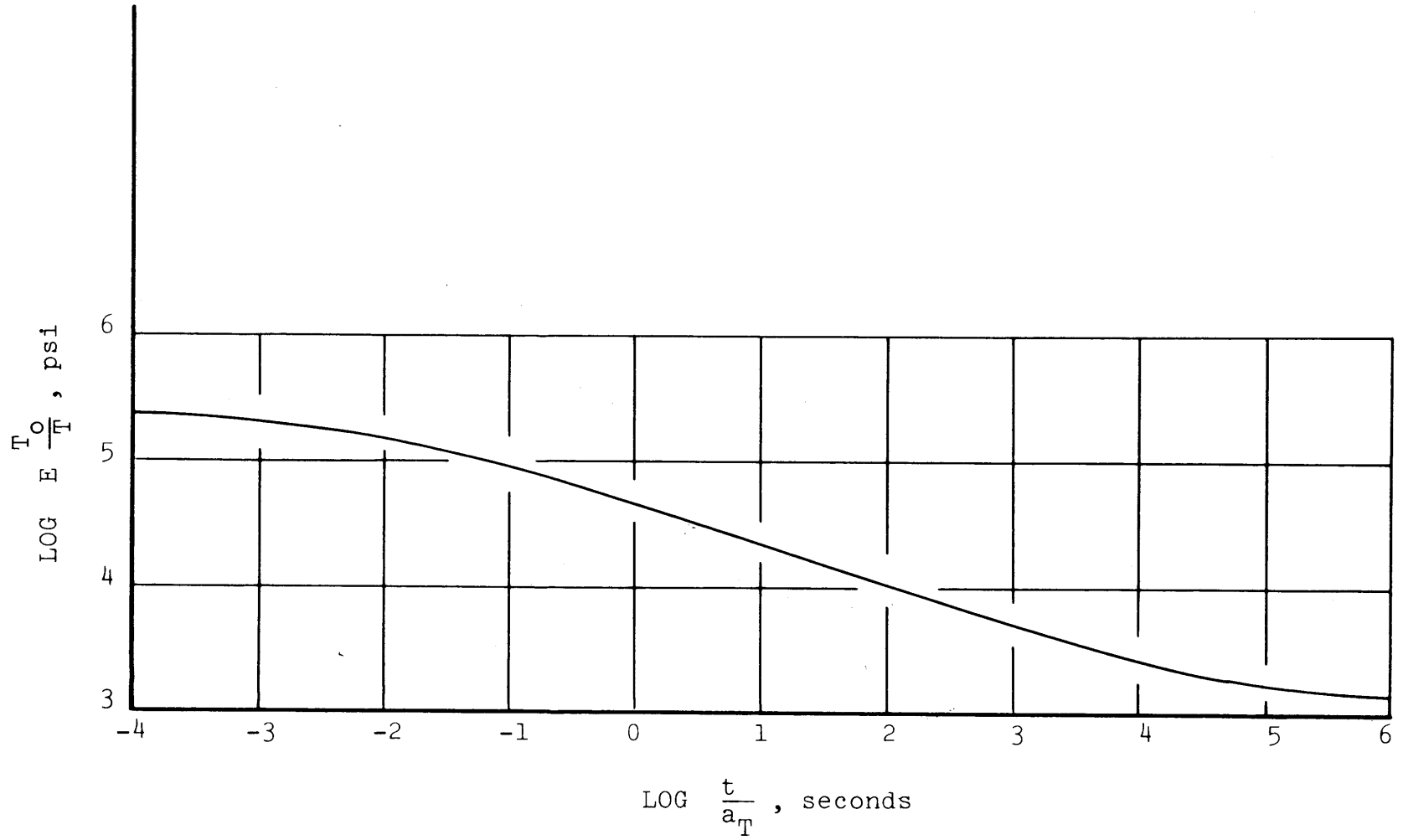
Figure 18.   Relaxation Modulus Master Curve Reduced at T_o = 298°K

creep tests are the same. This indicates that the sand-asphalt mixture used is a thermorheologically simple material. The shift factor represents the function of temperature at a given time, while the master curve represents the function of time at a given temperature.

Analytical Expression of Master Curves: To express the relaxation and the creep characteristic functions analytically, the experimental data was handled using Dirichlet series. The technique is described in section III of this study. The number of terms was chosen approximately equal to the number of decades of time where the curves have a significant slope. The relaxation modulus $E_r(t)$ and the creep compliance $D_c(t)$ are:

$$E_r(t) = E_\infty + \sum_{i=1}^{11} E_i e^{-\alpha_i t}$$

and

$$D_c(t) = D_\infty + \sum_{i=1}^{11} D_i e^{-\alpha_i t}$$

The numerical values obtained for coefficients E_i, D_i and α_i are given in Table 7. E_∞ and D_∞ are the values of the relaxation and the creep compliance at infinite time. A computer program to perform this collocation was written for this study and it is listed in the Appendix.

-106-

TABLE 7

Series Fitting of Master Curves

Creep Compliance: $\quad D_c(t) = D_\infty + \sum_{i=1}^{11} D_i\, e^{-\alpha_i t}$

Relaxation Modulus: $\quad E_r(t) = E_\infty + \sum_{i=1}^{11} E_i\, e^{-\alpha_i t}$

where: $\quad \alpha_i = 0.5 \times 10^{(5-i)} \quad$ for $\quad 1 \leqslant i \leqslant 11$

$D_1 = -0.697 \times 10^{-6}$	$E_1 = +0.545 \times 10^5$
$D_2 = +0.458 \times 10^{-7}$	$E_2 = +0.231 \times 10^5$
$D_3 = -0.165 \times 10^{-5}$	$E_3 = +0.706 \times 10^5$
$D_4 = -0.330 \times 10^{-5}$	$E_4 = +0.526 \times 10^5$
$D_5 = -0.213 \times 10^{-4}$	$E_5 = +0.299 \times 10^5$
$D_6 = -0.245 \times 10^{-4}$	$E_6 = +0.143 \times 10^5$
$D_7 = -0.546 \times 10^{-4}$	$E_7 = +0.659 \times 10^4$
$D_8 = -0.662 \times 10^{-4}$	$E_8 = +0.317 \times 10^4$
$D_9 = -0.797 \times 10^{-4}$	$E_9 = +0.126 \times 10^4$
$D_{10} = -0.133 \times 10^{-3}$	$E_{10} = +0.478 \times 10^3$
$D_{11} = -0.361 \times 10^{-3}$	$E_{11} = +0.160 \times 10^3$
$D_\infty = +0.750 \times 10^{-3}$	$E_\infty = +0.130 \times 10^4$

The same program was used previously in viscoelastic study of cement paste [34].

The use of this technique in certain cases may result in certain coefficients with opposite sign. When such variations in sign of the coefficient occurs, it means that too many terms were used to approximate the transition region. Since the coefficients (E_i) and $(-D_i)$ can be considered as an approximation to a continuous spectral distribution function or as a discrete spectral distribution [22], it seems to be physically unacceptable to have the coefficients (E_i) or $(-D_i)$ with negative values.

In Figure 19, log E_i and log $(-D_i)$ are plotted vs. log $1/\alpha_i$. It should be kept in mind that coefficient D_i's are negative, thus $(-D_i)$'s are positive quantities. This plot can be considered as a discrete spectral representation of the transient functions. For the sake of clarity of the figure, instead of plotting the values of (E_i) and $(-D_i)$, their logarithms are plotted. Thus the negative value $(-D_2)$ found in the series fitting, could not be shown since it does not have a logarithm.

The occurrence of this negative value $(-D_2)$ could be avoided in the series either by changing the number of terms or by choosing other values for the exponents α_i. This value was kept, however, in the fitting series, since this representation is considered as a purely mathematical

LOG $H_n(\tau_i)$

LOG $L_n(\tau_i)$

LOG τ_i

or

LOG $\frac{1}{\alpha_i}$

- - Creep

—— Relaxation
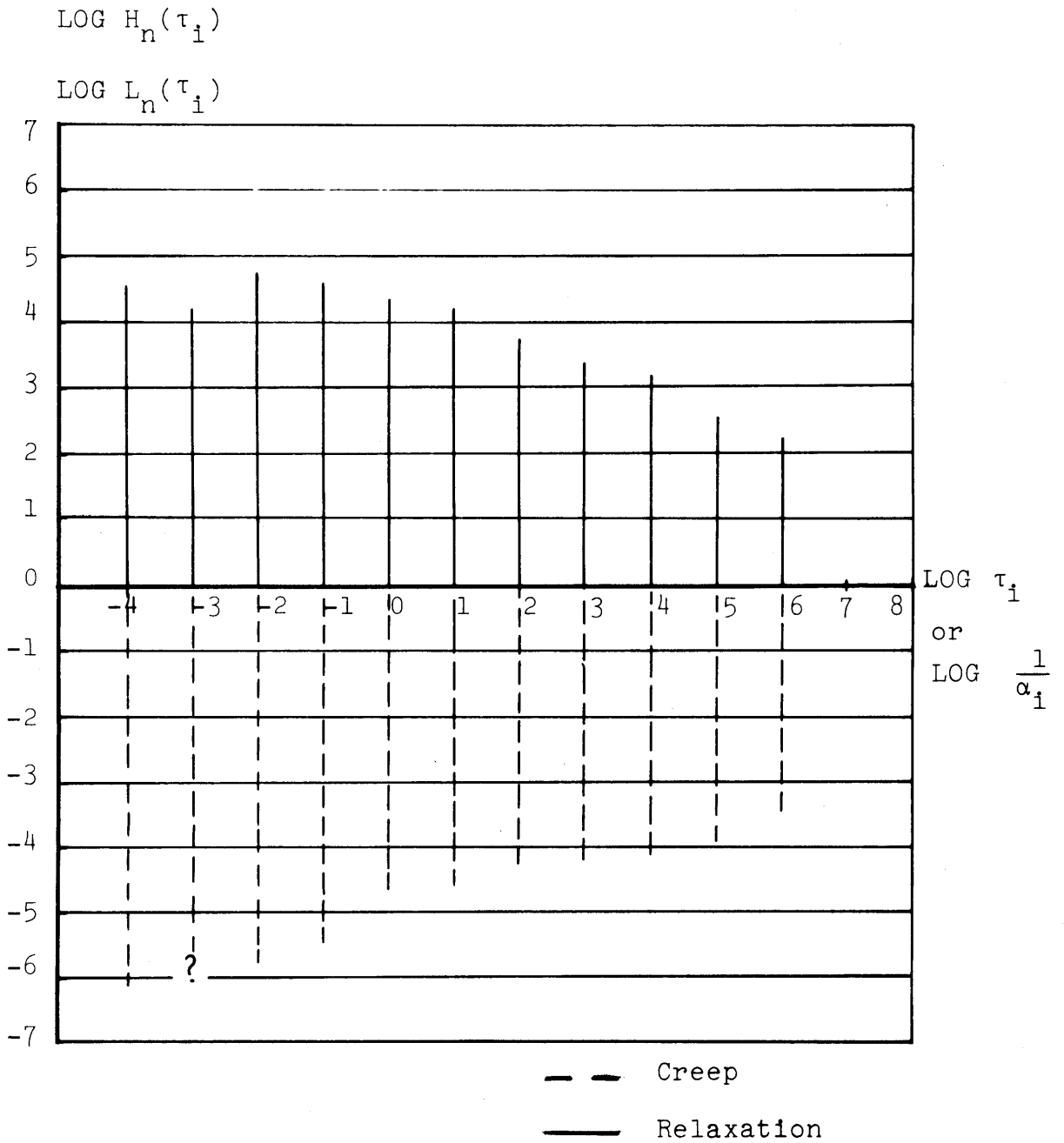
Figure 19.   Discrete Spectral Representation

expression.

Comparison in Laplace Domain: The above curve fitting
technique provides an excellent means to establish the
relationships which exist among the various viscoelastic
functions of a material.   For example a comparison of the
relaxation modulus and the creep compliance may be done
easily in the Laplace domain.   This can be achieved using
the Laplace transform of the above expressions for $E_r(t)$
and $D_c(t)$, that is:

$$\overline{E}(p) = p\overline{E}_r(p) = p \int_0^\infty E_r(t)\ e^{-pt}\ dt$$

$$\overline{E}(p) = p\left[\frac{E_\infty}{p} + \sum_{i=1}^{11} \frac{E_i}{p+\alpha_i}\right]$$

and

$$\overline{D}(p) = p\overline{D}_c(p) = p \int_0^\infty D_c(t)\ e^{-pt}\ dt$$

$$\overline{D}(p) = p\left[\frac{D_\infty}{p} + \sum_{i=1}^{11} \frac{D_i}{p+\alpha_i}\right]$$

In Laplace domain, these quantities are simply the
inverse of each other such that $\overline{E}(p) = [\overline{D}(p)]^{-1}$ or
$p\overline{E}_r(p) = [p\overline{D}_c(p)]^{-1}$.   The values of $\overline{E}(p)$ and
$[\overline{D}(p)]^{-1}$ are plotted vs.   p   in Figure 20.   This figure
shows that a good correspondence exists between the results

-110-

LOG E(p)

LOG $\dfrac{1}{D(p)}$
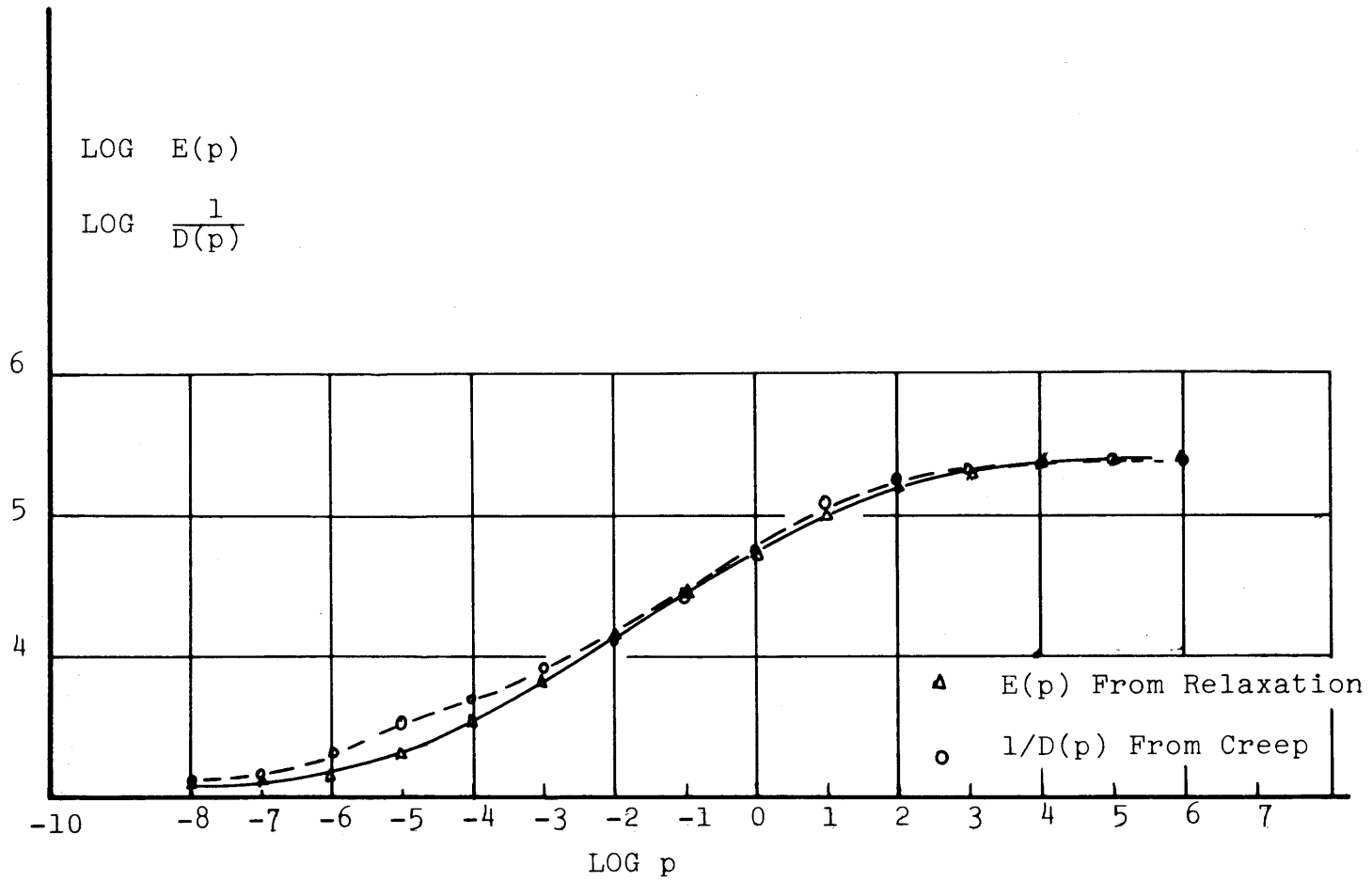
Figure 20. . Laplace Transforms $\overline{E}(p)$ and $\dfrac{1}{\overline{D(p)}}$

of the creep and the relaxation tests in all regions
except in certain transition parts, where the two values
deviate from each other. This deviation is attributed
to experimental variation occurring in the preconditioning
stage. Figure 11 shows the extent of this variation for
the relaxation results. Moreover the time-temperature
superposition principle may increase considerably the
experimental errors in the master curves because an error
in the evaluation of the shift factor a_T for one
temperature is cumulative throughout the graphical shift
procedure.

Direct Conversion of Master Curves: In Figures 21 and 22,
direct comparison of the two functions in the time domain
is obtained using numerical integration of Volterra
equations:

$$\int_o^t E_r(t-\tau) \, D_c(\tau) \, d\tau = t$$

and

$$\int_o^t D_c(t-\tau) \, E_r(\tau) \, d\tau = t$$

The procedure used was that of Hamming and Hopkins
numerical technique which is described in previous sections,
and the FORTRAN listing of a computer program using this
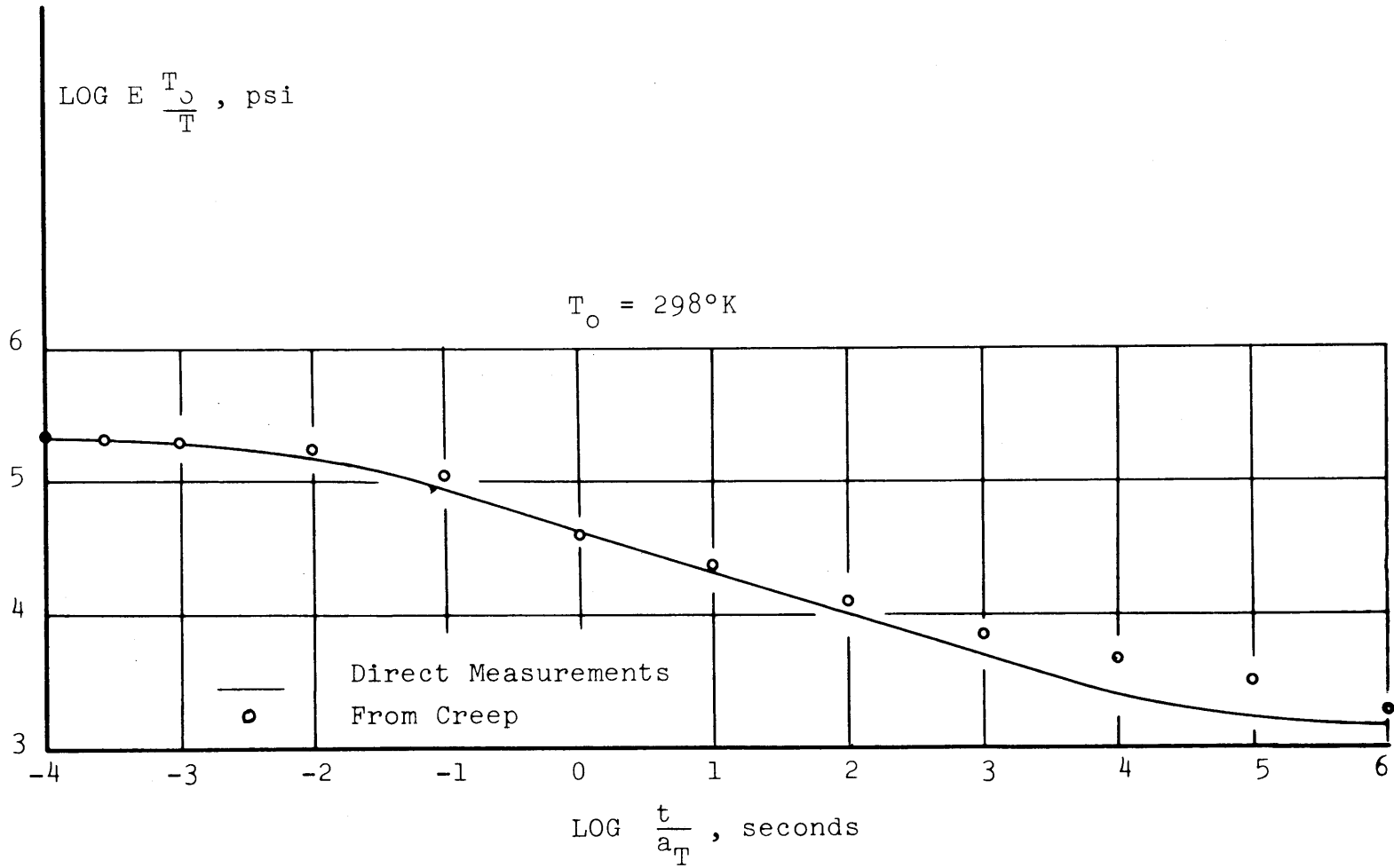
Figure 21. Comparison of Experimental Relaxation Modulus Curve with
Values Obtained by Numerical Conversion of the Creep
Compliance
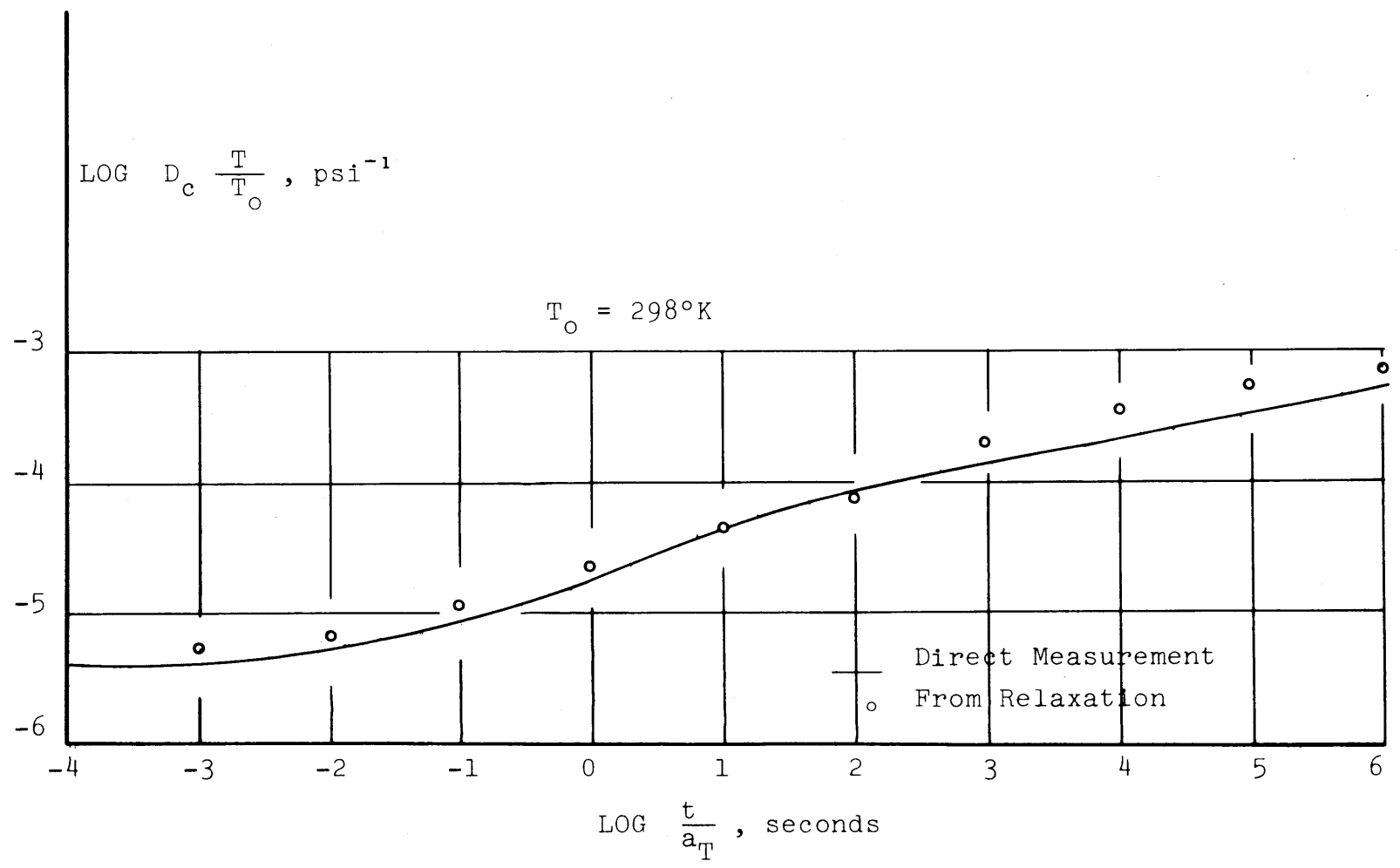
Figure 22.   Comparison of Experimental Creep Compliance Curve with
Values Obtained by Numerical Conversion of the Relaxation
Modulus

procedure is in the Appendix. Comparisons of creep and
relaxation results in Figures 20, 21 and 22 show similar
trends in Laplace and time domains; a good comparison
in the glassy region and part of the transition region
and some deviations occurring towards the end of the
transition region. This corresponds to the curves obtained
from high temperatures and long times. In this region the
cycling effect was most pronounced and the limit of
linearity was very low, which would suggest that either
another way of preparing the specimens to minimize this
cycling effect should be found or non linearity of the
material occurring in this region should be accounted for.

Comparison of Complex Functions: Substitution of $(i\omega)$
where ω is the circular frequency of a dynamic testing,
for p in the analytical expressions of the associated
functions $\overline{E}(p)$ and $\overline{D}(p)$, gives the complex functions:

$$E^*(i\omega) = E_\infty + \sum_{i=1}^{n} \frac{E_i(i\omega)}{i\omega + \alpha_i}$$

and

$$E^*(i\omega) = E_1 + iE_2$$

where
$$E_1(\omega) = E_\infty + \sum_{i=1}^{n} \frac{E_i\omega^2}{\alpha_i + \omega^2}$$

$$E_2(\omega) = \sum_{i=1}^{n} \frac{E_i \alpha_i}{\alpha_i + \omega^2}$$

Similar expressions are obtained from the Dirichlet
expansion of the creep compliance. Figure 23 is a plot of
$D_1(\omega)$ and $D_2(\omega)$ obtained from $D_c(t)$, and Figure 24 is
a plot of $E_1(\omega)$ and $E_2(\omega)$ obtained from $E_r(t)$. These
dynamic functions derived from two independent sets of
results, creep compliances and relaxation moduli, can be
directly compared.

From $D_1(\omega) + iD_2(\omega) = \dfrac{1}{E_1(\omega) + iE_2(\omega)}$ it can be shown
easily that:

$$D_1(\omega) = \frac{E_1}{(E_1)^2 + (E_2)^2}$$

and

$$D_2(\omega) = \frac{-E_2}{(E_1)^2 + (E_2)^2}$$

The values of $D_1(\omega)$ and $D_2(\omega)$ calculated directly
from $D_c(t)$ are compared in Figure 25 with the values
computed from $E_r(t)$ and $E_1(\omega)$ and $E_2(\omega)$. The
deviation that occurs corresponds to the same deviation
observed in the former comparisons made in Figures 20, 21
and 22 in Laplace and time domains. Finally the two
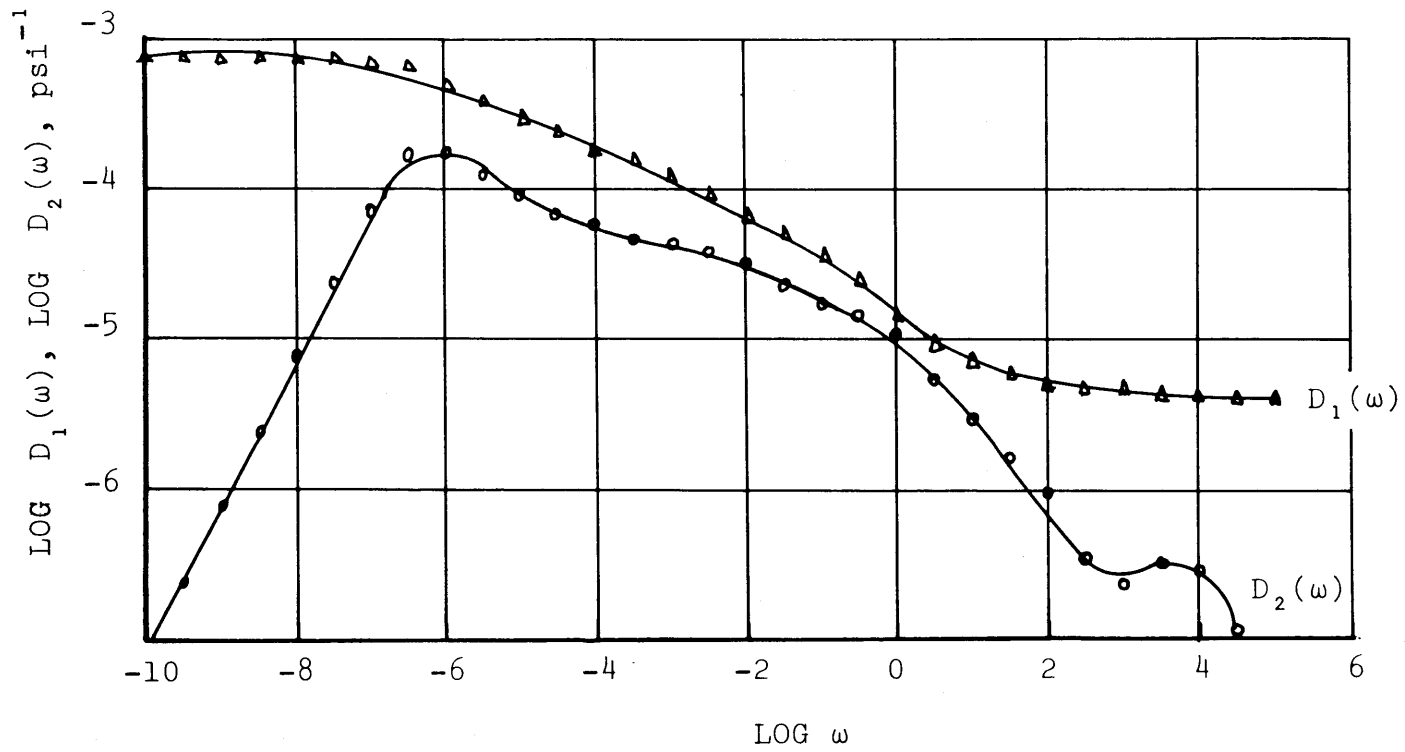
Figure 23. Complex Compliance Calculated from $D_c(t)$
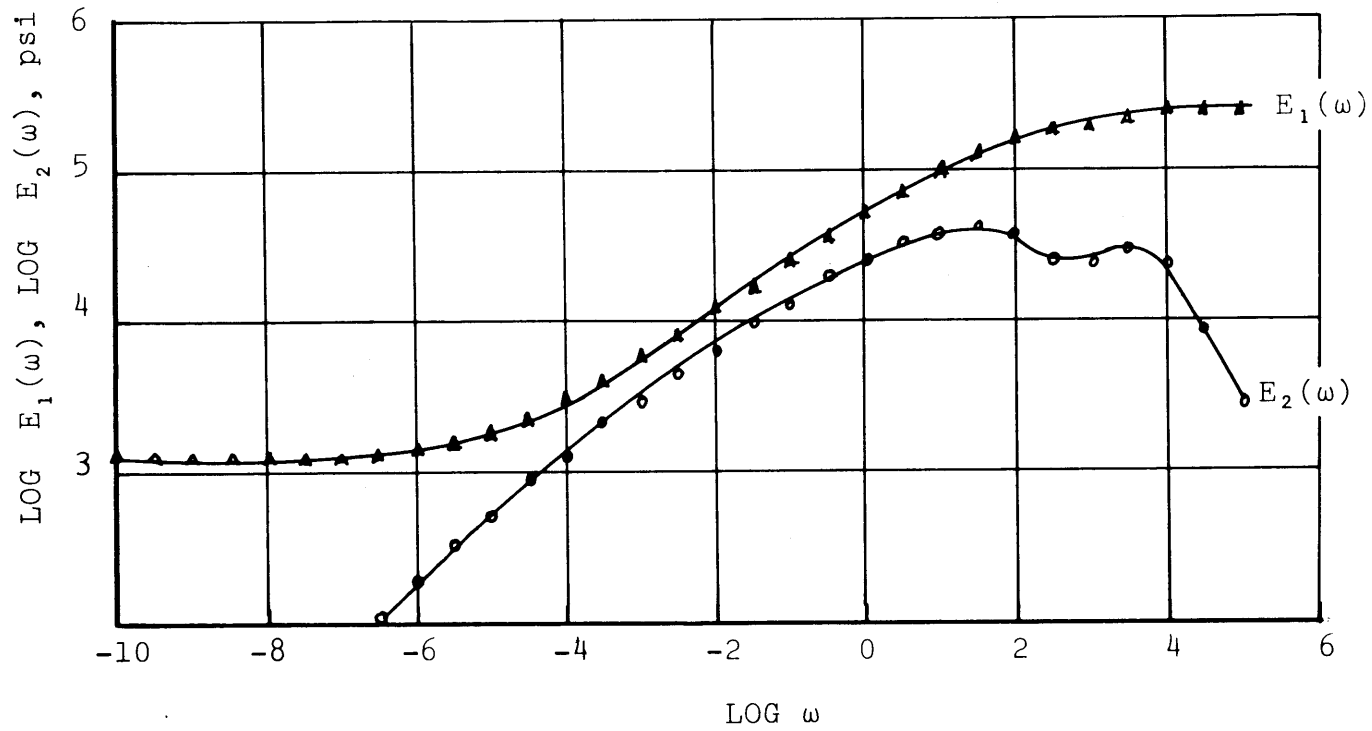
Figure 24.   Complex Modulus Calculated from $E_r(t)$
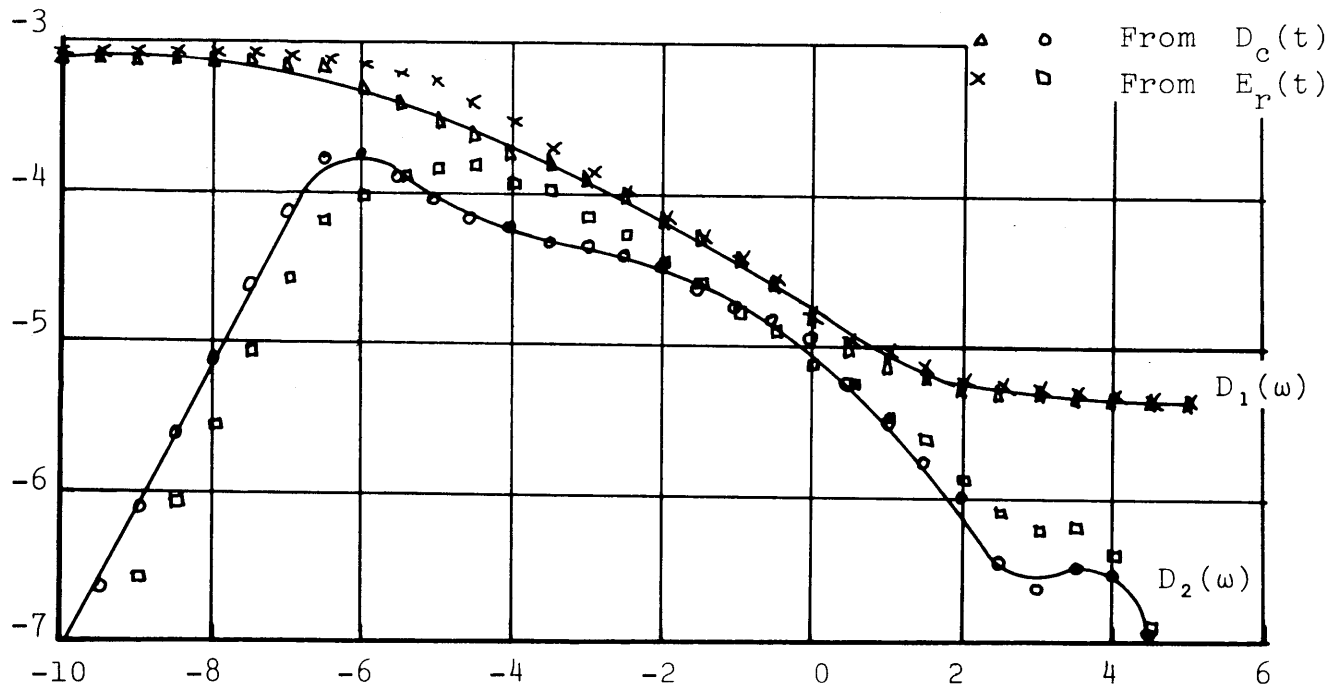
Figure 25.   Comparison of the Complex Compliance Components

different complex functions are compared by the
evaluation of their loss tangent, in Figure 26:

$$\tan\ \delta(\omega)\ =\ \frac{E_2(\omega)}{E_1(\omega)}\ =\ \frac{-D_2(\omega)}{D_1(\omega)}$$

In this plot the deviations are emphasized due to the
addition of the errors obtained from $E_r(t)$ and $D_c(t)$
and then increased because of the division of the imagi-
nary and the real part of the complex function.

Summary of Results:

The results presented above indicate that the
sand-asphalt mixture used in this study exhibits a
distinct time dependent behavior which is highly tempera-
ture susceptible. The application of theories of linear
viscoelasticity to time dependent response of this
material indicated that to within a certain degree of
approximation the material can be assumed as linear
viscoelastic. The temperature dependency of the material
was found to be within the realm of thermorheologically
simple materials and the time-temperature superposition
principle is applicable to the response of the material.
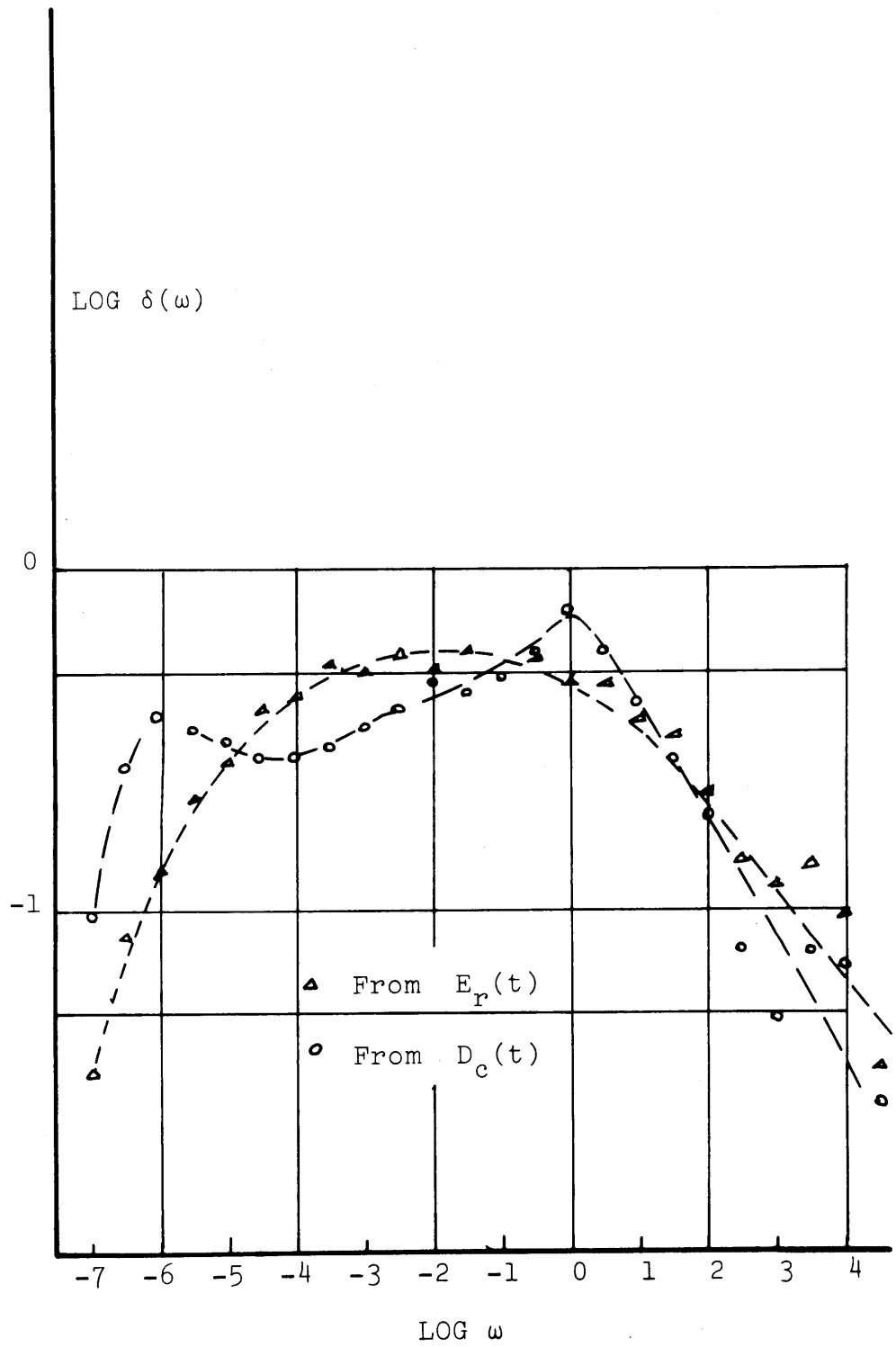
Figure 26.   Loss Tangent

VI. CONCLUSIONS

The results of this study have demonstrated a few basic points:

1. The response of sand-asphalt mixture to creep and relaxation modes of testing is similar to that of a linear viscoelastic material, providing the levels of imposed stresses and/or strains are small, and the work hardening effect is minimized.

2. The time-temperature superposition is applicable to the response of such a material in creep or relaxation tests, and the necessary shift factors in these two modes of testing are almost identical. In order to minimize the cumulative errors produced by the shift factors, however, it seems preferable to extend as much as possible the experimental range of time such that the number of temperatures necessary to complete the master curve can be reduced.

3. Exponential series can be used for analytical representation of creep and relaxation functions and they provide for easy transformation of one set of viscoelastic functions into another. They allow a good representation of the experimental data over a very wide time or frequency range. The accurate prediction of the complex functions from

the results of transient functions (creep and relaxation) depends on the degree of accuracy by which the transient functions are related to each other. Thus a unique transient function, accounting for the experimental errors, should be used to predict the complex values.

4. The numerical methods allowing direct conversion of one transient function to another can be used to obtain the necessary functional transformations with a high degree of accuracy.

5. The study of the characterization of sand-asphalt mixtures should be completed by performing some dynamic tests and comparing the actual results with values predicted from creep and relaxation tests. Also an independent visco-elastic function should be measured experimentally, as the Poisson's ratio. The numerical techniques described above using the indirect method would then be checked on sand-asphalt mixtures to see if only the initial value of this independent function is necessary. The study may then be extended to an investigation of the effect of the asphalt content and the asphalt type on the viscoelastic behavior.

LIST OF REFERENCES

1. Aklonis, J.J., Tobolsky, A.V., "Relationship Between Creep and Stress Relaxation," Journal of Applied Physics, Vol. 37, No. 5, April 1966, pp. 1949-51.

2. Al-Ani, H.M., "The Rheological Characteristics of Sand-Asphalt Mixtures," Thesis presented in partial fulfillment of the requirements for the degree of Master of Science, Ohio State University, 1965, (unpublished).

3. Alexander, R.L., "Limits of Linear Viscoelastic Behavior of an Asphalt Concrete in Tension and Compression," D. Eng. Thesis, University of California, Berkeley, Department of Civil Engineering, 1964.

4. Alfrey, T., Mechanical Behavior of High Polymers, Interscience Publishers, New York, 1948.

5. Alfrey, T., and Doty, P., "The Methods of Specifying the Properties of Viscoelastic Materials," Journal of Applied Physics, 16, 700, 1945.

6. Andrews, R.D., "Correlation of Dynamic and Static Measurements on Rubberlike Materials," Industrial Engineering Chemistry, Vol. 44, p. 407, April 1952.

7. Ashton, J.E., and Moavenzadeh, F., "Analysis of Stresses and Displacements in a Three-Layered Viscoelastic System," Proc. Sec. International Conference on the Structural Design of Asphalt Pavements, 1967.

8. Billmeyer, F.W., Textbook of Polymer Science, Interscience Publishers, New York, 1962.

9. Biot, M.A., "Theory of Stress-Strain Relations in Anisotropic Viscoelasticity and Relaxation Phenomena," Journal of Applied Physics, Vol. II, No. 25, 1954, p. 1385.

10. Bland, D.R., The Theory of Linear Viscoelasticity, Pergamon Press, New York, 1960.

11. Brisbane, J.J., "Characterization of Linear Visco-
elastic Materials," Bulletin Second Meeting Working
Group on Mechanical Behavior, CPIA, Pub. No. 27,
1963, P. 327.

12. Britton, S.C., "Characterization of Solid Propellants
as Structural Materials," Solid Rocket Structural
Integrity Abstracts, Vol. II, No. 4, October 1965.

13. Catsiff, E., and Tobolsky, A.V., "Stress Relaxation
of Polyisobutylene in the Transition Region," Journal
of Coll. Science, 10, 1955, p. 375-392.

14. Clauser, J.F., and Knauss, W.G., "On the Numerical
Determination of Relaxation and Retardation Spectra
for Linearly Viscoelastic Materials," GALCIT SM67-6,
August 1967.

15. Coleman, B.D., and Noll, W., "Foundations of Linear
Viscoelasticity," Review of Modern Physics, Vol. 33,
No. 2, April 1961, p. 239.

16. Cost, T.L., "Approximate Laplace Transform Inversions
in Viscoelastic Stress Analysis," AIAA Journal, Vol.
2, No. 12, December 1964, p. 2157.

17. Ferry, J.D., Viscoelastic Properties of Polymers, John
Wiley and Sons, Inc., New York, 1960, pp. 41-81.

18. Ferry, J.D., and Williams, M.L., "Second Approximation
Methods for Determining the Relaxation Time Spectrum
of a Viscoelastic Material," Journal Coll. Science,
1952, pp. 347-353.

19. Freudenthal, A.M., The Inelastic Behavior of Engineering
Materials and Structures, John Wiley and Sons, New
York, 1950.

20. Fung, Y.C., Foundations of Solid Mechanics, Prentice-
Hall, Inc., New Jersey, 1965.

21. Fuoss, R.M., and Kirkwood, J.G., "Electrical Properties
of Solids, VIII Dipole Moments in Polyvinyl Chloride
Diphenyl Systems," Journal Amer. Chem. Society, 63,
1941, p. 385.

22. Gross, B.,Mathematical Structure of the Theories of
Viscoelasticity, Hermann and Cie, Paris, 1953.

23. Gurtin, M.E., and Sternberg, E., "On the Linear Theory of Viscoelasticity," Archive for Rational Mechanics Analysis, Vol, II, 1962, p. 20.

24. Hilton, H.H., "Viscoelastic Analysis," in Engineering Design for Plastics, Ed. Eric Baer, Reinhold Publishing Corporation, New York, 1964.

25. Hopkins, I.L., and Hamming, R.W., "On Creep and Relaxation," Journal of Applied Physics, Vol. 28, No. 8, August 1957.

26. Khazanovich, T.N., "Derivation of the Equations of Linear Viscoelasticity," App. Mathematics and Mechanics, Vol. 28, No. 6, 1964, pp. 1123-1126.

27. Kittel, C., Introduction to Solid State Physics, 3rd Edition, John Wiley and Sons, Inc. New York, 1966.

28. Leaderman, H., Elastic and Creep Properties of Filamentous Materials and Other High Polymers, Textile Foundation, Washington, D.C., 1943.

29. Leaderman, H., "Rheology of Polyisobutylene IV; Calculation of the Retardation Time Function and Dynamic Response from Creep Data," Proc. Second International Congress on Rheology, 1954, pp. 203-212.

30. Lee, E.H., and Rogers, T.G., "Solution of Viscoelastic Stress Analysis Problems Using Measured Creep or Relaxation Functions," Journal of Applied Mechanics, Transactions of ASME, March 1963.

31. Lottman, R.P., "A Thermorheological Approach to the Design of Asphaltic Mixtures," A Dissertation Presented in partial fulfillment of the requirements for the degree of Doctor of Philosophy, Ohio State University, 1965.

32. Malone, D.W., "The Complete Mathematical Characterization of Linearly Viscoelastic Materials," a term report for Course 1.48, Special Studies in Materials, M.I.T, September 1967, (unpublished).

33. Marvin, R.S., "A New Approximate Conversion Method for Relating Stress Relaxation and Dynamic Modulus," Phys. Review, 1952, 86, 644.

34. Nemec, J., Jr., "Viscoelastic Study of Cement Paste," a dissertation presented in partial fulfillment of the requirements for the degree Doctor of Philosophy, M.I.T., 1967.

35. Ninomiya, K., and Ferry, J.D., "Some Approximate Equations Useful in the Phenomenological Treatment of Linear Viscoelastic Data," J. Coll. Science, 14, 1959, pp. 37-48.

36. Pagen, C.A., "An Analysis of the Thermorheological Response of Bituminous Concrete," Engineering Experiment Station, Project No. EES 199, Ohio State University, March 1963.

37. Papazian, H.S., "The Response of Linear Viscoelastic Materials in the Frequency Domain," Engineering Experiment Station, Bulletin 192, Ohio State University, 1962.

38. Papoulis, A., "A New Method of Inversion of the Laplace Transform," Quarterly of Applied Mathematics, Vol. 14, 1957, pp. 405-414.

39. Parr, C.H., "The Application of Numerical Methods to the Solution of Structural Integrity Problems of Solid Propellant Rockets," Solid Rocket Structural Integrity Abstracts, Vol. 1, No. 2, October 1964.

40. Roesler, F.C.,"Some Applications of Fourier Series in the Numerical Treatment of Linear Behavior,"Proc. Physical Society, Section B, January 1955-December 1955, Vol. 68.

41. Roesler, F.C., and Twyman, W.A., "An Iteration Method for the Determination of Relaxation Spectra," Proc. Physical Society, Section B, January 1955-December 1955, Vol. 68.

42. Schapery, R.A., "Approximate Methods of Transform Inversion for Viscoelastic Stress Analysis," Proc. Fourth U.S. National Congress Applied Mechanics, 2. 1075, 1962.

43. Schwarzl, F., and Staverman, A.J., "Higher Approximations of Relaxation Spectra," Physica, 18, 1952, pp. 791-798.

44. Schwarzl, F., and Staverman, A.J., "Time-Temperature Dependence of Linear Viscoelastic Behavior," Journal of Applied Physics, Vol. 23, 1952, pp. 838-843.

45. Smith, T.L., "Approximate Equations for Interconverting the Various Mechanical Properties of Linear Visco-elastic Materials," Trans. Soc. Rheology, 2, 1958, pp. 131-151.

46. Taylor, R.L., "Creep and Relaxation," AIAA Journal, Vol. 2, No. 9, pp. 1659-1660.

47. Ter Haar, D., "A Phenomenological Theory of Visco-elastic Behavior," Physica 16, 1950, pp. 719, 738, 839.

48. Theocaris, P.S., "Affine Transformations of Visco-elastic Functions," Rev. Roum. Sci. Techn. - Mec. Appl. Tomell, No. 4, Bucarest, 1966, pp. 953-975.

49. Theocaris, P.S., "Phenomenological Analysis of Linear Viscoelastic Media," Rev. Roum. Sci. Techn. - Mec. Appl. Tomell, No. 5, Bucarest, 1966, p. 1185.

50. Tobolsky, A.V., "Stress Relaxation Studies of the Visco-elastic Properties of Polymers," Journal of Applied Physics, Vol. 27, No. 7, July 1956, p. 673.

51. Tobolsky, A.V., Properties and Structure of Polymers, John Wiley and Sons, Inc., New York, 1960, pp. 103-122.

52. Truesdell, C., The Elements of Continuum Mechanics, Springer-Verlag, New York, Inc., 1966.

53. Volterra, V., Theory of Functionals and of Integral and Integro-Differential Equations, Edmund Whittaker, New York, Dover Publications, 1959.

54. Williams, M.L., "Structural Analysis of Viscoelastic Materials," AIAA Journal, May 1964, Vol. 2, No. 5.

55. Zener, C., Elasticity and Anelasticity of Metals, University of Chicago Press, Chicago, 1948.

APPENDICES

APPENDIX A

LIST OF TABLES

APPENDIX B

LIST OF FIGURES

APPENDIX C

DETAILED FIGURES
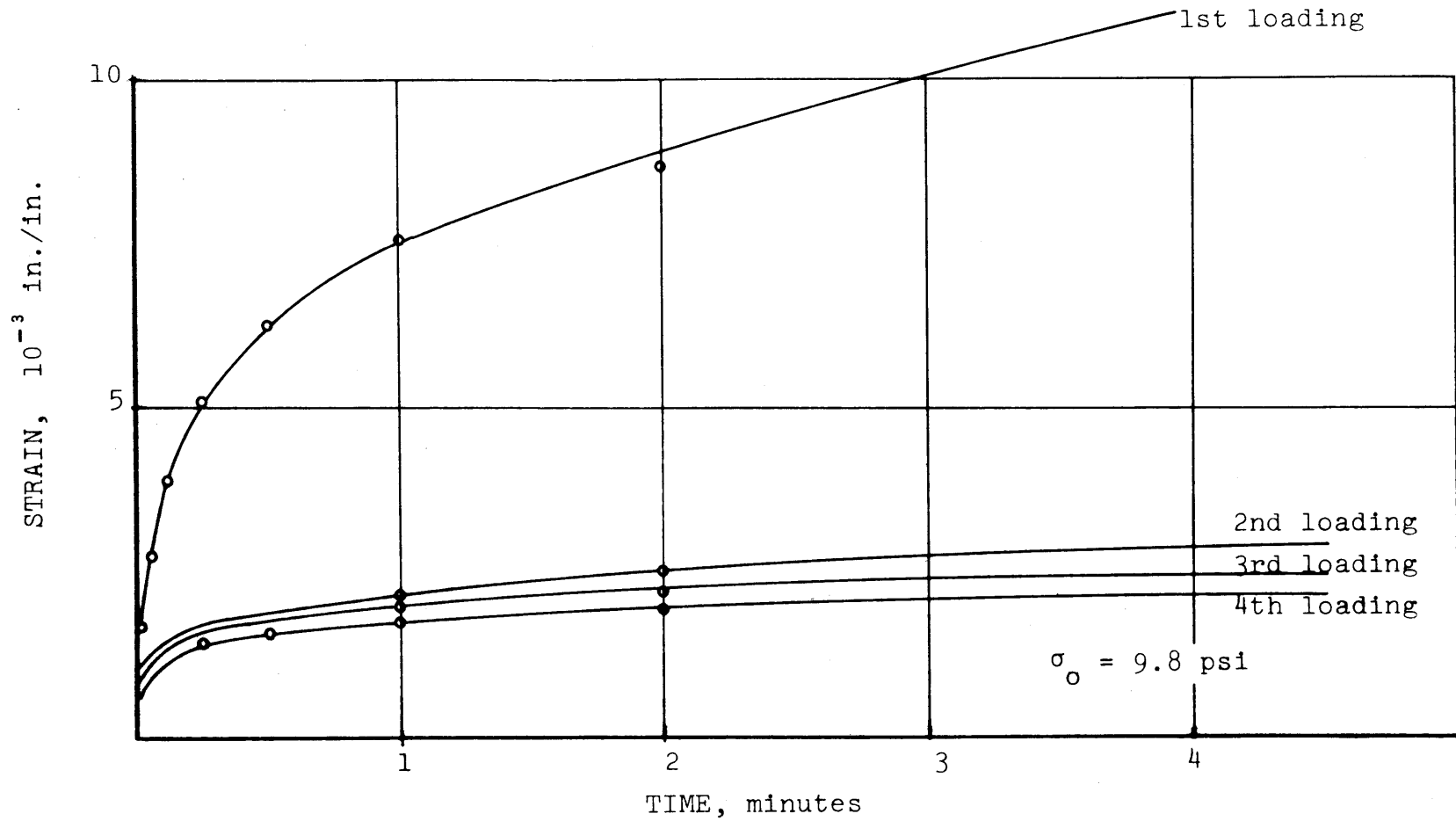
Figure 27.   Effect of Repetition of loading on Creep Curves at 35°C
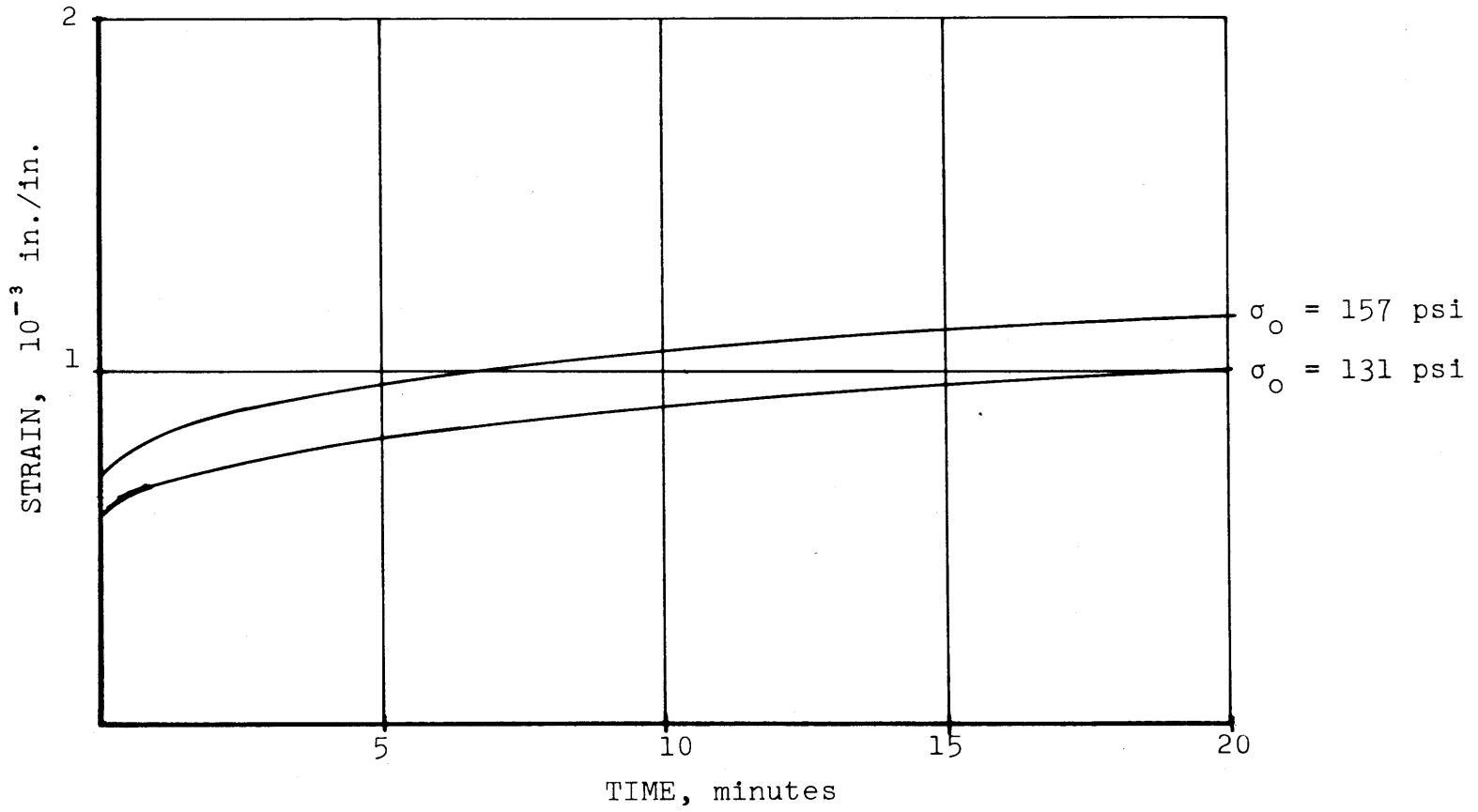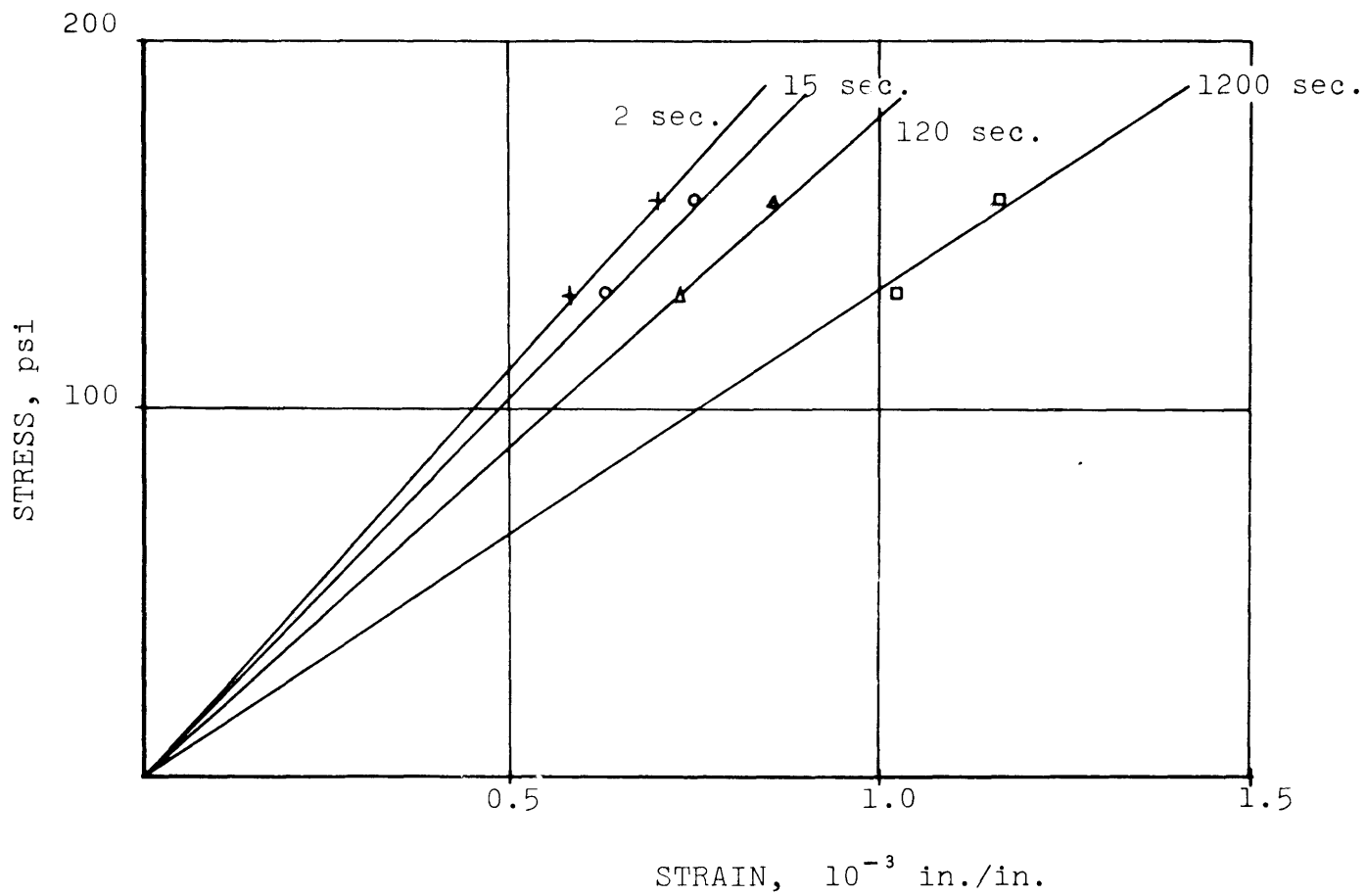
Figure 28.   Creep Curves at -5°C

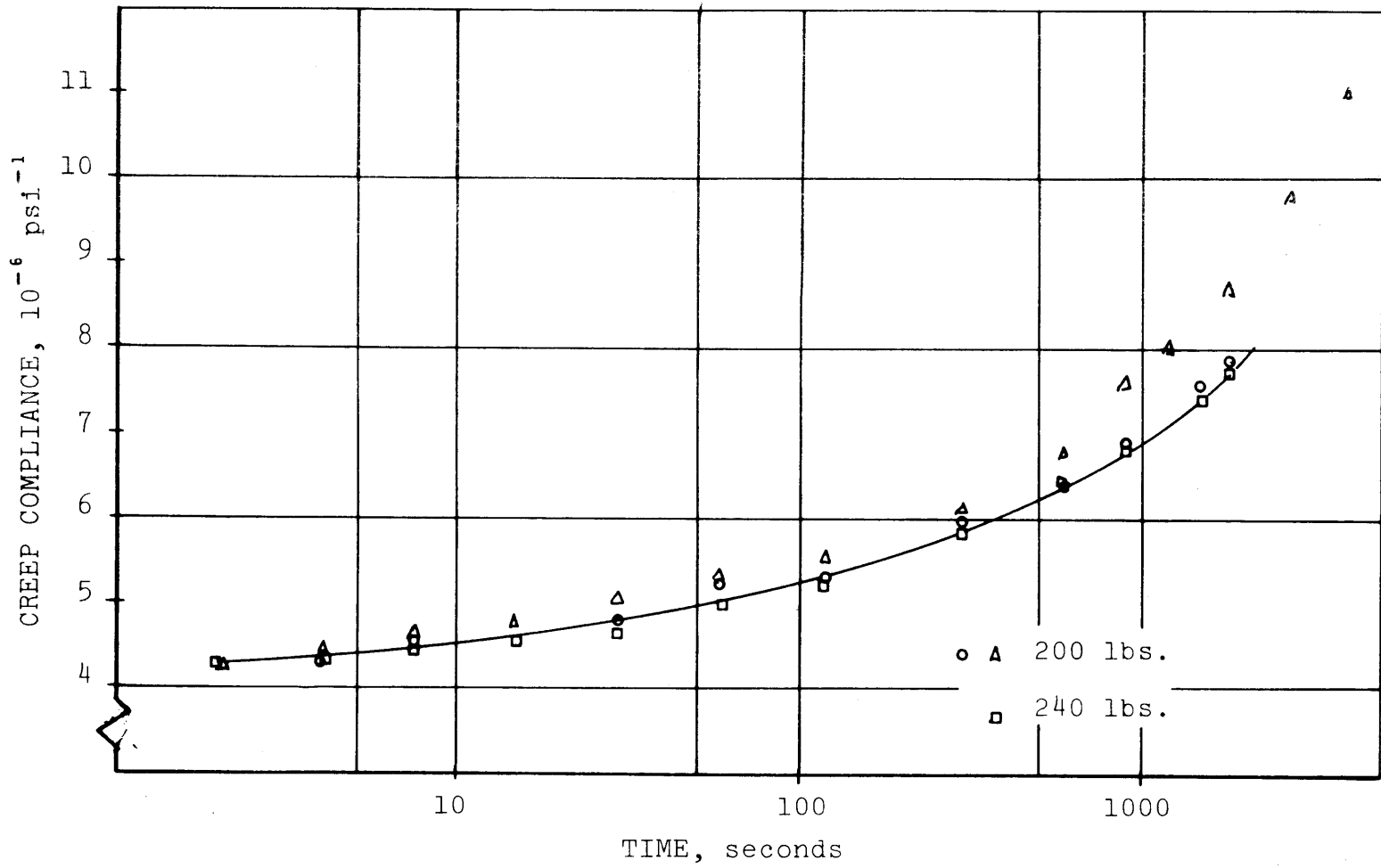Figure 29.   Isochrones from Creep at -5°C

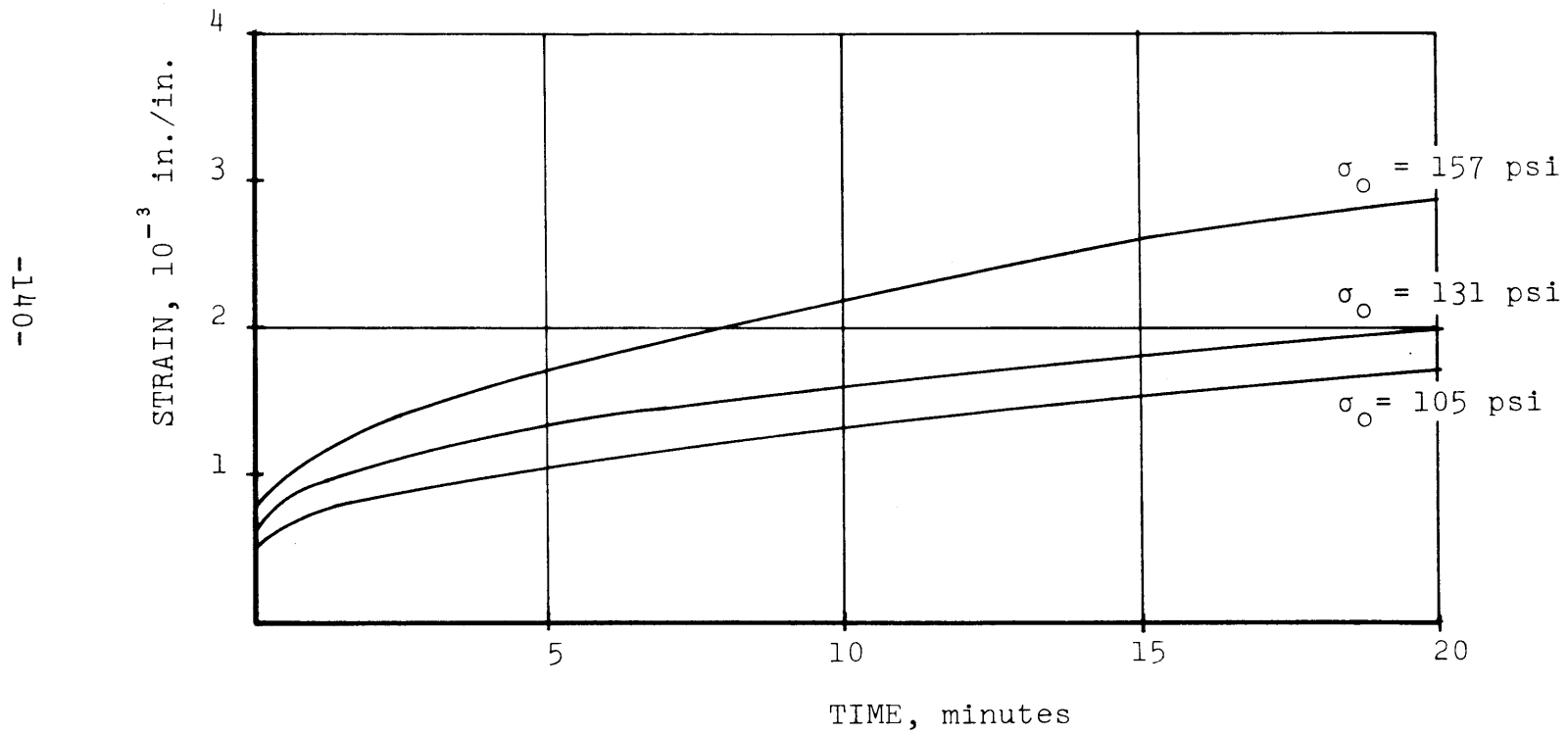Figure 30.   Creep Compliance at -5°C
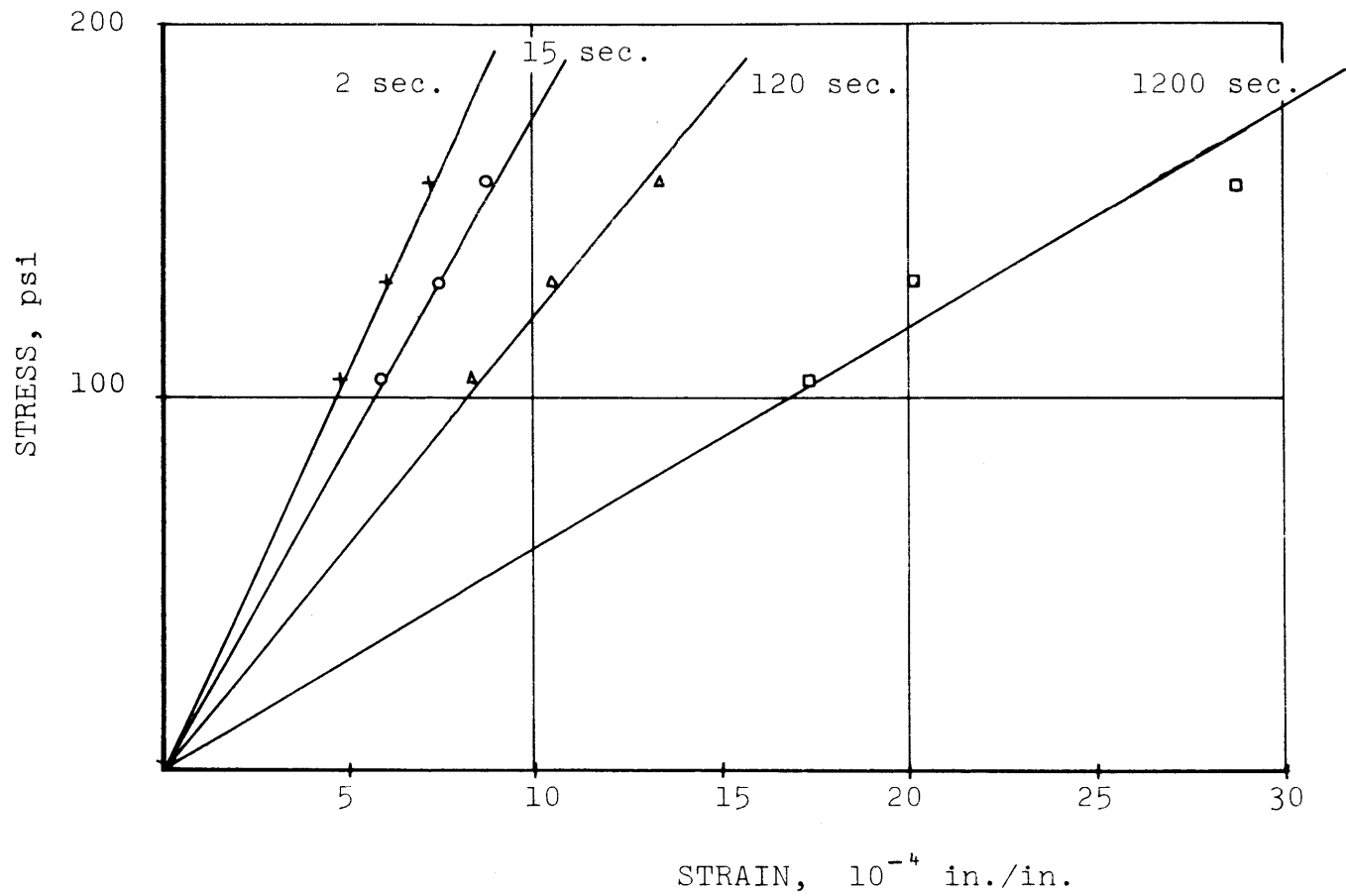
Figure 31.   Creep Curves at 5°C
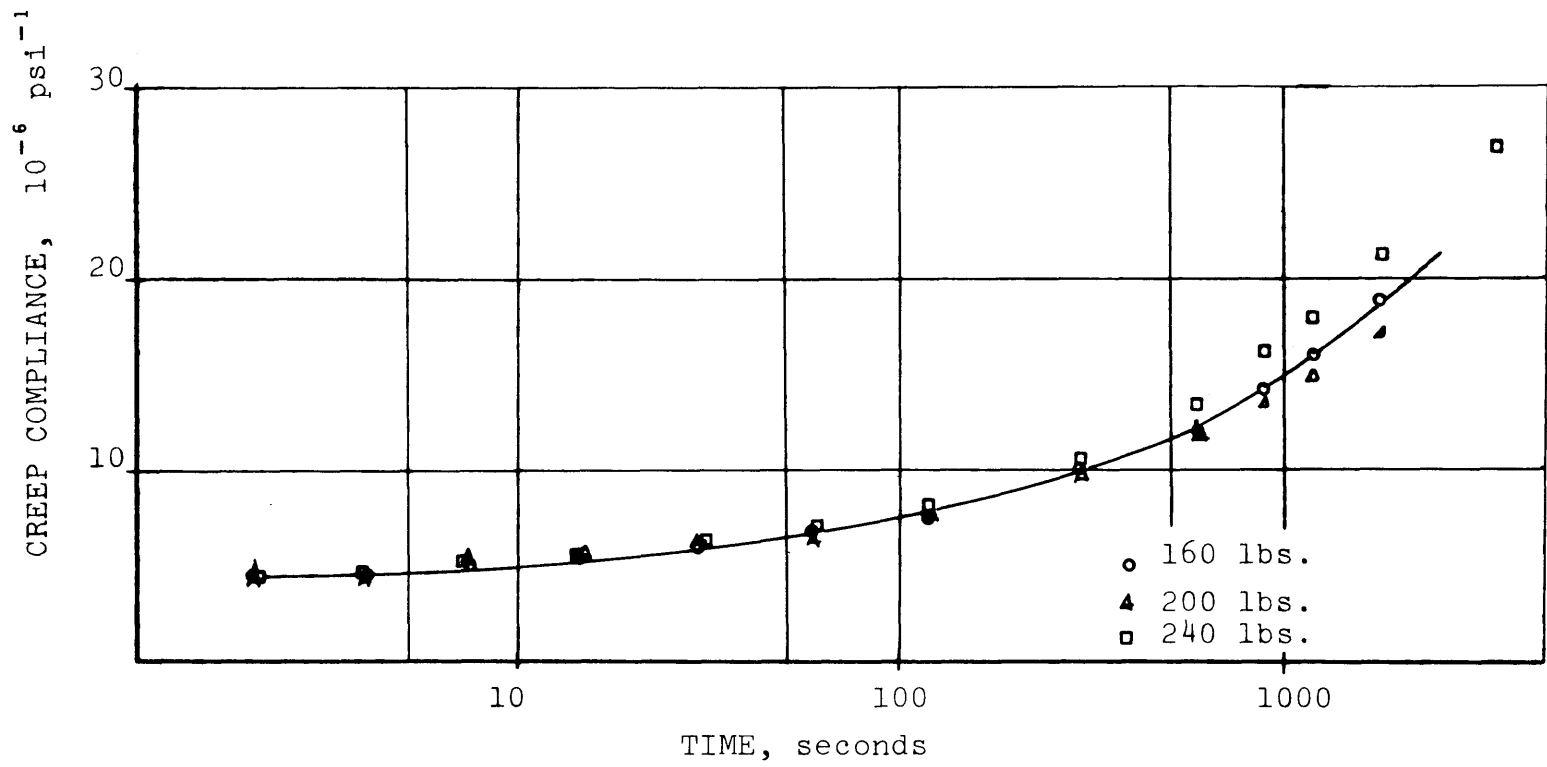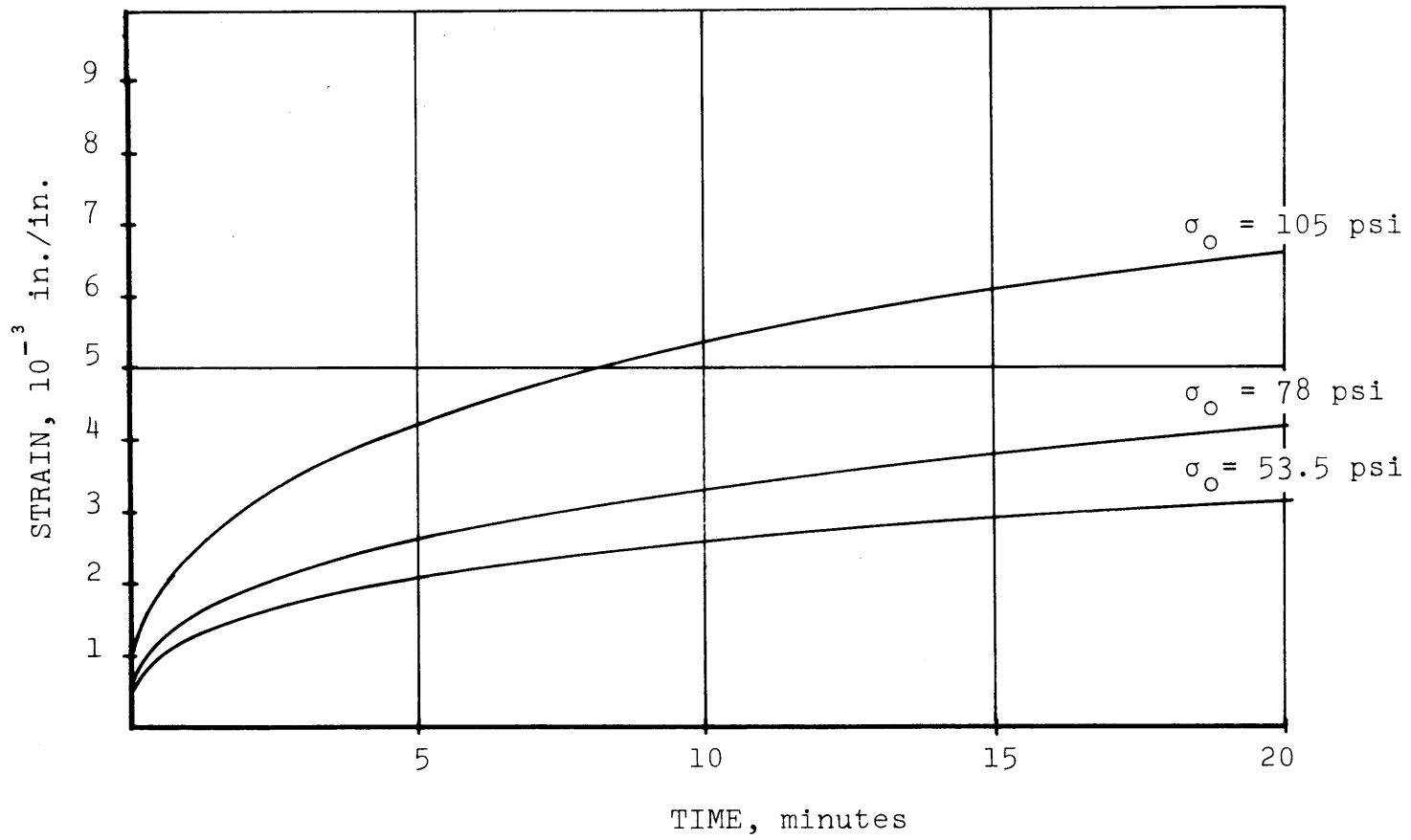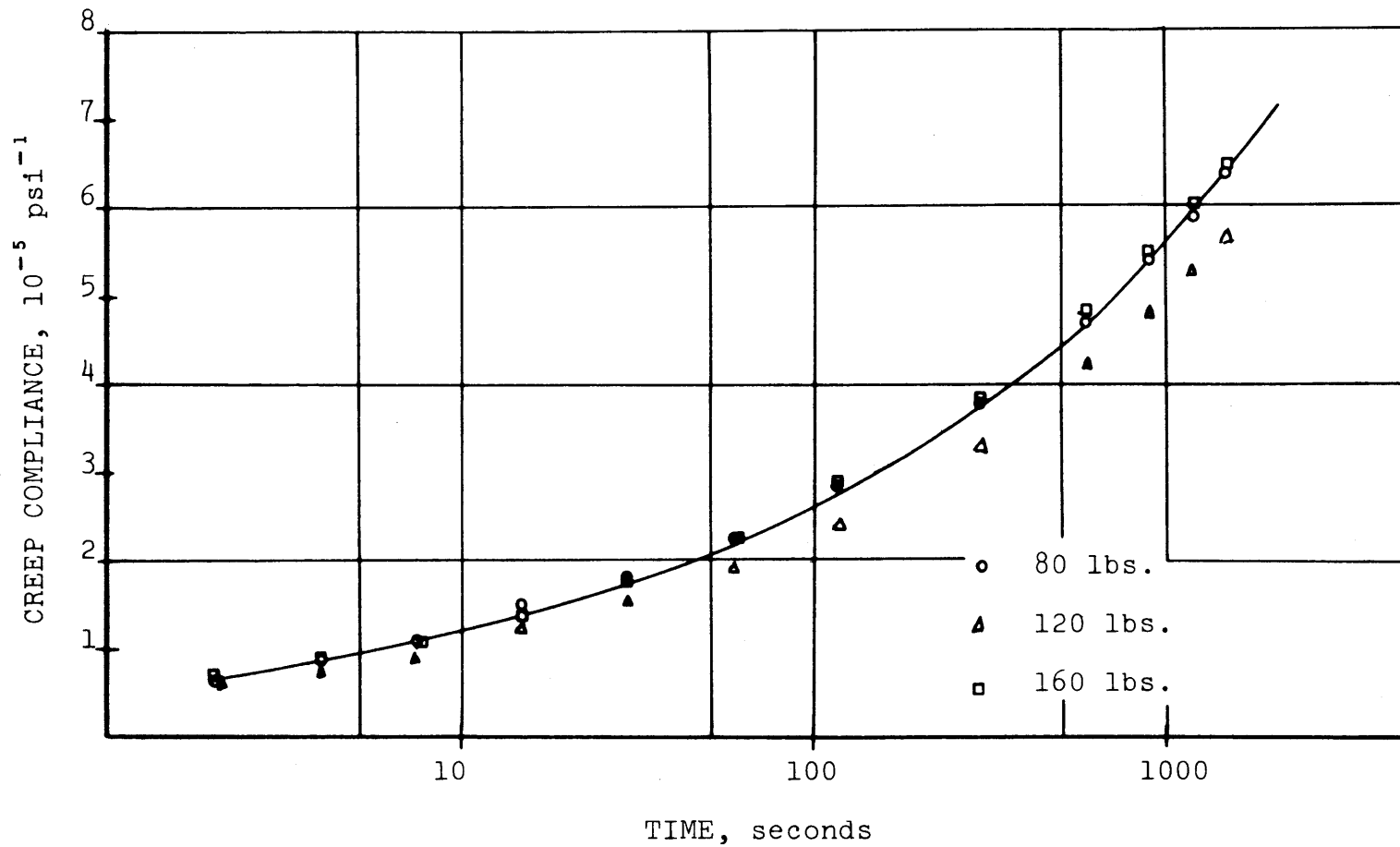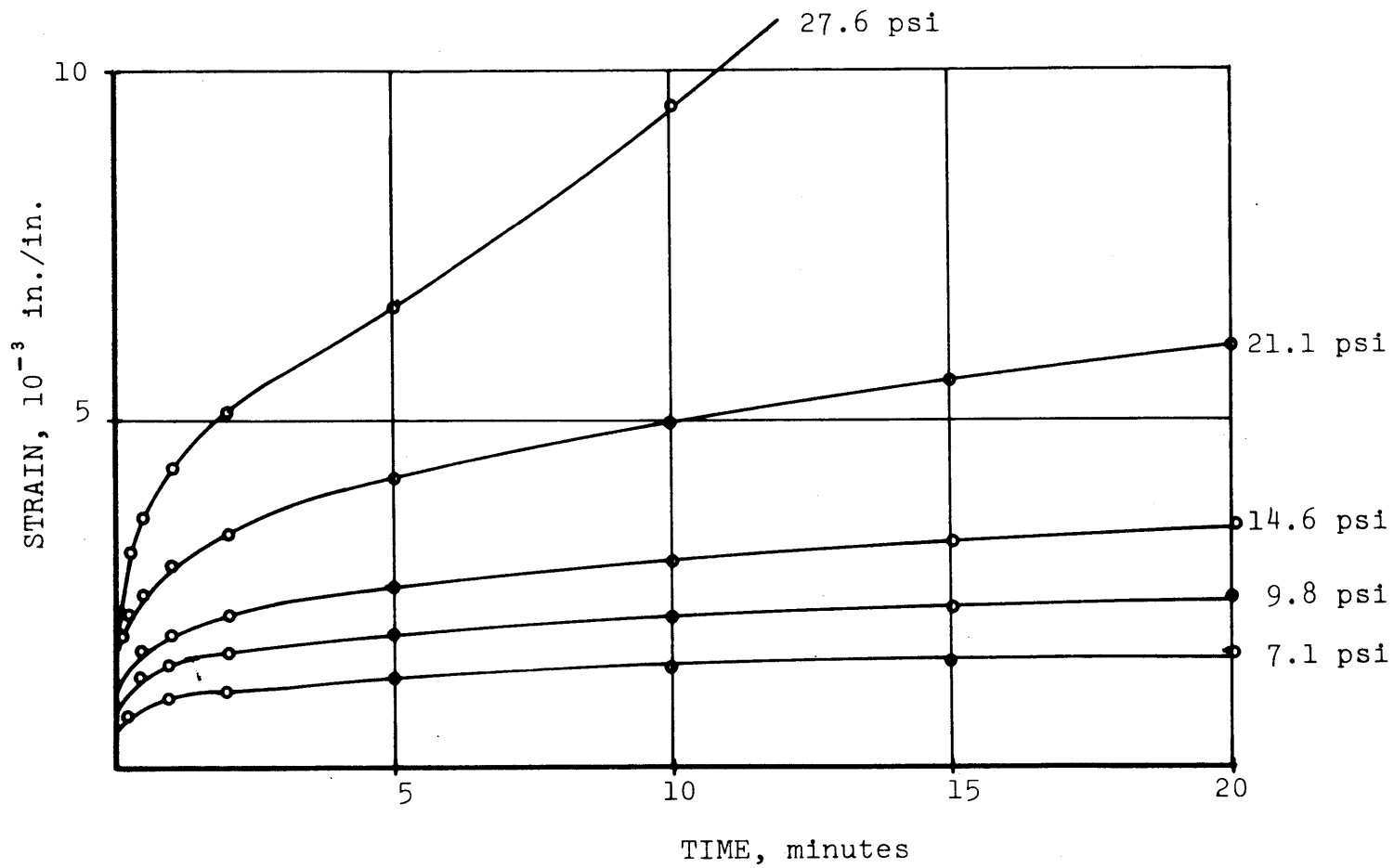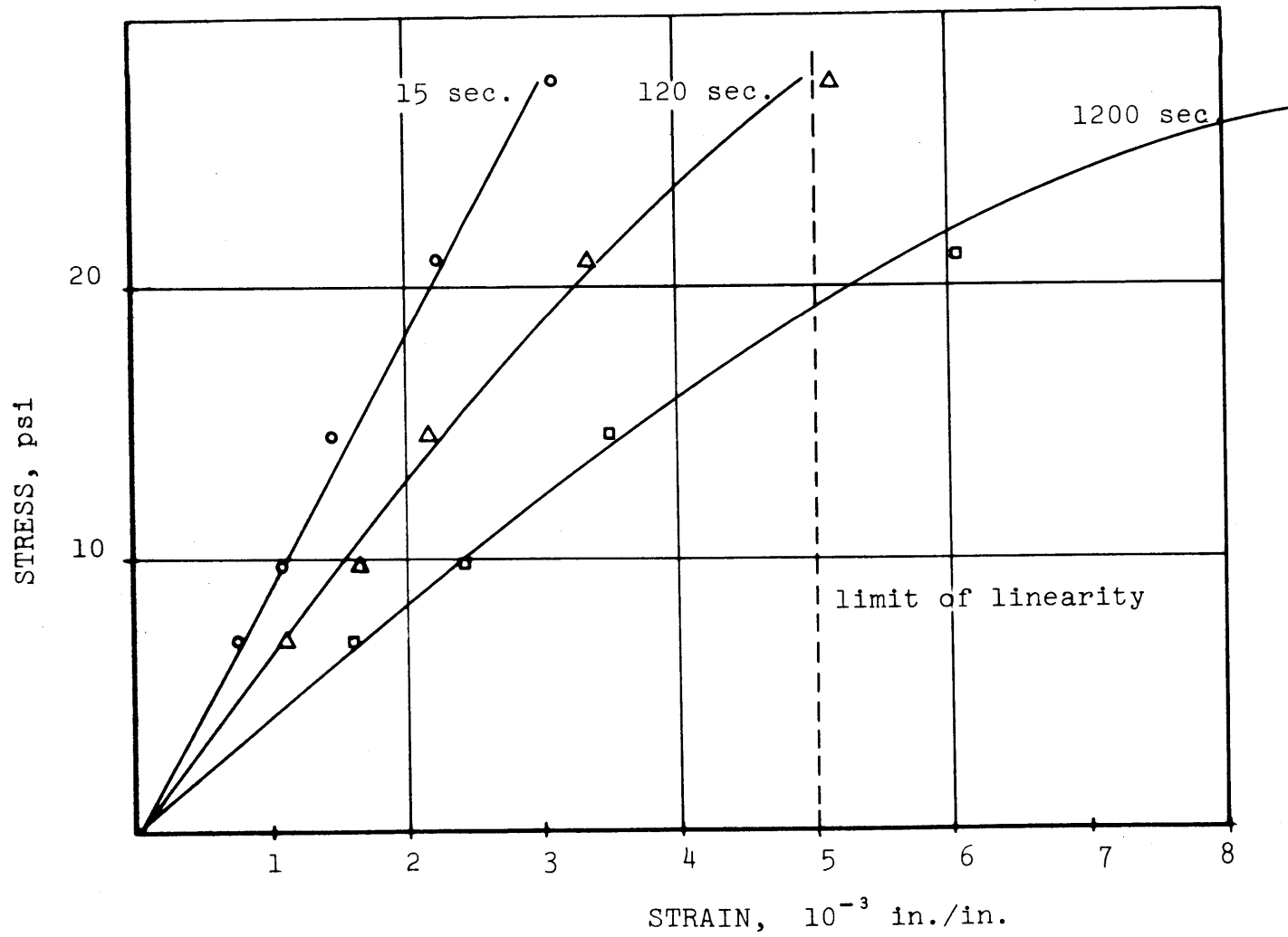
Figure 32.   Isochrones from Creep at 5°C

Figure 33. Creep Compliance at 5°C

Figure 34.   Creep Curves at 15°C

Figure 36.   Creep Compliance at 15°C

Figure 37.   Creep Curves at 35°C
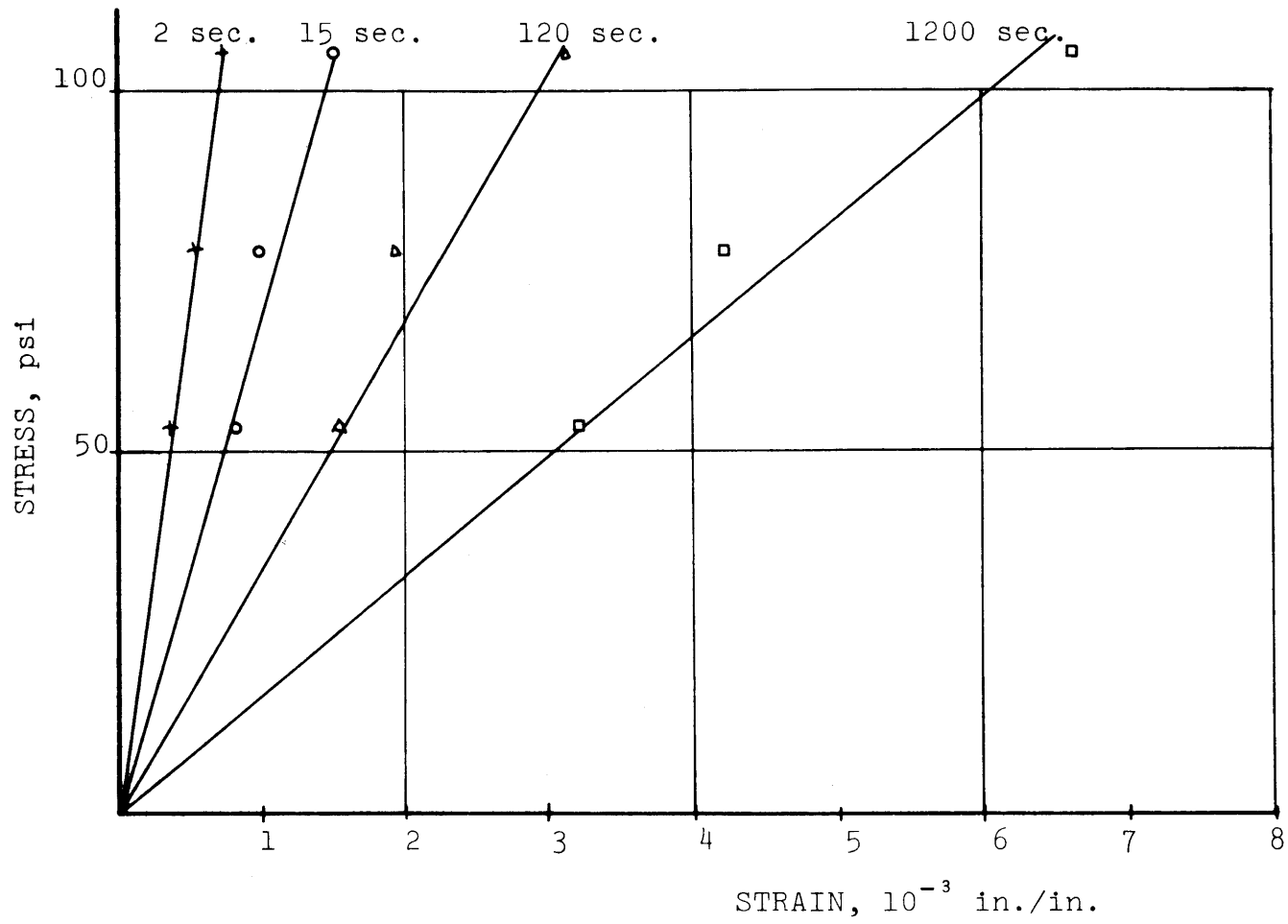
Figure 38.   Isochrones from Creep at 35°C

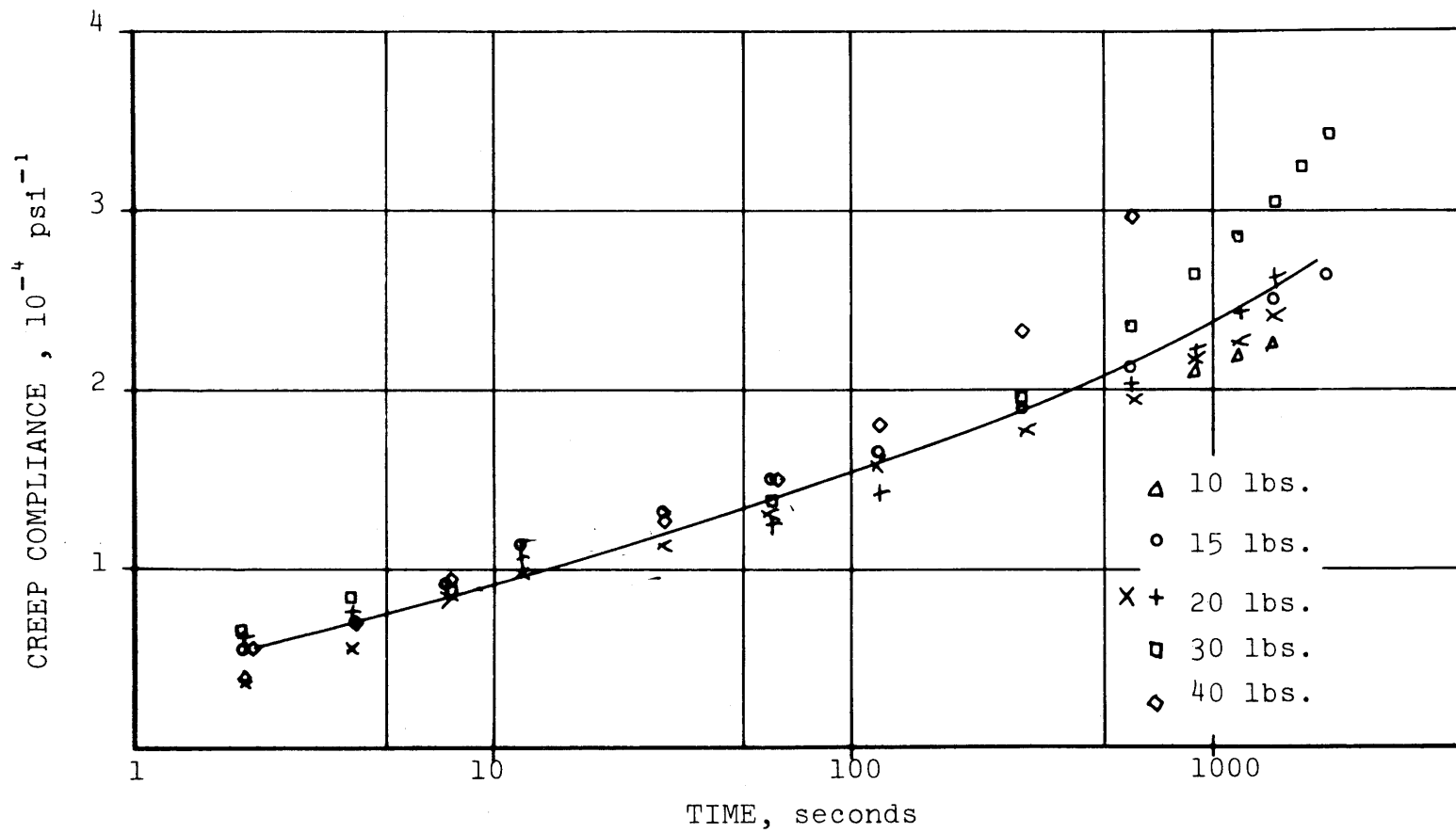Figure 35.   Isochrones from Creep at 15°C
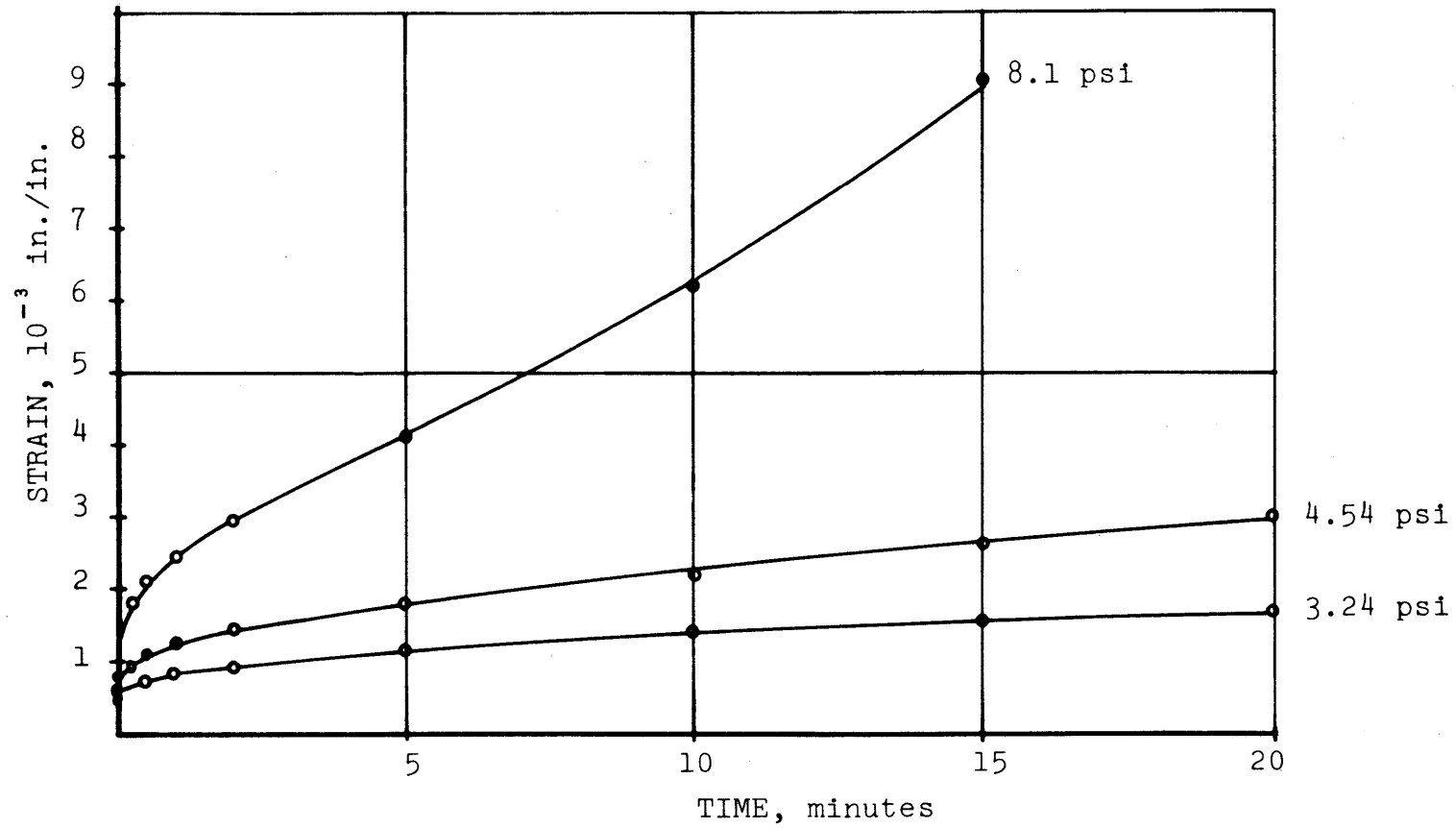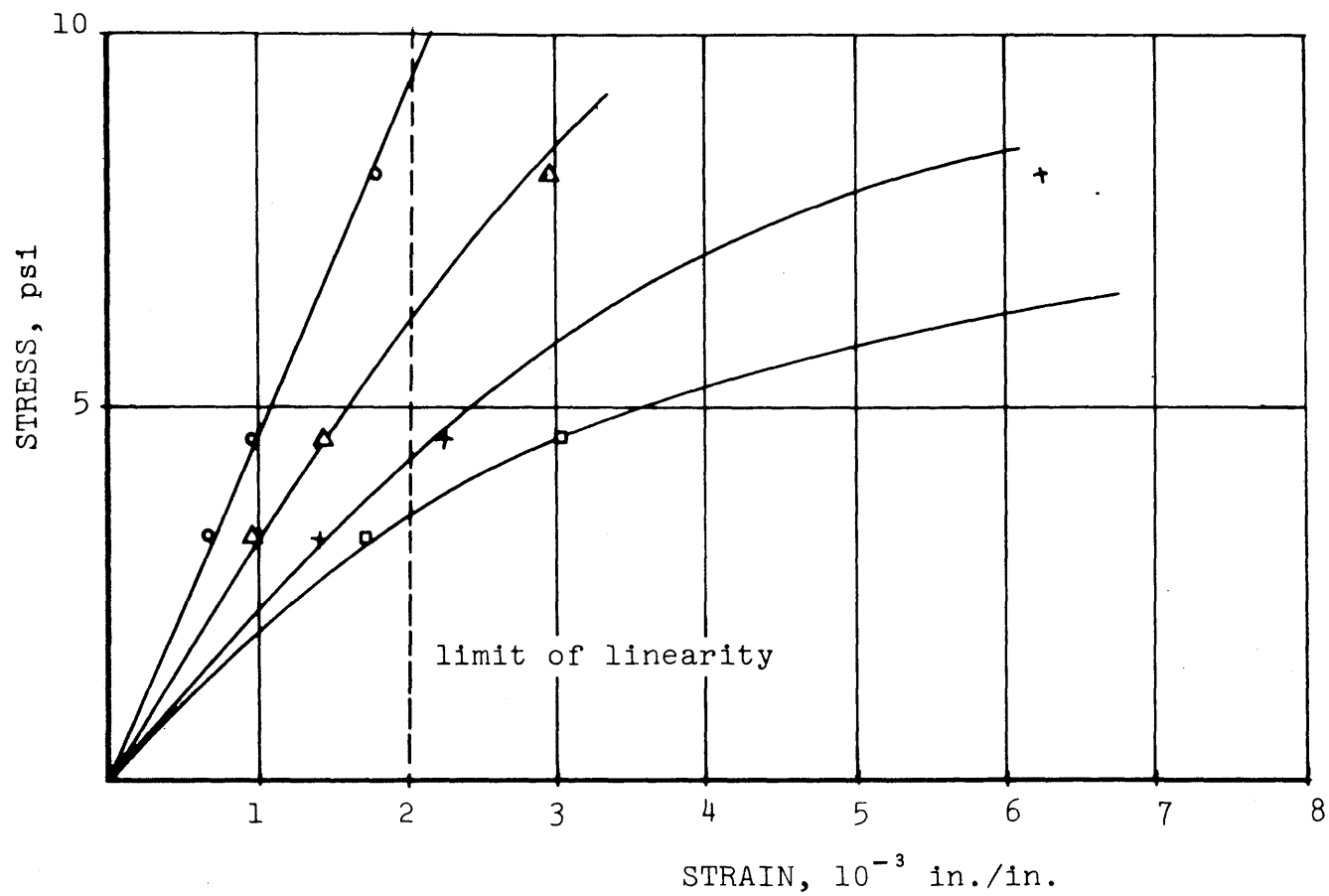
Figure 39.   Creep Compliance at 35°C

Figure 40. Creep Curves at 45°C

Figure 41.   Isochrones from Creep at 45°C

Figure 42.   Creep Compliance at 45°C

STRESS, 10^2 psi

$\varepsilon_o = 4.96 \times 10^{-3}$ in./in.

$\varepsilon_o = 2.68 \times 10^{-3}$ in./in.

TIME, minutes

Figure 43.   Stress Relaxation Curves
             at -5°C

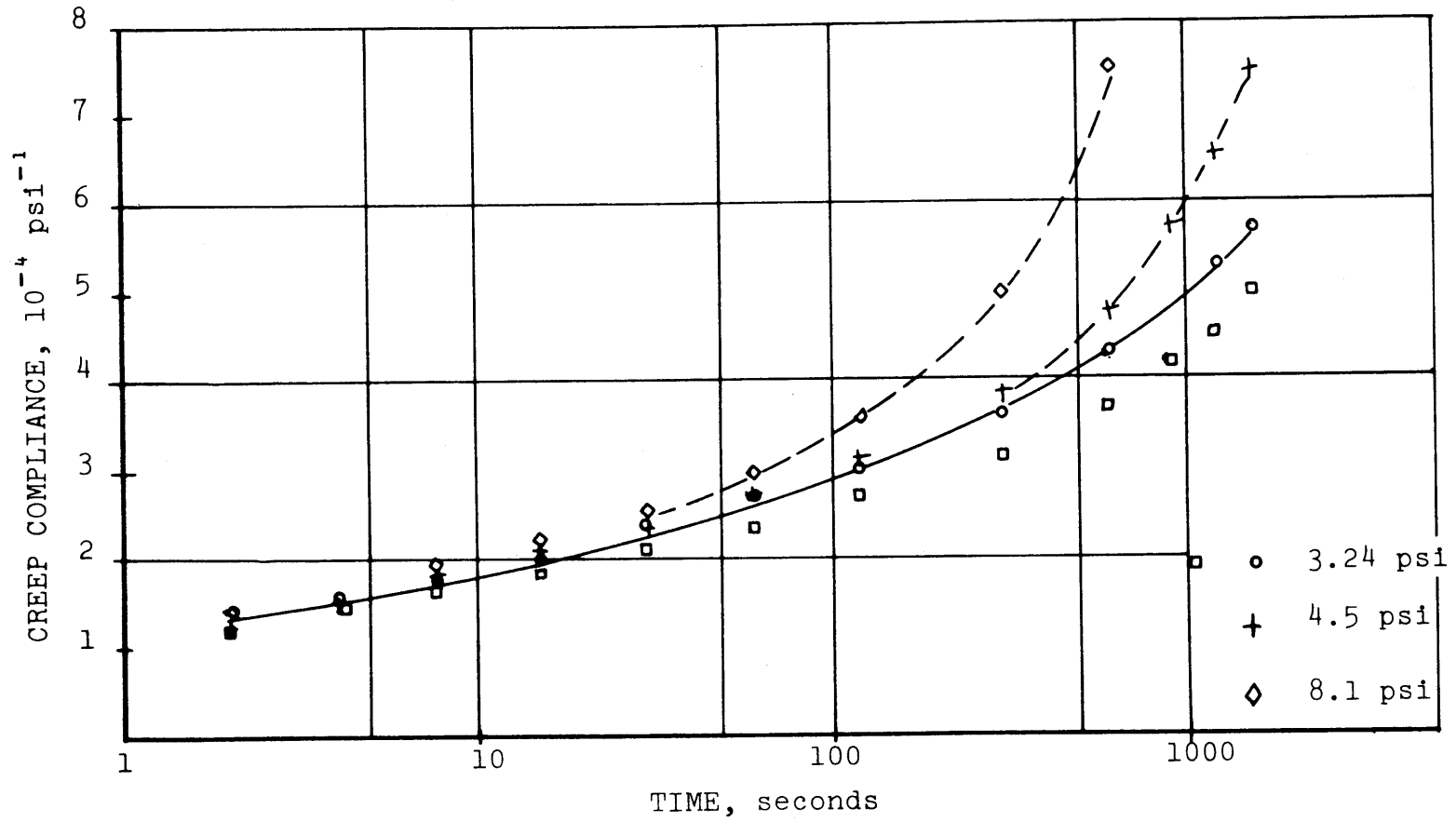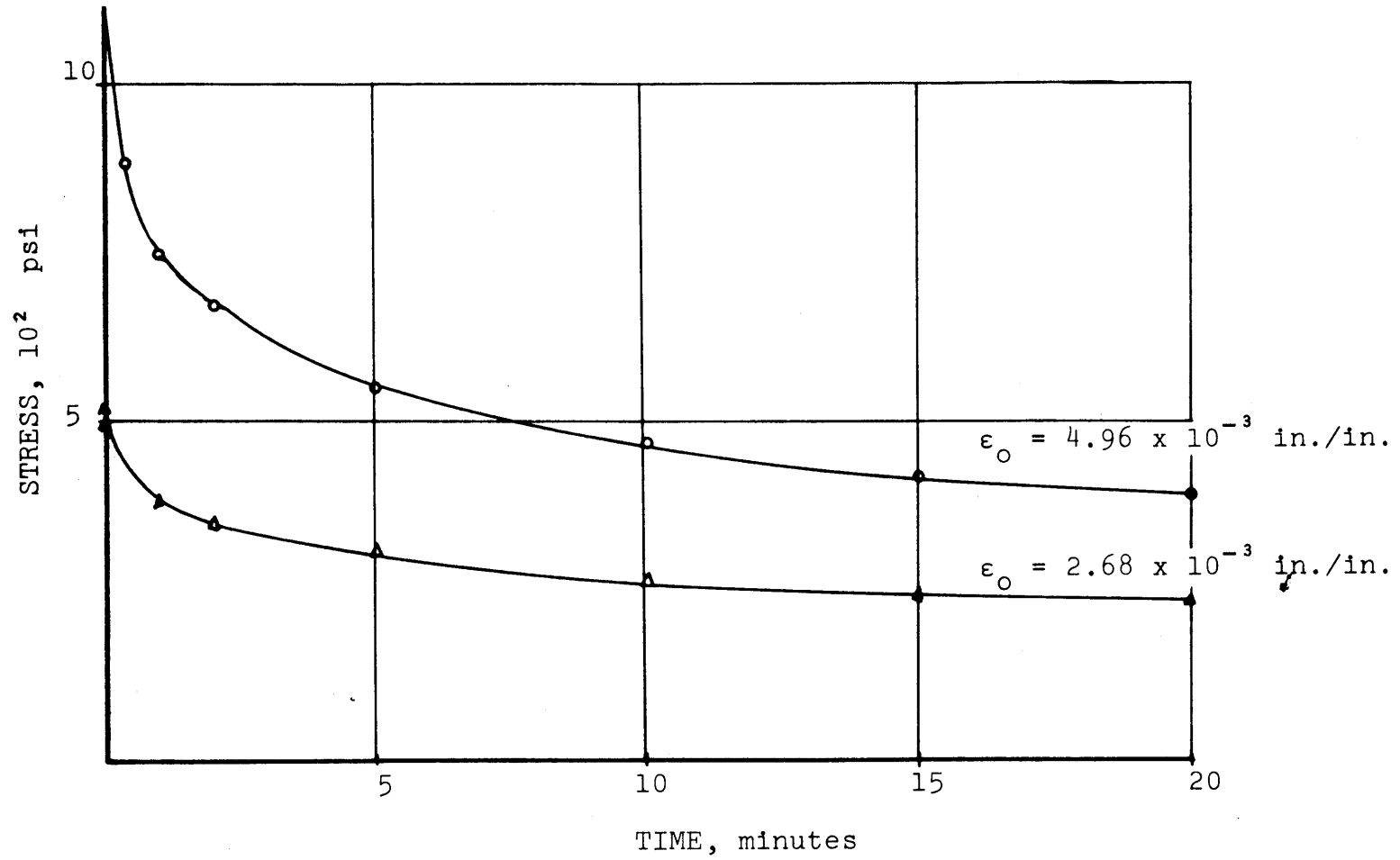Figure 44.   Isochrones from Stress Relaxation at
-5°C

Figure 45. Relaxation Modulus at -5°C

Figure 46.   Stress Relaxation Curves at 5°C

Figure 47.   Isochrones from Stress Relaxation
at 5°C

Figure 48.   Relaxation Modulus at 5°C

Figure 49. Stress Relaxation Curves at 15°C

Figure 50.   Isochrones from Stress Relaxation at 15°C

Figure 51. Relaxation Modulus at 15°C

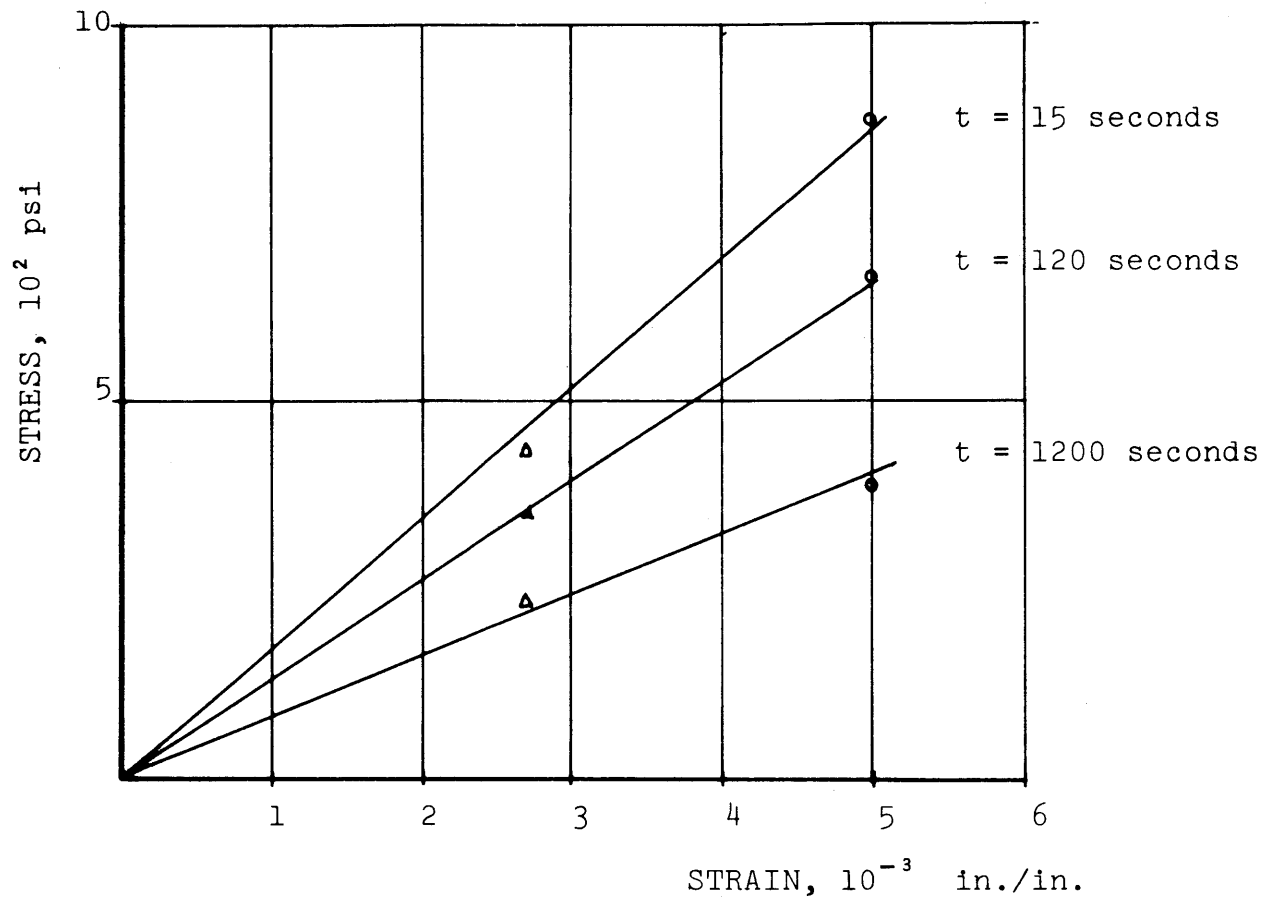Figure 52.   Stress Relaxation Curves at 35°C

Figure 53.   Isochrones from Stress Relaxation at 35°C
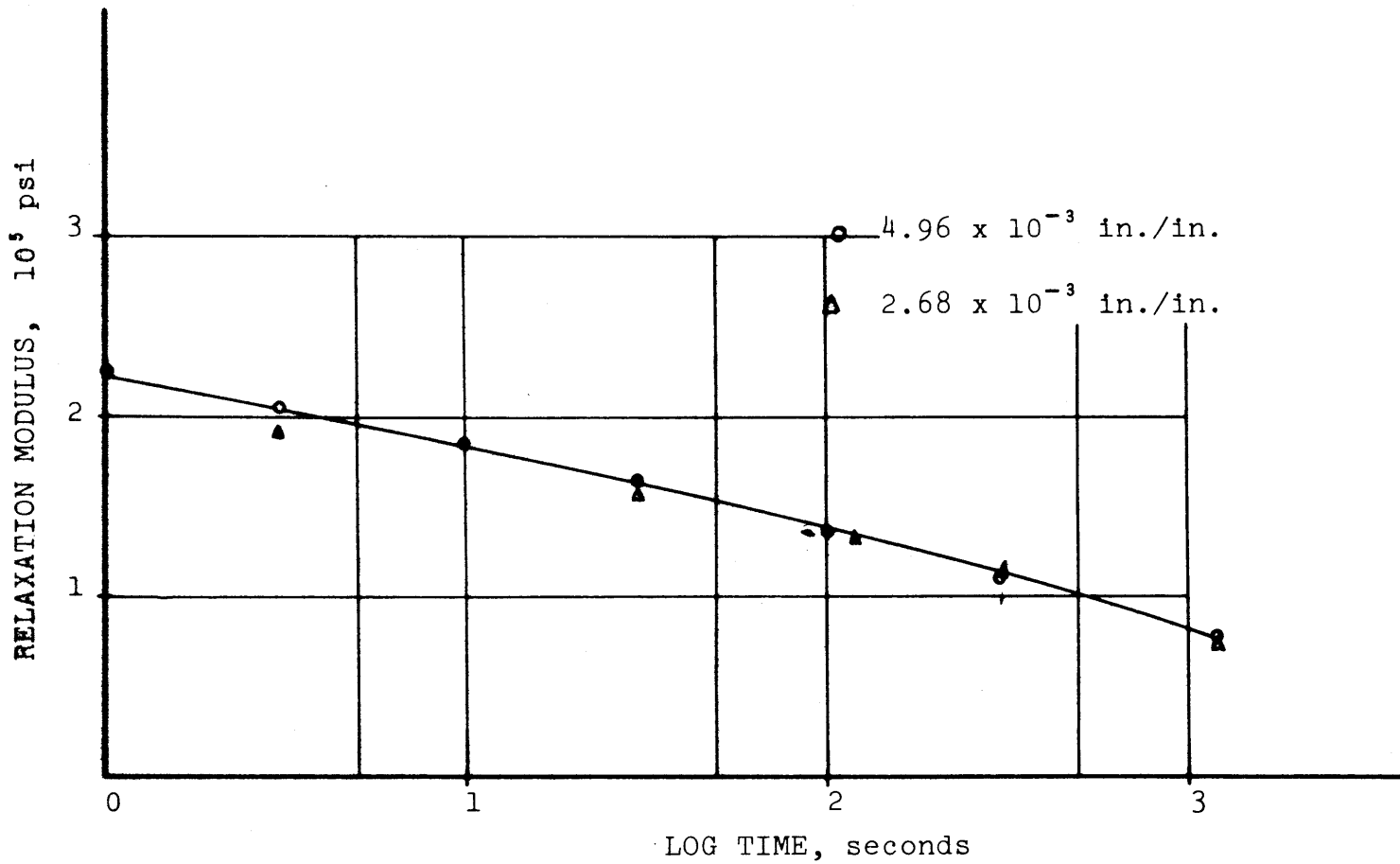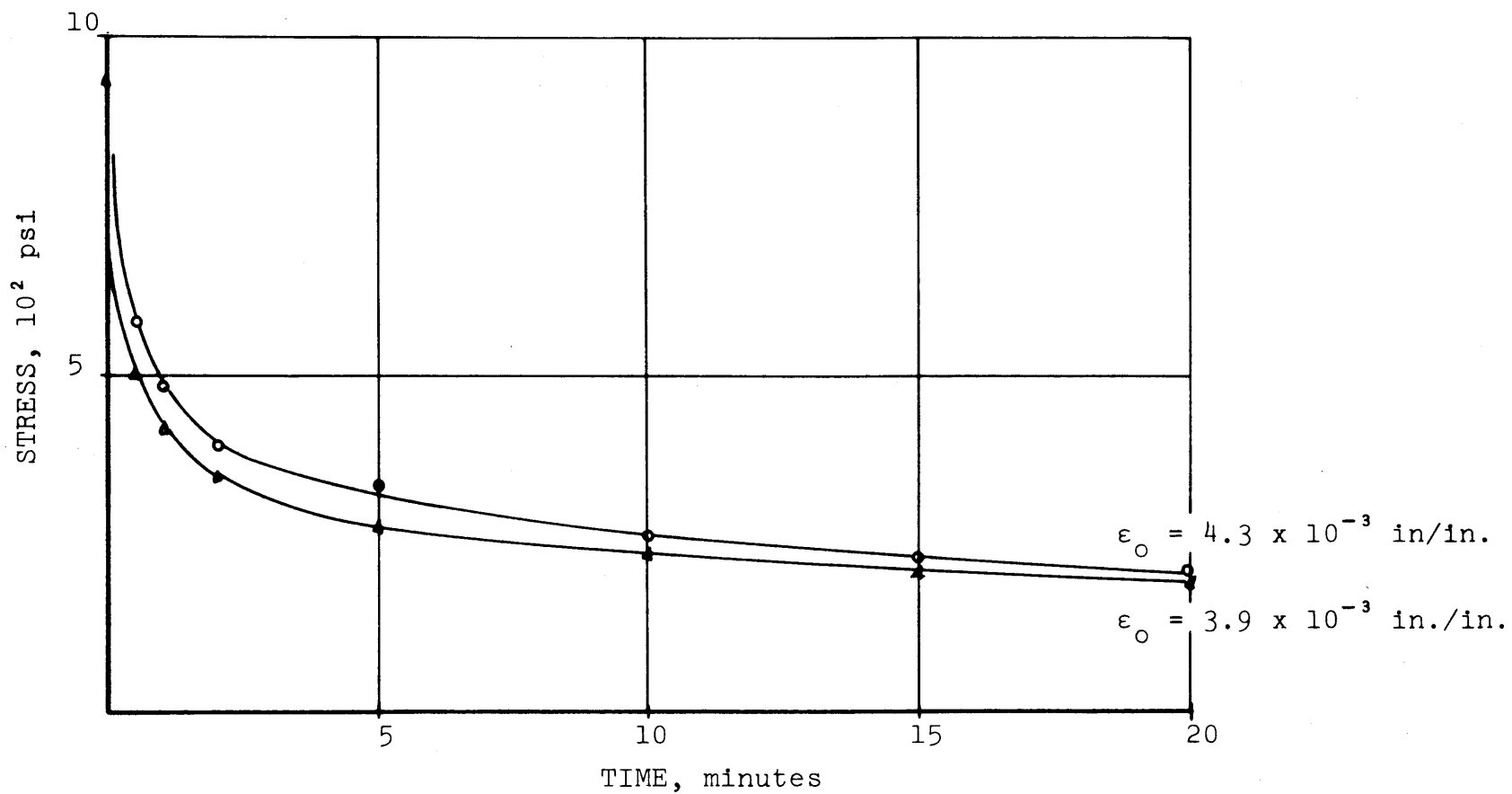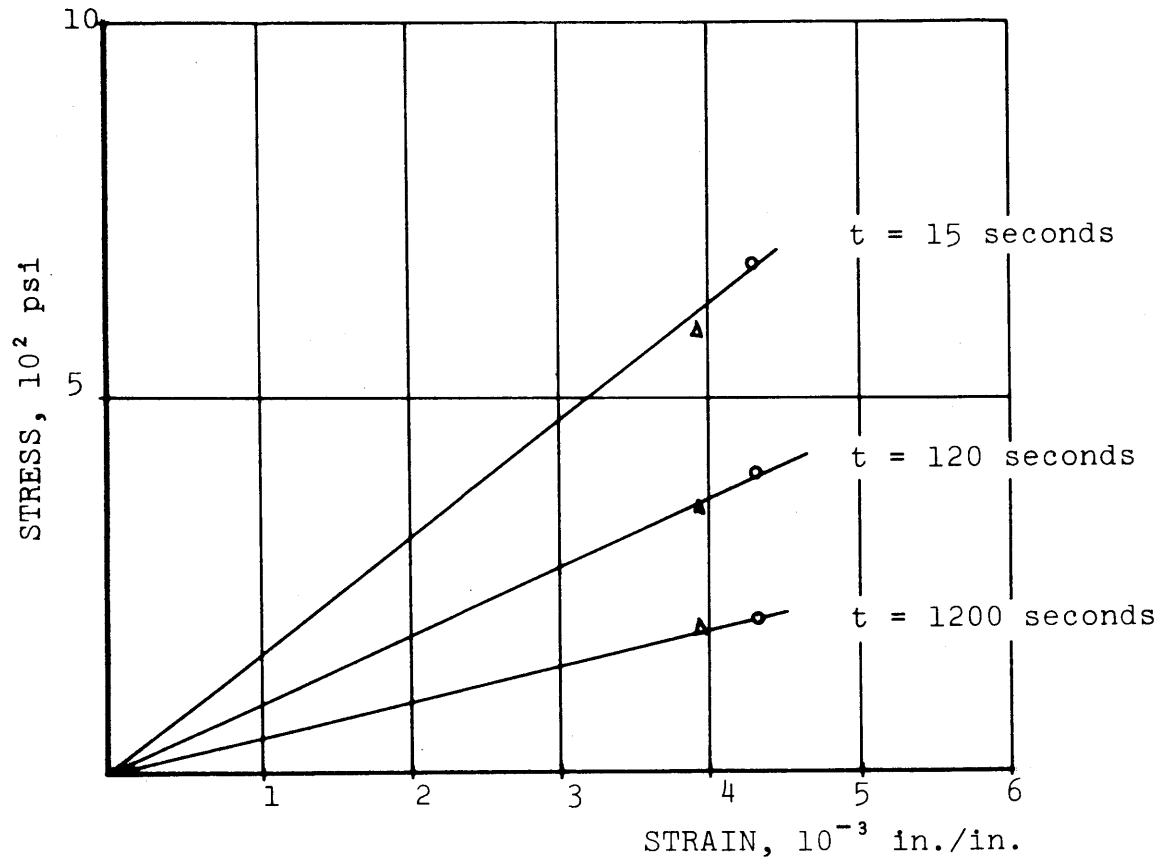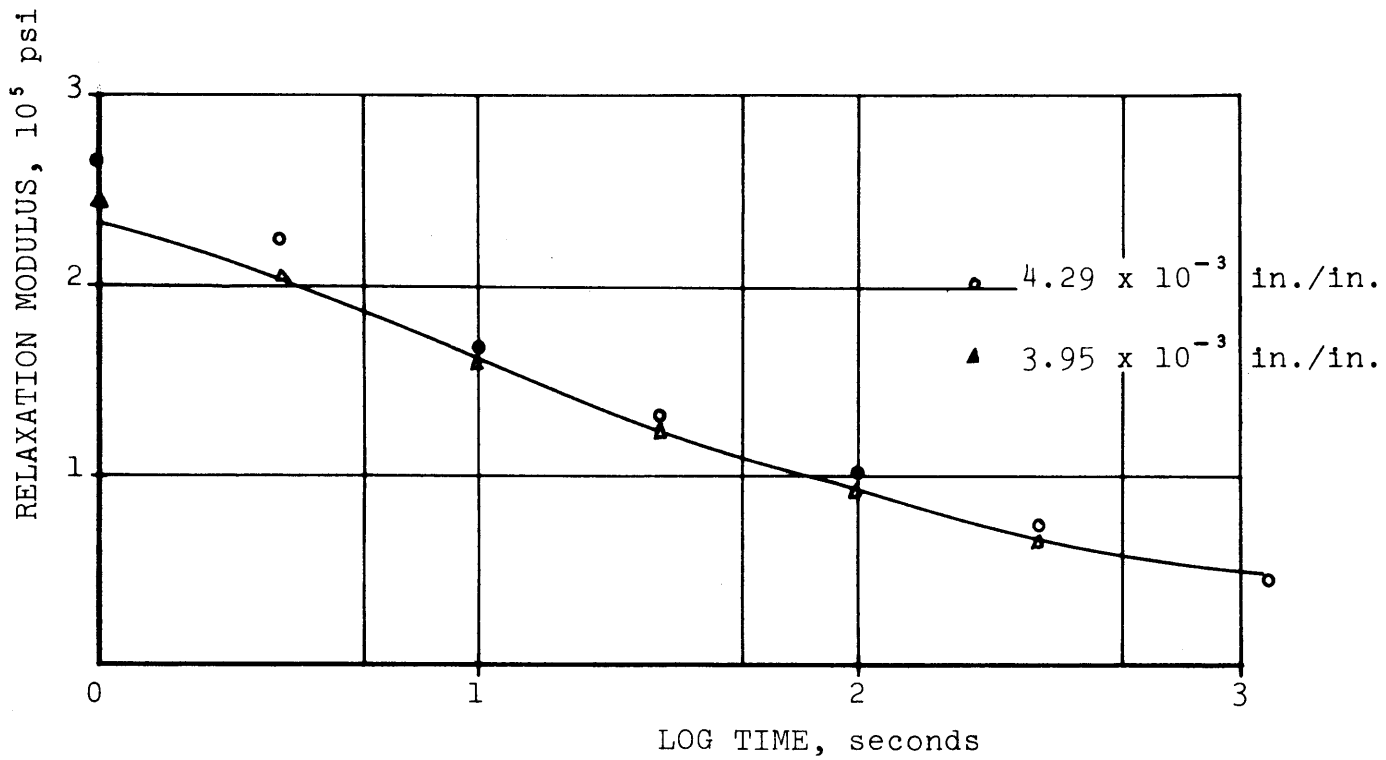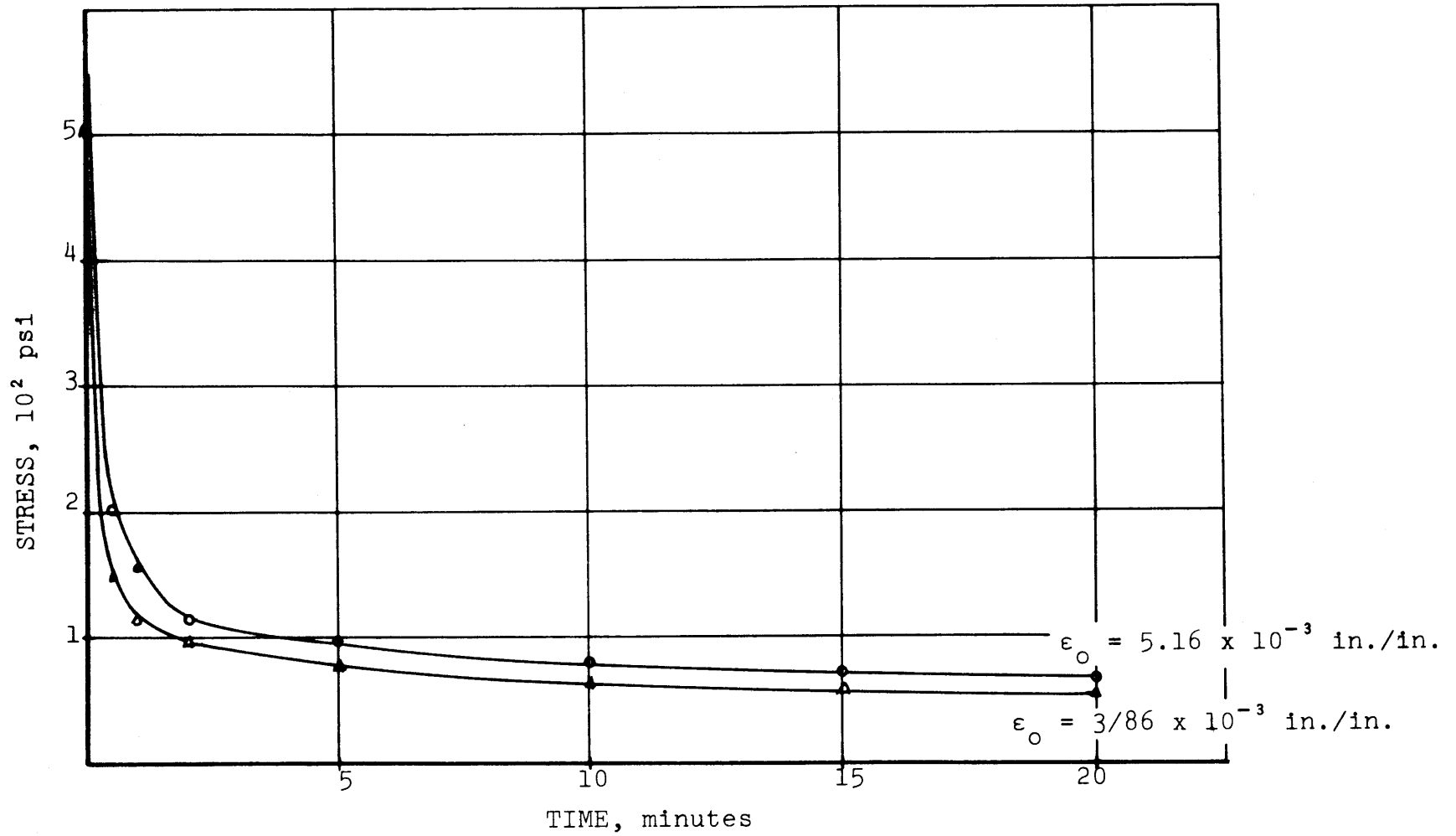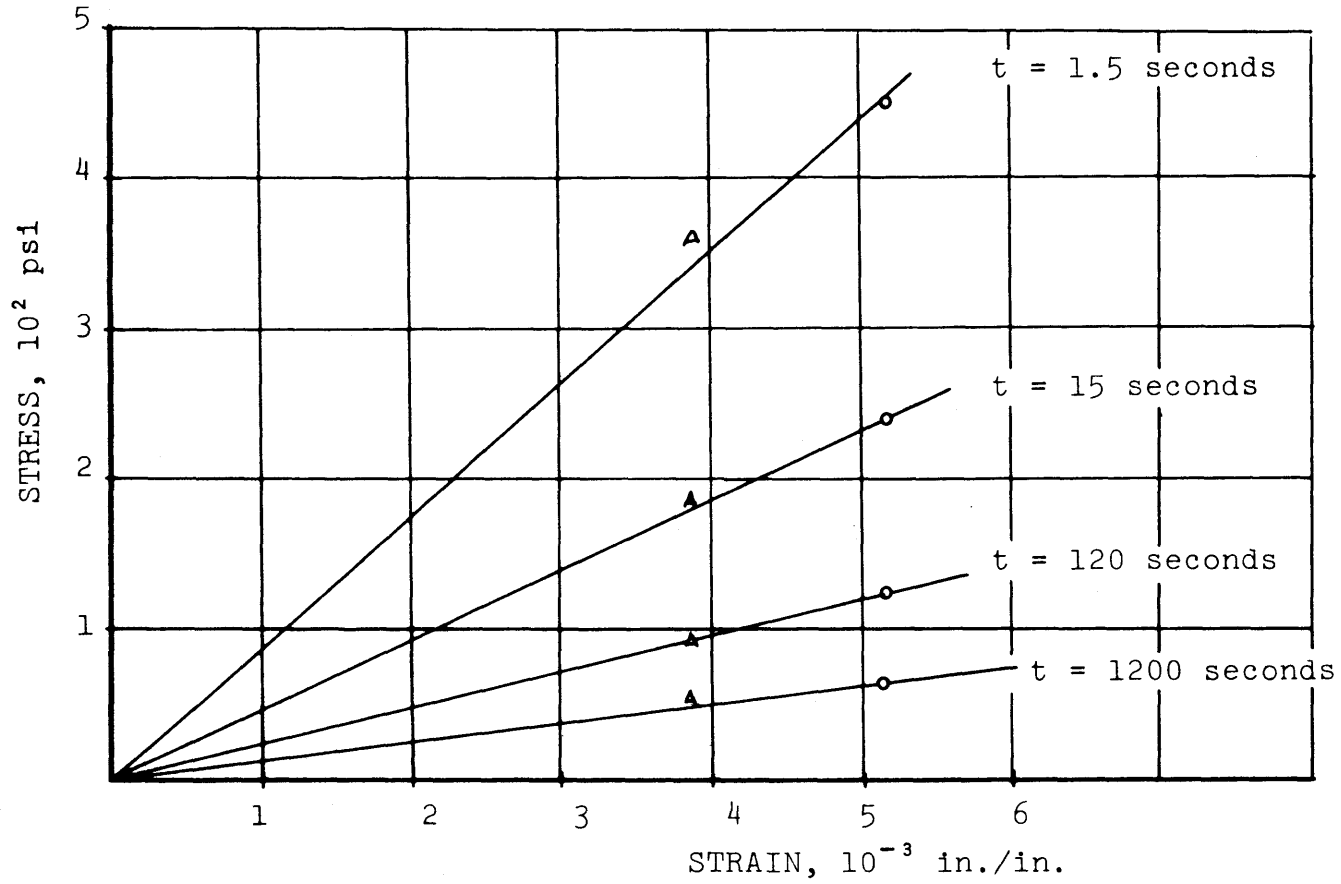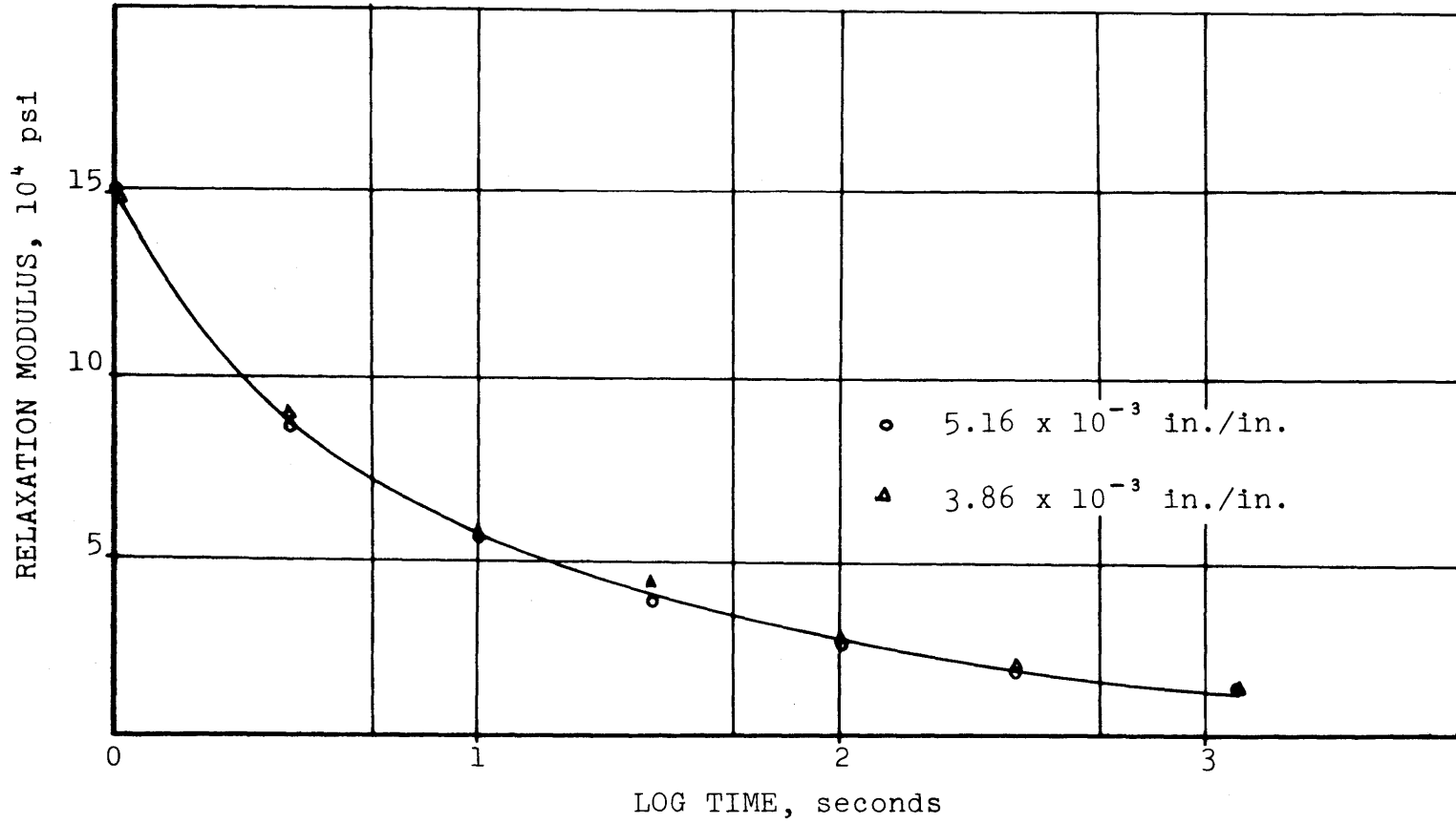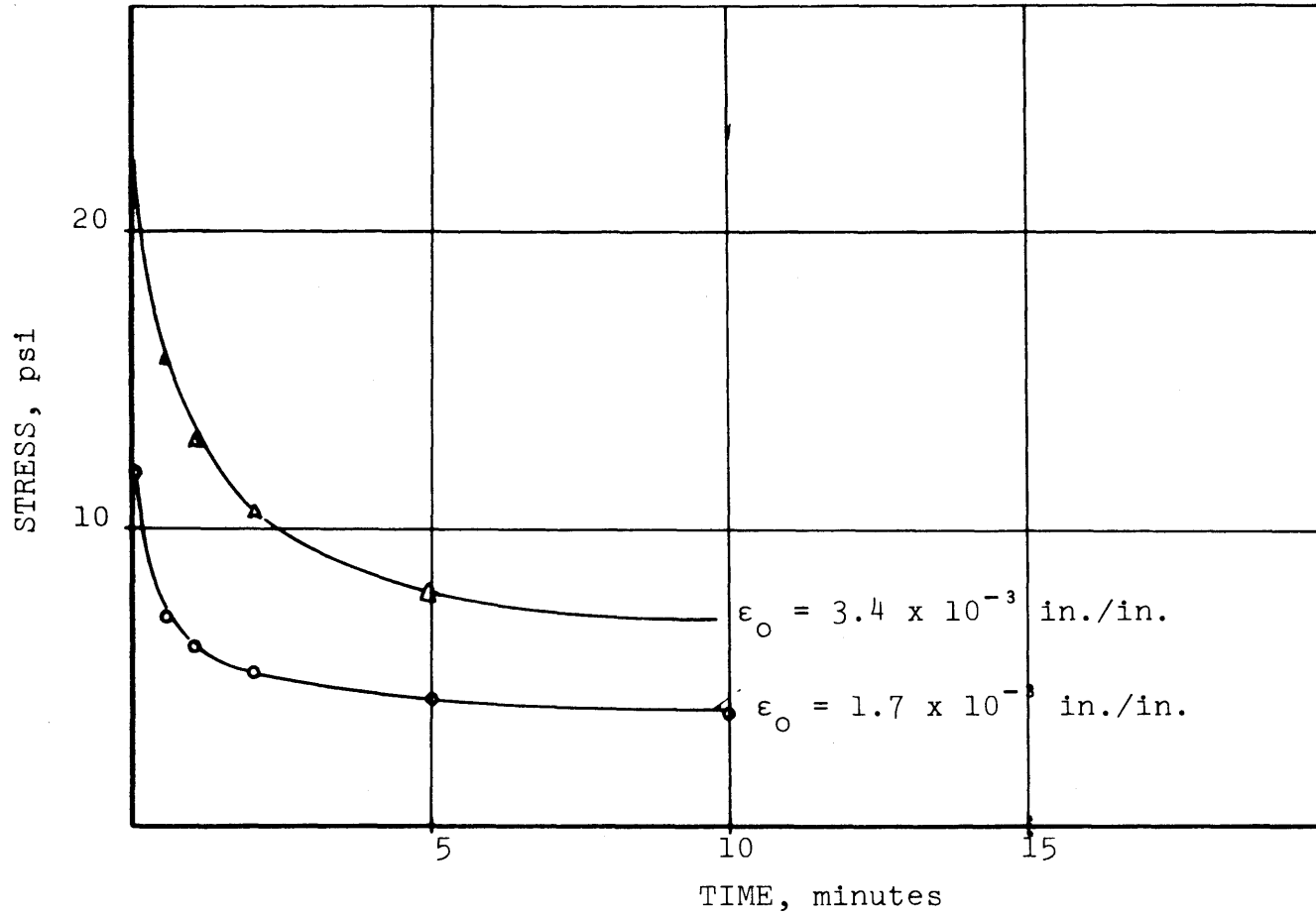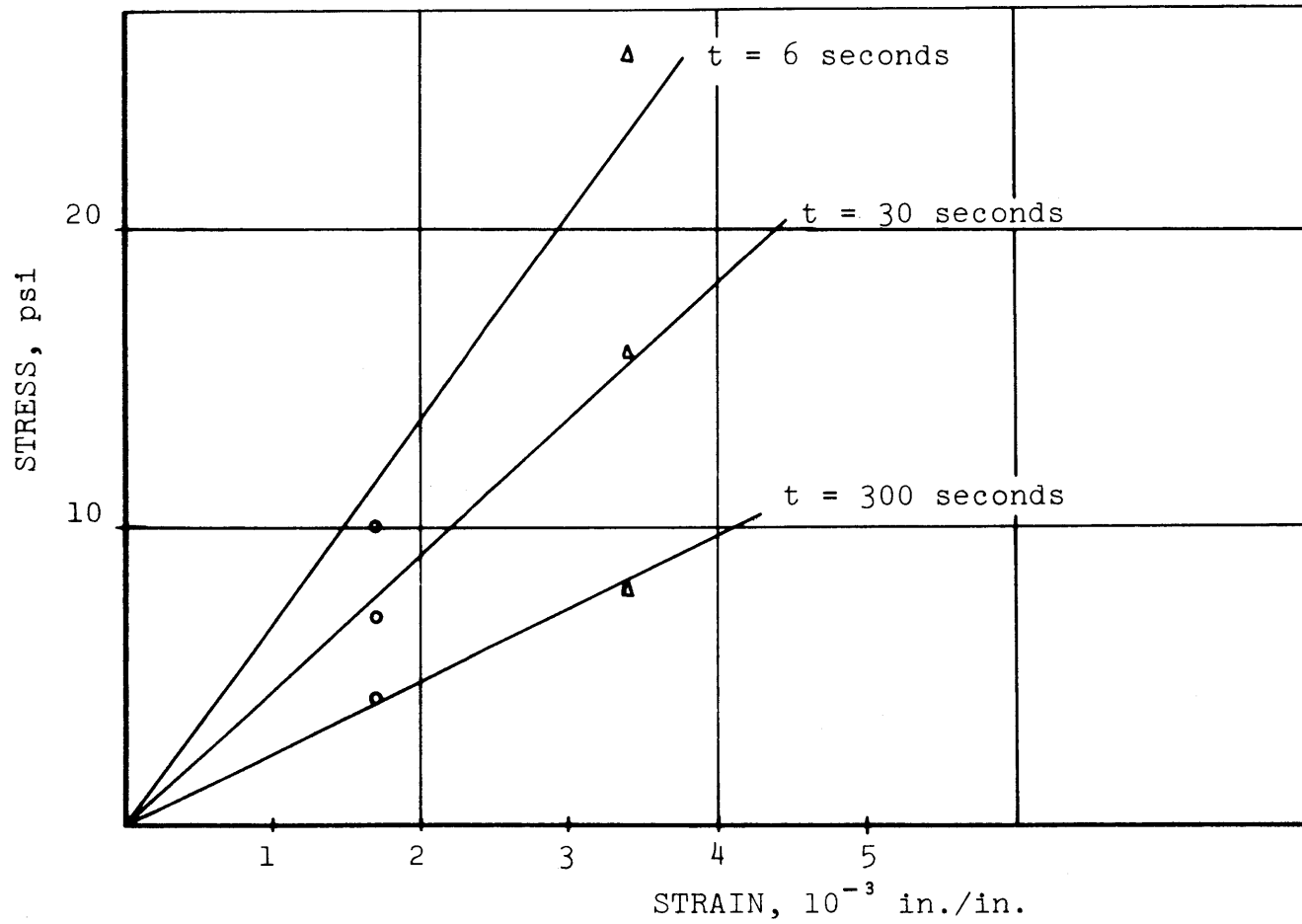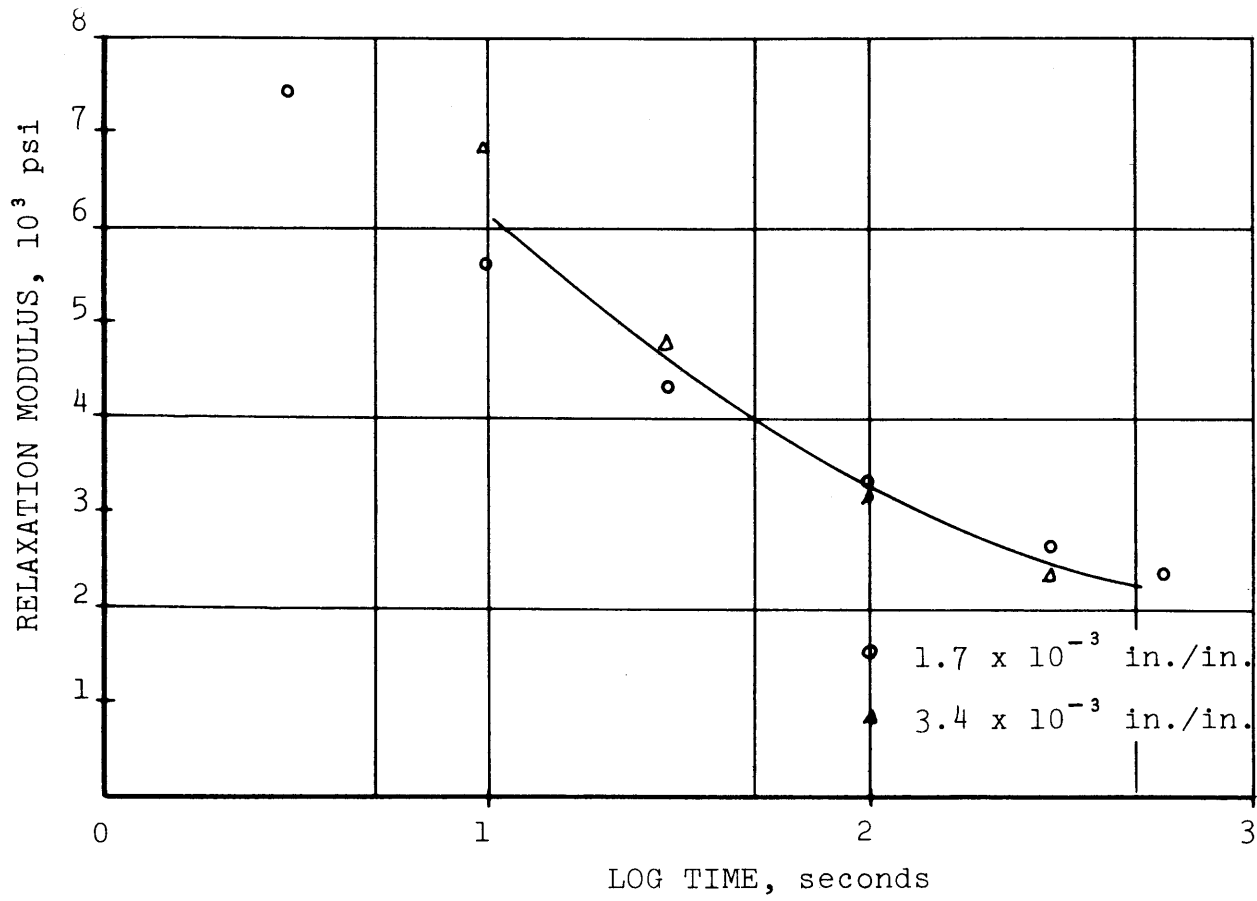
Figure 54.   Relaxation Modulus at 35°C

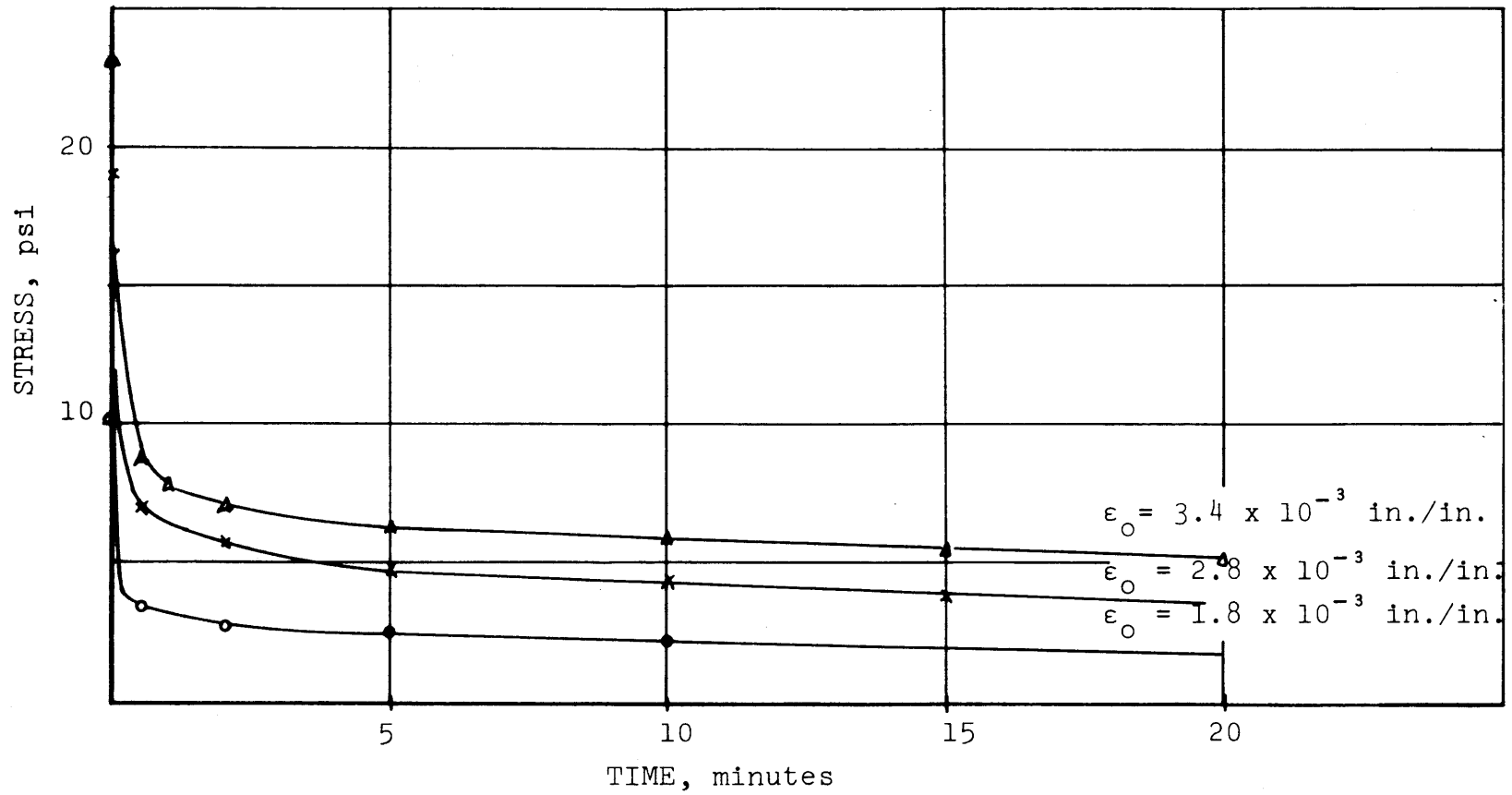Figure 55.   Stress Relaxation Curves
at 45°C
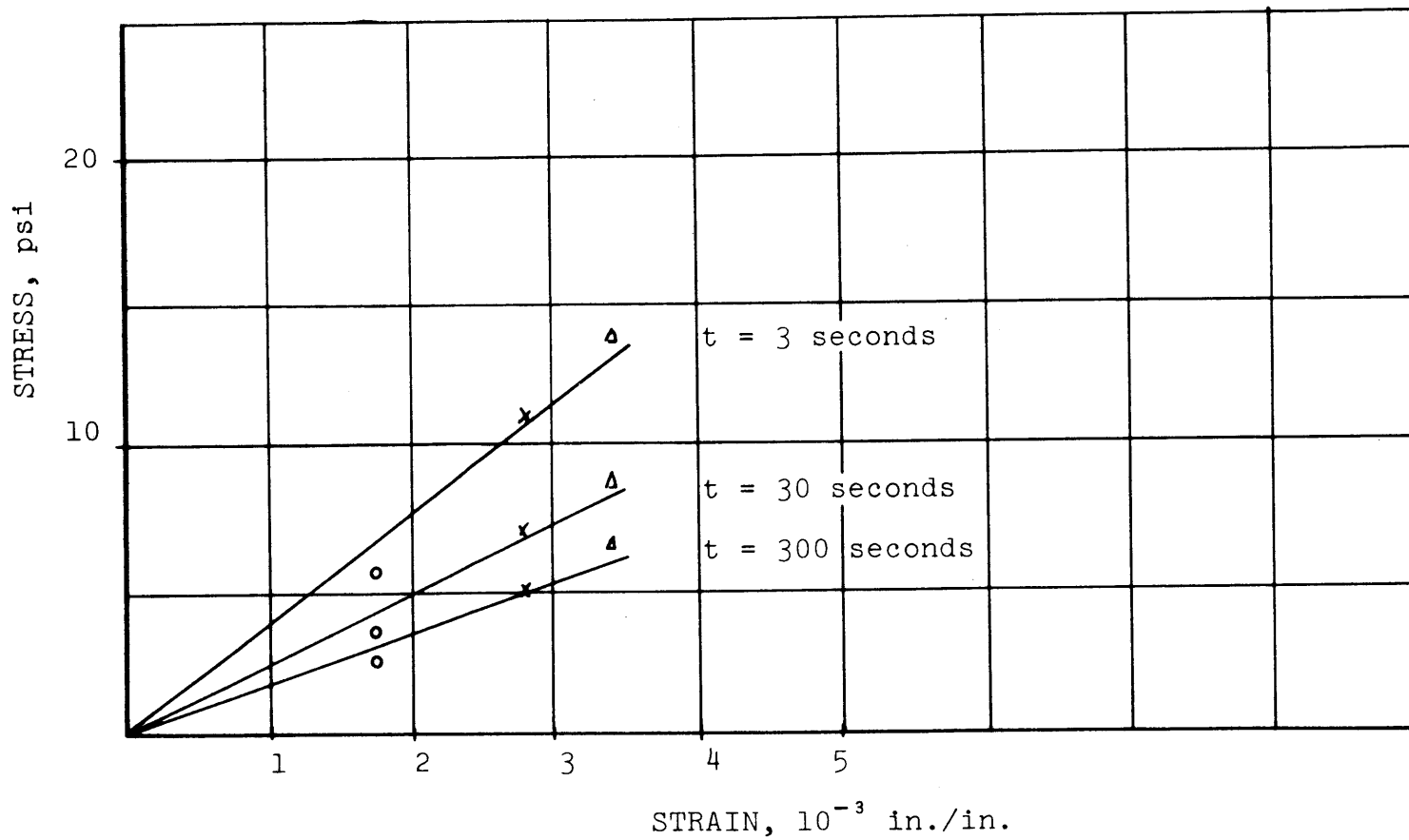
Figure 56.   Isochrones from Stress Relaxation at 45°C
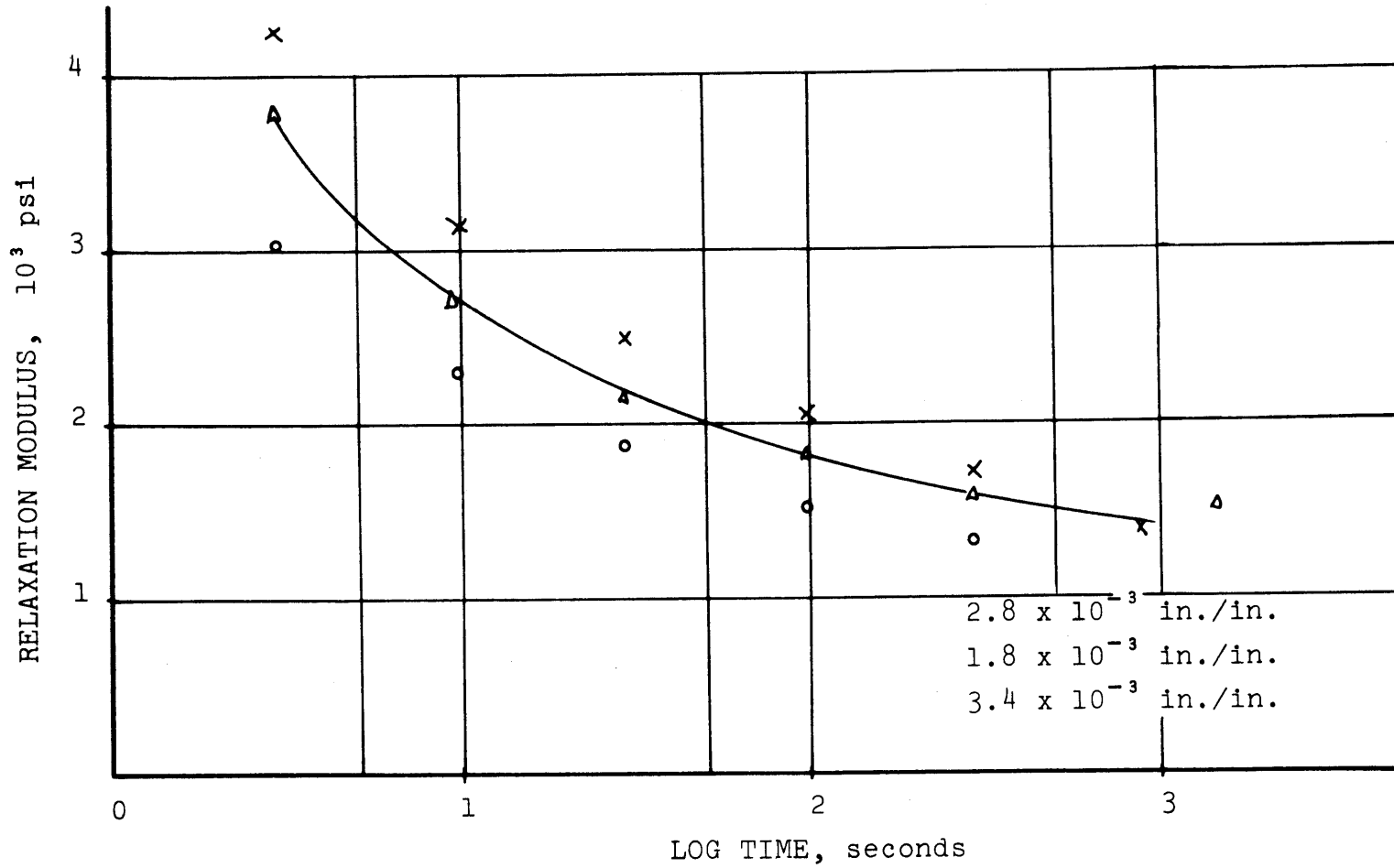
Figure 57.   Relaxation Modulus at 45°C

APPENDIX D

COMPUTER PROGRAMS LISTINGS

```
C         PROGRAM FOR CURVE FITTING AND RAMP CORRECTION
C         J AND L ARE IDENTIFICATION NUMBERS
C         M=N=NUMBER OF TERMS IN SERIES
C         CNOT=ASYMPTOTIC VALUE FOR INFINITE TIME
C         TNOT=LOADING TIME
C         RATE=VALUE OF CONSTANT RATE OF STRAIN
C         SIGMA=EXPERIMENTAL VALUE OF RELAXATION LOAD
C         RAT=AREA OF CROSS SECTION
C         ALPHA=VALUE OF EXPONENTS
C         HCOEF=COEFFICIENTS OF FITTING SERIES
C         DCOEF=COEFFICIENTS OF CORRECTED SERIES REPRESENTATION
C         DCOEF=COEFFICIENTS OF CORRECTED SERIES REPRESENTING
C         RELAXATION MODULUS
C         DNOT=ASYMPTOTIC VALUE OF RELAXATION MODULUS
          DIMENSION SIGMA(20),T(20),ALPHA(20),HCOEF(20),D(20,20)
          DIMENSION A(20,20),FRS(20),F(20,20),FR(20)
          DIMENSION COEF(20),DCOEF(20)
          DIMENSION BM(20,20),CM(20,20)
999       READ(5,1)J,L,M,N,CNOT
1         FORMAT(4I5,F10.5)
          READ(5,231)RAT
231       FORMAT(5X,F10.3)
          WRITE(6,231)RAT
          CNOT=CNOT/RAT
          WRITE(6,100)J,L,M,N,CNOT
100       FORMAT(4I5,F10.5)
          READ(5,15)TNOT,RATE
15        FORMAT(2F10.5)
          WRITE(6,15)TNOT,RATE
          READ(5,3)(T(I),I=1,N)
3         FORMAT (8F10.5)
          WRITE(6,102) (T(I),I=1,N)
102       FORMAT (8F10.5)
          READ(5,2)(SIGMA(I),I=1,N)
2         FORMAT (8F10.5)
          DO 232 I=1,N
          SIGMA(I)=SIGMA(I)/RAT
232       CONTINUE
          WRITE(6,101)(SIGMA(I),I=1,N)
101       FORMAT (8F10.5)
C         COMPUTE COEFFICIENTS
          DO 4 I=1,N
          ALPHA(I)=1./(2.*T(I))
4         CONTINUE
          WRITE(6,103) (ALPHA(I),I=1,N)
103       FORMAT('COEFFICIENTS OF EXPONENTS.=',7F10.4,//)
          DO 5 I=1,N
          D(I,1)=SIGMA(I)-CNOT
5         WRITE(6,98)D(I,1)
98        FORMAT(1F10.4)
          DO 6 I=2,N
          DO 6 J=1,M
          A(I,J)=0.0
          FRS(I)=-T(I)*ALPHA(J)
          A(I,J)=A(I,J)+EXP(FRS(I))
6         CONTINUE
          DO 61 J=1,M
61        A(1,J)=1.
```

```
       DO 99 I=1,M
 99    WRITE(6,104)(A(I,J),J=1,M)
 104   FORMAT(7F10.5)
       DO 1000 I=1,M
       DO 1000 J=1,M
 1000  BM(I,J)=A(I,J)
       CALL MATINV(A,M)
       DO 7 I=1,M
 7     WRITE(6,106)(A(I,J),J=1,M)
 106   FORMAT(4X,7E10.5)
       CALL MULTP(A,BM,CM,M,M,M,M,ISUCC,0)
       DO 2000 I=1,M
 2000  WRITE(6,106)(CM(I,J),J=1,M)
       CALL MULTP(A,D,F,M,M,M,1,ISUCC,0)
       WRITE(6,105)(F(I,1),I=1,M)
 105   FORMAT(4X,'RAMP COEFFICIENTS.=',10E10.3,//)
C      COMPUTE MODULUS COEFFICIENTS
       DO 8 I=1,N
 8     HCOEF(I)=F(I,1)
       CALL PLOT(M,ALPHA,HCOFF,CNOT)
       DO 9 I=1,N
       S=ALPHA(I)*TNOT
       IF( ABS(S)-50) 85,90,90
 85    DCOEF(I)=(HCOEF(I)*(EXP(S))*ALPHA(I))/(RATE*(EXP(S)-1.))
       GO TO 9
 90    DCOEF(I)=(HCOEF(I)/(RATE*TNOT))
 9     CONTINUE
       WRITE(6,107)(DCOEF(I),I=1,N)
 107   FORMAT(4X,'MODULUS COEFFICIENTS.=',7E10.3,//)
C      COMPUTE CONSTANT VALUF OF MODULUS
       DNOT=CNOT/(TNOT*RATE)
       WRITE(6,108)DNOT
 108   FORMAT (4X,'CONSTANT VALUE OF MODULUS.=',1E10.3,//)
       CALL PLOT(M,ALPHA,DCOFF,DNOT)
       GO TO 999
       END
```

```
      SUBROUTINE MULTP(A,B,C,MA,NA,MB,NB,ISSUC,IB)
C     A=MA*NA MATRIX
C     B=MB*NB MATRIX
C     C=PRODUCT MATRIX
C     ISSUC=TEST FOR CONFORMABILITY
C     IB=TEST FOR HOMOGENEOUS SYSTEM
      DIMENSION A(20,20),B(20,20),C(20,20),TEMP(400)
      IF(NA-MB)1,2,1
1     ISSUC=2
      WRITE (6,40)
      GO TO 35
2     ISSUC=1
      IF(IB-0)15,5,15
5     DO 10 I=1,MA
      DO 10 J=1,NB
      C(I,J)=0.0
      DO 10 K=1,NA
10    C(I,J)=C(I,J)+A(I,K)*B(K,J)
      GO TO 35
15    CONTINUE
      DO 30 J=1,NB
      DO 20 I=1,MA
      TEMP(I)=0.0
      DO 20 K=1,NA
20    TEMP(I)=TEMP(I)+A(I,K)*B(K,J)
      DO 30 I=1,MA
      B(I,J)=TEMP(I)
30    CONTINUE
40    FORMAT ('MATRICES ARE NOT COMFORMABLE')
35    RETURN
      END
```

```
      SUBROUTINE MATINV(A,N)
C     MATRIX INVERSION BY PARTITIONING
      DIMENSION A(20,20),B(30),C(30)
      NN=N-1
      A(1,1)=1./A(1,1)
      DO 1110 M=1,NN
      K=M+1
      DO 1160 I=1,M
      B(I)=0.0
      DO 1160 J=1,M
 1160 B(I)=B(I)+A(I,J)*A(J,K)
      R=0.0
      DO 1170 I=1,M
 1170 R=R+A(K,I)*B(I)
      R=-R+A(K,K)
      A(K,K)=1./R
      DO 1180 I=1,M
 1180 A(I,K)=-B(I)*A(K,K)
      DO 1190 J=1,M
      C(J)=0.0
      DO 1190 I=1,M
 1190 C(J)=C(J)+A(K,I)*A(I,J)
      DO 1100 J=1,M
 1100 A(K,J)=-C(J)*A(K,K)
      DO 1110 I=1,M
      DO 1110 J=1,M
 1110 A(I,J)=A(I,J)-B(I)*A(K,J)
      RETURN
      END
```

```fortran
      SUBROUTINE PLOT(M,ALPHA,DCOEF,DNOT)
      DIMENSION ALPHA(20),DCOEF(20),T(15)
      T(1)=0.1
      T(2)=0.3
      T(3)=0.5
      T(4)=1.
      T(5)=3.
      T(6)=5.
      T(7)=10.
      T(8)=30.
      T(9)=50.
      T(10)=100.
      T(11)=300.
      T(12)=500.
      T(13)=1000.
      T(14)=3000.
      T(15)=0.01
      DO 40 J=1,15
      D=DNOT
      DO 20 I=1,M
      S=ALPHA(I)*T(J)
      IF(S-60)4,20,20
4     IF(S+60)5,5,10
5     D=D+DCOEF(I)
      GO TO 20
10    D=D+DCOEF(I)/EXP(S)
20    CONTINUE
      WRITE(6,35)T(J),D
35    FORMAT(4X,'TIME   ',F7.1,10X,F10.3)
40    CONTINUE
      RETURN
      END
```

```
C          THIS SUBROUTINE SOLVES NUMERICALLY VOLTERRA
C          INTEGRAL EQUATION.
C          FOR CONVENIENCE DATA ARE GIVEN AS SERIES OF
C          EXPONENTIALS.F(T)=RRR+(COEFF(I)*EXP(-DELTA(I)*T))
C          WHERE THERE IS SUMMATION FOR I=1 TO I=K
C          K IS LESS THAN 20
C          T(J) ARE TIMES AT WHICH UNKNOWN FUNCTION Q(J)
C          IS COMPUTED.
           SUBROUTINE  CONV(K,COEFF,DELTA,RRR)
           DIMENSION T(500),DELTA(20),COEFF(20),Q(500)
           DIMENSION F(500),G(500)
           N=450
           REM=-6.
           RN=0.05
15         FORMAT(2F10.5)
           WRITE(6,4)N,K
4          FORMAT(4X,2I5)
           WRITE(6,15)RN,REM
           WRITE(6,5)(COEFF(I),I=1,K)
 5         FORMAT(4X,8E10.3)
           WRITE(6,5)(DELTA(J),J=1,K)
           CREM=REM
           CRN=RN
           T(1)=0.0
           NNN=N-1
           DO 6 JJ=1,NNN
           J=JJ+1
           CREM=CREM+CRN
           T(J)=10.**CREM
6          CONTINUE
           WRITE(6,21)(T(I),I=2,N)
           DO   31  JK=1,N
           G(JK)=0.0
           DO 30 I=1,K
           FT=-T(JK)*DELTA(I)
           G(JK)=G(JK)+COEFF(I)*EXP(FT)
30         CONTINUE
           G(JK)=G(JK)+RRR
31         CONTINUE
           WRITE(6,20)(G(J),J=1,N,10)
           F(1)=0.0
           MM=N-1
           DO 40 L=1,MM
           KI=L+1
           F(KI)=F(L)+0.5*(G(KI)+G(L))*(T(KI)-T(L))
40         CONTINUE
           WRITE(6,20)(F(J),J=1,N,10)
           DO 50 KT=3,N
           ST=0.0
           MMM=KT-1
           DO 45 I=2,MMM
           Q(2)=T(2)/F(2)
           KK=I-1
           PF=F(KT)-F(KK)
           PS=F(KT)-F(I)
45         ST=ST+Q(I)*(PF-PS)
           R=F(KT)-F(MMM)
           Q(KT)=(T(KT)-ST)/R
50         CONTINUE
```

```fortran
      WRITE(6,21)(Q(J),J=2,N)
20    FORMAT(4X,8E10.3)
21    FORMAT(4X,8E10.3,//)
      RETURN
      END
```

```
C          LAPLACE TRANSFORMATION OF DIRICHLET SERIES
C          ANOT =CONSTANT TERM IN SERIES
C          ALPHA(I)=COEFFICIENTS OF EXPONENTIALS
C          GAMMA(I)=COEFFICIENTS OF DIRICHLET SERIES
C          P(I)=LAPLACE PARAMETERS
C          NN=NUMBERS OF P PARAMETERS
C          CLAPL(I)=LAPLACE TRANSFORM OF CREEP
C          N= IDENTIFICATION NUMBER
C          M=1 CREEP
C          M=2 RELAXATION
C          MLAPL(I)=LAPLACE TRANSFORM OF MODULUS
           DIMENSION ALPHA(50),GAMMA(50),P(100),LAPL(50),SLAPL(50)
           DIMENSION PSUM(50),SUM(50)
           DIMENSION ACLAPL(50),ARLAPL(50)
           DIMENSION CLAPL(50),DLAPL(50),ELAPL(50)
           REAL MLAPL(50)
      999  READ(5,100)N,M,NN,ANOT
      100  FORMAT(3I5,E10.3)
           WRITE(6,104)N,M,NN,ANOT
      104  FORMAT(3I5,F10.3)
           READ(5,101)(ALPHA(I),I=1,N)
      101  FORMAT(8E10.3)
           WRITE(6,105)(ALPHA(I),I=1,N)
      105  FORMAT(8E10.3)
           READ(5,102)(GAMMA(I),I=1,N)
      102  FORMAT(8E10.3)
           WRITE(6,106)(GAMMA(I),I=1,N)
      106  FORMAT(8E10.3)
           READ(5,103)(P(J),J=1,NN)
      103  FORMAT(8E10.3)
           WRITE(6,107)(P(J),J=1,NN)
      107  FORMAT(8E10.3)
           IF(M-2)3,7,7
      7    J=1
      8    I=1
           SUM(I)=GAMMA(I)/(P(J)+ALPHA(I))
           DO 2 I=2,N
           PSUM(I)=GAMMA(I)/(P(J)+ALPHA(I))
           SUM(I)=SUM(I-1)+PSUM(I)
      2    WRITE(6,108)M,I,J,SUM(I)
      108  FORMAT(3I5,4X,E10.3)
           DLAPL(J)=ANOT/P(J)
           MLAPL(J)=DLAPL(J)+SUM(N)
           WRITE(6,109)M,I,J,MLAPL(J),DLAPL(J)
      109  FORMAT(3I5,4X,E10.3,4X,E10.3)
           ARLAPL(J)=P(J)*MLAPL(J)
           WRITE(6,200)P(J),ARLAPL(J)
      200  FORMAT( '    P(J)=  ',E10.3,'   P*MLAPL= ',E10.3)
           J=J+1
           IF(J-NN)8,8,999
      3    J=1
      9    I=1
           SUM(I)=GAMMA(I)/(P(J)+ALPHA(I))
           DO 20 I=2,N
           PSUM(I)=GAMMA(I)/(P(J)+ALPHA(I))
           SUM(I)=SUM(I-1)+PSUM(I)
      20   WRITE(6,111)M,I,J,SUM(I)
      111  FORMAT(3I5,4X,E10.3)
           DLAPL(J)=ANOT/P(J)
```

```
      CLAPL(J)=1./(DLAPL(J)+SUM(N))
      WRITE(6,110)M,I,J,CLAPL(J),DLAPL(J)
110   FORMAT(3I5,4X,E10.3,4X,E10.3)
      ACLAPL(J)=CLAPL(J)/P(J)
      WRITE(6,300)P(J),ACLAPL(J)
300   FORMAT( '        P(J)= ',E10.3,'     1/P*CLAPL=   ',E10.3)
      J=J+1
      IF(J-NN)9,9,999
      END
```

```fortran
C       THIS PROGRAM COMPUTE THE COMPONENTS OF DYNAMIC FUNCTIONS,
C       GIVEN TRANSIENT FUNCTIONS IN TERMS OF DIRICHLET SERIES.
C       D(T)=ANOT+(GAMMA(I)*EXP(-ALPHA(I)*T))
C       WHERE THERE IS SUMMATION FOR I=1 TO I=N.
C       N IS LESS THAN FIFTY.
C       P1 AND P2 ARE THE CIRCULAR FREQUENCIES AND THERE SQUARES.
        D1 AND D2 =REAL AND IMAGINARY PARTS OF D(T)
C       E1 AND E2 THE CORRESPONDING COMPONENTS OF OTHER FUNCTION
C       DABS IS ABSOLUTE VALUE OF COMPLEX FUNCTION D*
C       TANDEL=LOSS TANGENT
        SUBROUTINE DYNA(GAMMA,ALPHA,P1,P2,NN,N,ANOT)
        DIMENSION SUM(100),GAMMA(50),P1(100),P2(100),ALPHA(50)
        DIMENSION PSUM(100),DYNA(100),DYNAM(100),D1(100)
        DIMENSION D2(100),E1(100),E2(100)
        M=10
        J=1
8       I=1
        SUM(I)=GAMMA(I)/(P2(J)+ALPHA(I)**2)
        DO 2 I=2,N
        PSUM(I)=GAMMA(I)/(P2(J)+ALPHA(I)**2)
        SUM(I)=SUM(I-1)+PSUM(I)
2       WRITE(6,108)M,I,J,SUM(I)
108     FORMAT(3I5,4X,E10.3)
        DYNA(J)=ANOT/P2(J)
        DYNAM(J)=DYNA(J)+SUM(N)
        WRITE(6,109)M,I,J,DYNAM(J),DYNA(J)
109     FORMAT(3I5,4X,E10.3,4X,E10.3)
        D1(J)=P2(J)*DYNAM(J)
        D2(J)=0.
        DO 15 I=1,N
        D2(J)=D2(J)+(GAMMA(I)*ALPHA(I)*P1(J))/(P2(J)+ALPHA(I)**2)
15      CONTINUE
        SMOD=(D1(J)*D1(J))+(D2(J)*D2(J))
        DABS=SMOD**0.5
        E1(J)=D1(J)/SMOD
        E2(J)=D2(J)/SMOD
        TANDEL=D2(J)/D1(J)
        WRITE(6,200)P1(J),P2(J),D1(J),D2(J),E1(J),E2(J),DABS,TANDEL
200      FORMAT(4X,8(E10.3,2X))
        J=J+1
        IF(J-NN)8,8,999
999     RETURN
        END
```